UNIVERSITY OF STRATHCLYDE

Department of Civil and Environmental Engineering

An SHM-based decision support system for risk management of bridge scour

by

Andrea Maroni

BEng, MEng

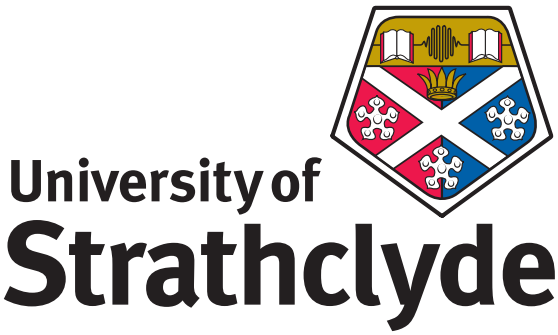

Thesis submitted in fulfilment of the
requirements for the degree of

Doctor of Philosophy

in

Civil and Environmental Engineering

July 2020

Glasgow, UK

This thesis is the result of the author's original research. It has been composed by the author and has not been previously submitted for examination which has led to the award of a degree.

Chapters that have been submitted for publication during the course of this degree are indicated. My contribution and those of the other authors to this work has been explicitly indicated below. I confirm that appropriate credit has been given within this thesis where reference has been made to the work of others.

Signed: _____

Date: _____

To my beloved Dalila.

Abstract

Flood-induced scour, the erosion of material around bridge foundations due to flowing water, is by far the leading cause of bridge failures worldwide. Although recent developments in sensor technology have resulted in more structures being monitored, practical applications of scour monitoring systems are limited. Thus, there is a need of quantifying the benefits stemming from the use of Structural Health Monitoring (SHM) systems for bridge scour assessment and of methodologies supporting the decision-making process of transport agencies responsible for scour risk management with information from scour sensors.

This thesis presents a probabilistic framework and a Decision Support System (DSS) for scour risk management of road and railways bridges, aiming to extend current procedures by incorporating *(i)* the various sources of uncertainty characterising the scour estimation, and *(ii)* information from scour sensors. The probabilistic framework for the estimation of bridge scour depth is based on a Bayesian network approach that exploits information from scour sensors to achieve a more precise estimate of the scour depth at unmonitored bridges. The DSS for bridge scour management is an SHM- and event-based decision model producing measurement-informed scour thresholds triggering bridge closure to traffic under heavy floods.

The functioning of the DSS is illustrated by considering as case study a network of road bridges crossing the same river in Scotland, under a heavy flood scenario. Only one of these bridges is instrumented with a scour monitoring system. The probabilistic framework demonstrates that the limited data from the scour sensors allow a significant reduction of uncertainty in the scour estimates at unmonitored bridge piers. This reduction is in the order of 70%, leading to a more precise classification of the bridge scour risk and to an increase of about 10% of the scour thresholds that trigger bridge closures compared to the ones chosen by transport agencies in their decision plans.

Contents

List of Figures

List of Tables

List of Symbols

Greek letters

ε	Dielectric permittivity of a material
ε_{m}	Bulk dielectric permittivity of a soil mixture
ε_{r}	Dielectric permittivity of a material relative to vacuum permittivity
θ	Volumetric water content

Latin letters

B_B	Channel width at bridge opening
$\overline{D}_R$	Measurement-informed scour threshold
d	Bed material grain size
D_C^*	Constriction scour measured in the middle of the channel
D_C	Constriction scour depth
D_F	Foundation depth
D_L	Local scour depth
D_T	Total scour depth
$D_{C,ave}$	Average constriction scour along the channel width
$D_{C,pier}$	Constriction scour depth at the pier

$^{(j)}e_M$	Uncorrelated model error of the Manning equation in the jth bridge
$^{(j)}e_{D_L}$	Uncorrelated model error of the local scour equation in the jth pier
$^{(j)}e_{v_{B,c}}$	Uncorrelated model error of the Colebrook–White equation in the jth bridge
e_M	Correlated model error of the Manning equation
e_{D_L}	Correlated model error of the local scour equation
$e_{D_{C,ave}}$	Error in the calculation of $D_{C,ave}$
e_{F_S}	Error in the constriction scour estimation where the river bends
$e_{v_{B,c}}$	Correlated model error of the Colebrook–White equation
F_S	Constriction scour distribution factor
n	Manning coefficient
N^k	Scaled frequency read by the kth sensor of EnviroSCAN probe
Q	River flow
s	Channel slope
v_B	Water velocity
$v_{B,c}$	Threshold velocity below which scour does not occur
W_P	Pier width
y_B	Water level through the bridge
y_U	Depth of flow upstream of the bridge

Abbreviations

BN	Bayesian network
cdf	Cumulative distribution function
DSS	Decision support system
DTU	Data transmission unit
FBG	Fiber–Bragg grating
FLM	Flood Level Marker
GPR	Ground-penetrating radar
GPS	Global Positioning System
InSAR	Interferometric synthetic aperture radar
LC	Inductor-Capacitor circuit (L is the symbol for inductance)
MCMC	Markov chain Monte Carlo
MSC	Magnetic sliding collar
NR	Network Rail
pdf	Probability density function
RV	Random variable
SD	Standard deviation
SHM	Structural health monitoring
SVI	Scour vulnerability index
TDR	Time-domain reflectometry
TMCMC	Transitional Markov chain Monte Carlo
TS	Transport Scotland

CHAPTER 1

Introduction

1.1 Problem statement

Scour is defined as the excavation and removal of ground material in water streams due to the erosive action of flowing water. This is mainly due to natural environmental changes in the river flow and the presence of bridges or hydraulic structures over the rivers. Scour threatens the safety of many civil engineering structures with foundations in riverbeds and, in fact, it is recognised as the leading cause for the collapse of bridges worldwide. The review of 1,502 failures of structures crossing rivers in the United States in the period 1966 - 2005 revealed that 58% of the recorded collapses have been attributed to scour (Briaud *et al.*, 2007). The same proportion of scour-related bridge failures was highlighted in Imhof (2004), where the author gathered a comprehensive collection of bridge failure data worldwide, and by the Federal Highway Administration (FHWA), which collected its samples among the bridges collapsed in the USA alone (Richardson and Davis, 2001). Moreover, the analysis carried out by Wardhana and Hadipriono (2003)—using a data set obtained from the New York State Department of Transportation (NYSDOT)—on the failure of 500 bridges in the US in the 1990s showed again that 53% of the total cases were due to floods and scour. Reviews carried out by Cook *et al.* (2015) and Flint *et al.* (2017), based on the NYSDOT

data set as well, drew the same conclusion.

In the UK, scour was responsible for at least 138 railway bridge failures between 1846 and 2013, (i.e., 1 bridge fails every 2.44 years) (Benn, 2013; van Leeuwen and Lamb, 2014), causing 15 fatalities. Bridges in Cumbria, a non-metropolitan county in North West England, have been particularly affected by flood events in the last decade. Several bridges were damaged in the aftermath of extreme events in November 2009 and December 2015, including two scour-related collapses (Cumbria Intelligence Observatory, 2010; Szoenyi *et al.*, 2015). Unfortunately, both storm events led to one death. The problem of scour is also exacerbated by climate changes in the UK, and particularly in Scotland, where the clear upward trend in winter precipitation will contribute to increased scour risk in the future, particularly for older bridge assets that have not been designed to withstand scouring (Dikanski *et al.*, 2016; Dikanski, 2018; Ekuje, 2018).

Current approaches for bridge scour risk management in the UK provide transport agencies with a classification of bridges based on estimates of their scour risk, thus forming the basis for prioritising and planning inspection and scour risk mitigation measures. The risk assessment is based on an essentially deterministic approach, with a prefixed flood scenario (e.g., the 1 in 200 years flood) and disregarding the various uncertainties that may characterize the problem. The scour estimation process is mainly based on visual inspections, which provide unreliable estimates of scour and of its effects, also considering the difficulties in visually monitoring the riverbed erosion around foundations.

Transport agencies' response to the threat of adverse weather is defined in their action plans establishing a systematic and structured approach. The purpose of these strategy documents is to provide the action to be taken during or following an extreme weather event, and hence defining the decision processes. According to these plans, the decision of whether to close a bridge to traffic or not in the occurrence of a heavy flood is based on the comparison between the water level at the upstream section of the bridge and the critical

water level, represented by a marker installed on the bridge. This flood level marker can be set to correspond to a specific return period of the flood (e.g., 200 years return period) defined by considering other potential problems for the bridge (e.g., deck uplifting).

It is worth noting that measurement of the scour depth does not enter directly into the decision process, and an inspection of the scour depth is taken only when water levels recede so that inspectors can safely carry out checks. Moreover, scour is a very complex phenomenon and triggering bridge closures according to flood level markers does not allow the directly control of scour risk under floods. In fact, the critical water level cannot be directly associated to a precise level of scour at the bridge foundations (Pizarro *et al.*, 2020). This is mainly due to many uncertainties that affect the problem (Tubaldi *et al.*, 2017; Pizarro and Tubaldi, 2019), reducing the correlation between water level and scour depth. Furthermore, an intense flood event (i.e., water level above the marker) does not directly lead to a significant scour hole because of bed material deposition during the live-bed scour regime. At the same time, multiple flood events with small intensity (i.e., below the marker) might lead to scour accumulation problem, thus threatening the safety of the bridge. In essence, visual inspections and water levels are very rough indicators of bridge scour risk.

A way to overcome these limitations is to install scour monitoring systems, which are techniques and devices aiming to provide in near-real time reliable measures of the scour depth and/or of the condition of the structural components. The use of structural health monitoring (SHM) systems permanently installed around a bridge pier or abutment is very promising, considering the wide range of techniques developed in the past decades; yet, continuous monitoring campaigns for scour depths are still scarce due to accessibility issues under flood events and their costs.

Although there are many studies in the literature on the benefits of SHM campaigns for asset management, bridge operators are still sceptical about the advantages of the deployment of sensors and SHM systems. Outputs of monitoring systems are affected by

uncertainties (i.e., it is also difficult to quantify them) and operators act based on their engineering judgement and experience because often SHM data are not converted into useful information for manager. Consequently, if their budget is limited, they might prefer to undertake retrofitting work instead of investing in SHM systems. For these reasons, there is a need to introduce a system that, during and after an extreme weather event, is capable not only of monitoring the evolution of scour at bridge foundations, but also of supplementing the agencies' decision process with clear and direct information about scour and the bridge state in order to support them in taking the optimal decision about keeping bridges in service.

1.2 Objectives

This thesis aims to develop a probabilistic framework and a Decision Support System (DSS) for scour risk management of road and railway bridges (Figure 1.1), which enhances the safety of users, while minimizing traffic disruptions and operational costs. In particular, the proposed scour risk management system aims at extending and complementing current scour risk rating procedures and action plans of UK transport agencies by incorporating (i) the various sources of uncertainty inherent to the hydrological and hydraulic parameters as well as the models employed for evaluating the scour depth at a bridge, and (ii) the information from scour sensors. A more explicit consideration of the sources of uncertainty facilitates the shift from a deterministic to a probabilistic approach for scour risk assessment, whereas observations from scour sensors allow the reduction of the uncertainty in the scour risk estimates and hence helping bridge operators take the optimal decisions concerning bridge scour risk management.

The main objectives of this research are:

(i) Developing a pilot scour monitoring system based on smart probes equipped with

capacitive sensors at different depths along the probe's height. The monitoring technique allows distinguishing between water, saturated soil and deposited soil, which is useful to assess whether the scour hole has been refilled after the flood peak has receded. The SHM can provide quantitative information about the structure condition to be used in the process of risk evaluation and supplementing the flood level threshold after which a bridge is closed.

(ii) Producing a probabilistic framework for the estimation of bridge scour depth based on a Bayesian network (BN) approach, which considers the various sources of uncertainty characterising the scour problem and integrates information from the scour sensors into the assessment. This latter information is expanded by the BN to other unmonitored locations in the bridge infrastructure network to achieve a more confined scour estimate. This probabilistic framework constitutes the first application of BNs to bridge scour risk management.

(iii) Proposing an SHM-based scour risk classification for bridge performance in the occurrence of a flood event using the outcomes of the probabilistic framework and SHM scour data. It provides a more fair and accurate scour risk assessment that reflects the uncertainties characterizing the problem and allows the integration of real-time scour measurements. The risk classification could drive strategic maintenance, repair and rehabilitation (MR&R) actions and help to reduce bridge risk misclassification.

(iv) Developing an SHM-based event-based DSS that produces measurement-informed scour thresholds triggering bridge closure to traffic under heavy floods by incorporating real-time scour measurements in the decision-making process. The DSS could help bridge asset operators in reducing the times that bridges might be closed unnecessarily as a precautionary action.

The rationale of the proposed risk-based decision support system is depicted in Figure 1.1.

Starting from the river water flow Q and the data collected by gauging stations, the total scour depth D_T at each bridge is subsequently estimated though the probabilistic framework, based on a BN reproducing the scour estimation process used by transport operators (i.e., second objective). Bridge geometry, river hydraulic parameters and past scour inspection records enter the BN for the scour estimation. As the flood occurs, the estimate of scour depth D_T is continuously updated based on the observations from scour monitoring systems (first objective), using a Bayesian updating approach. These updated estimates of the probabilistic distribution of scour are the used to classify the bridge performance under an extreme event, thus reproducing, in a probabilistic form, the scour risk rating method (third objective). Moreover, the BN's output and observations of scour monitoring system inform the decision model by producing measurement-informed scour thresholds (fourth objective) that suggest whether the bridge should undergo traffic restrictions or closure during the high-flow event.

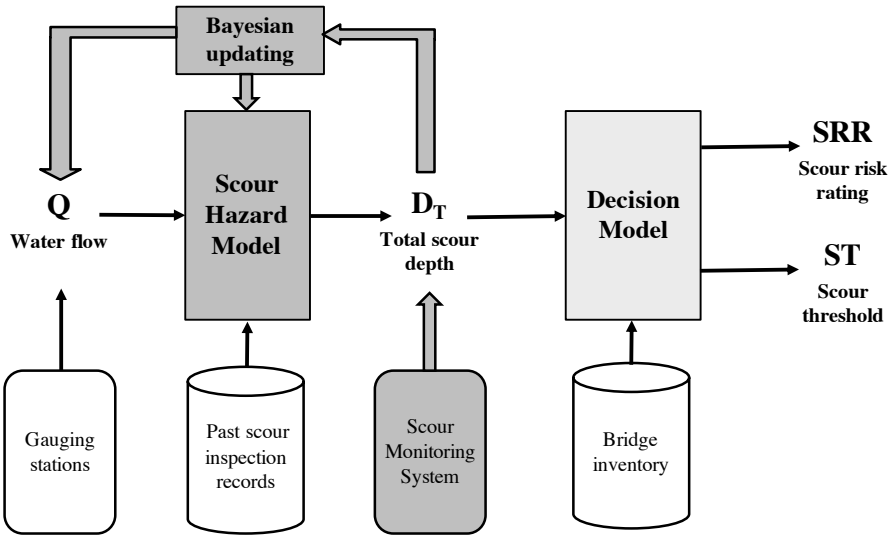

Figure 1.1: *Schematic rationale of the Decision Support System*

The functioning of the developed DSS is tested using a small bridge network, consisting of bridges managed by Transport Scotland in south-west Scotland. The bridges cross the same river (River Nith) and only Bridge 1 is assumed to be instrumented with a scour

monitoring system. The objectives will be achieved by applying experimental, numerical and theoretical approaches.

It is noteworthy that although earlier work on DSS, SHM and scour estimation methods have been singularly presented and SHM-based DSSs have been developed as well, to the author's knowledge, this is the first application of an SHM-based DSS for scour risk management of bridges. This is also the first application of smart probes with electromagnetic sensors to a real case-study for continuous scour monitoring.

1.3 Outline of the thesis

The thesis is structured as follows. This Chapter provides a general overview of the motivations and objectives of the research. *Chapter 2* contains a review of the current state-of-the-art of scour risk assessment, monitoring, and management. It starts with the description of the scour process and then reviews the current scour risk assessment frameworks by illustrating contributions from the academic community and the procedures followed by transport operators in the UK. The rest of the Chapter covers the literature used as a basis for the development of the DSS, by illustrating the existing scour monitoring techniques, the principal concepts of the Bayesian networks and an introduction of SHM-based decision-making processes.

Chapter 3 describes the concept, installation and functioning of a pilot scour monitoring system based on the use of smart electromagnetic probes and installed on the A76 200 bridge over the River Nith in New Cumnock, UK. The work presented in this Chapter was published in the special issue *"Innovative Sensors for Civil Infrastructure Condition Assessment"* of the international journal *Sensors* as *"Electromagnetic sensors for underwater scour monitoring"* by Andrea Maroni (student), Dr. Enrico Tubaldi (PhD lead supervisor), Dr. Neil Ferguson, Prof. Alessandro Tarantino, Dr. Hazel McDonald and Prof. Daniele

Zonta (PhD second supervisor), vol. 20, issue 15 (2020).

Chapter 4 presents a scour hazard model in the form of a probabilistic framework for the assessment of the scour hazard of bridges in a network based on a BN. The work presented in this Chapter has been submitted to the international journal *Structural Health Monitoring*, as *"Using Bayesian networks for the assessment of underwater scour for road and railway bridges"* by Andrea Maroni (student), Dr. Enrico Tubaldi (PhD lead supervisor), Prof. Dimitri V. Val, Dr. Hazel McDonald and Prof. Daniele Zonta (PhD second supervisor). The manuscript has been accepted for publication.

Chapter 5 illustrates the development of the DSS for bridge scour management, able to supplement transport operators' decision frameworks with real-time information from scour monitoring systems and scour estimates achieved by the scour hazard model. The work presented in this Chapter will be submitted to the international journal *Structure and Infrastructure Engineering* as *"SHM-based decision support system for bridge scour management"* by Andrea Maroni (student), Dr. Enrico Tubaldi (PhD lead supervisor), Dr. Hazel McDonald and Prof. Daniele Zonta (PhD second supervisor).

A summary and a discussion of the results are presented at the end of each Chapter. Finally, *Chapter 6* summarises the major findings of this doctoral dissertation, discusses the outcome of the research project and outlines future research work.

1.4 Funding

This study has been carried out within the project titled "Early warning decision support system for the management of underwater scour risk for road and railway bridges", which has received funding from the NERC ERIIP (Environmental Risk to Infrastructure Innovation Programme) under grant agreement no. NE/R009090/1. The procurement and installation of the probes at the Nith bridge in New Cumnock (South-West Scotland) was supported by

Transport Scotland.

1.5 List of publications

The following is the full list of peer reviewed journal publications that resulted and/or are related with this thesis.

Journals

[1] Maroni, A., Tubaldi, E., Ferguson, N. S., Tarantino, A., McDonald, H., and Zonta, D. (2020a). "Electromagnetic sensors for underwater scour monitoring". *Sensors*, **20**(15), 4096.

[2] Maroni, A., Tubaldi, E., Val, D. V., McDonald, H., and Zonta, D. (2020b). "Using Bayesian networks for the assessment of underwater scour for road and railway bridges". *Structural Health Monitoring*, Jan 2020, *ACCEPTED FOR PUBLICATION*.

[3] Maroni, A., Tubaldi, E., McDonald, H., and Zonta, D. (2020c). "SHM-based decision support system for bridge scour management". Submitted for publication to *Structure and Infrastructure Engineering*, June 2020.

CHAPTER 2

Literature review

2.1 Introduction

Developed countries have a vast stock of bridges, whose level of safety should be guaranteed by adequate control and maintenance measures aimed to ensure the safety of their users. Although a large proportion of the bridge stock is in a good state, ageing, degradation, increase of traffic and natural hazards pose a significant threat to their safety (Figure 2.1a). A multitude of bridges could be below the current required standard and in some cases they may be subjected to higher loads than the ones they were originally designed and constructed. In Europe, 16% of the 1 million road bridges are more than 60 years old and 41% are 40–60 years old (Woodward, 2002). Railway overpasses are even older, since 35% of the total stock (i.e., 500,000 bridges) are more than 100 years old (Olofsson *et al.*, 2005). In the US, more than 600,000 highway bridges are 50 years old on average (ASCE, 2017), while in Japan there are 50,000 bridges with more than 50 years old Fujino and Siringoringo (2008). If long-term deterioration is left unchecked (Figure 2.1a), it can lead to catastrophes similar to the collapse of the Morandi bridge in Genova, Italy (Figure 2.1b), in August 2018, which killed 43 people and injured eleven (The Guardian, 2019*b*).

(a)

(b)

Figure 2.1: ***(a)*** *Long-term deteriorations make the steel reinforcement visible in piers and beams (The Boston Globe, 2009) and* ***(b)*** *the collapsed Morandi bridge in Genova in the 2018 (The Guardian, 2019a)*

Research in this field and revision of current management procedures are essential to address the problem. In this context, the EU-funded project "Sustainable bridges" (Sustainable Bridges, 2008) proposed improved methods and engineering solutions aiming to increase the residual service life of existing railway bridges in Europe. The procedures consist of new bridge condition assessment methods (e.g., using radar tomography or ultrasonic echo methods), developing probabilistic frameworks for load capacity and bridge resistance appraisal and the deployment of structural health monitoring systems.

In recent years, researchers have also looked at the main causes of bridge collapse in order to provide a comprehensive summary of information needed to understand the bridge collapse mechanisms. Bridge collapses are due to several factors that are generally broken down into two categories: *(i)* natural factors (e.g., f earthquake, flood, scour, hurricane, landslide, etc.) and *(ii)* human factors (e.g., lack of inspection and maintenance, fire, collision, imperfect design or construction, etc.) (Deng *et al.*, 2016). In the majority of these reviews, flood-induced scour has emerged as one of the most common cause of bridge failures worldwide (Briaud *et al.*, 2007; Cook *et al.*, 2015; Flint *et al.*, 2017; Imhof, 2004; Wardhana and Hadipriono, 2003), culminating in traffic disruption, loss of lives and notable economic losses.

In the last century, more frequent extreme flood events throughout the world have exposed river crossings at high peril of collapse due to scour. Figure 2.2a shows a typical bridge failure due to scour. Scour can be defined as the excavation and removal of material from the bed of streams around bridge foundations as a result of the erosive action of flowing water, as depicted in Figure 2.2b.

(a) ***(b)***

Figure 2.2: ***(a)*** *Bridge failure due to scour (Texas A&M Transportation Institute, 2014) and* ***(b)*** *detail of scour hole around a bridge pier (Dundee Tunnel Research, 2012)*

Bridges, culverts and every hydraulic structure founded on riverbed are prone to scour around their foundations (Richardson and Davis, 2001)). When the depth of scour becomes significant, the load-bearing capacity of pier foundations may be severely compromised, resulting in loss of structural stability and eventually catastrophic failures.

The current practice for scour risk management of bridges relies mainly on visual checks carried out by inspectors. These inspections are expensive and time-consuming; furthermore, the information they provide is often qualitative and subjective. A wide range of sensor and communication technologies offer the possibility to overcome these limitations, by allowing a real-time assessment of the scour depth at bridge foundations. However, practical applications of real-time bridge scour are very limited because of accessibility issues under flood events and the involved cost. Therefore, transport operators estimate the scour depths

and assess the scour risk at their asset (i.e., ranking the bridges in scour risk classes) before a flood event, exploiting information collected during visual inspections and assuming a conventional flood scenario with a prefixed return period. No measure of the actual scour depth enters their decision process. In fact, during an extreme weather event, transport operators make decision to close the bridge to traffic based only on a visual comparison between the water level and a fixed flood level marker. Only when water levels have receded inspectors can safely carry out safety checks and assess the scour evolution.

This Chapter provides a literature review of bridge scour risk assessment and management: Section 2.2 outlines the principal concepts of the scour process and reviews the scour bridge failures occurred in the past decades. Section 2.3 contains a brief literature review of current scour risk assessment frameworks by including both the works developed by the academic community and the procedures follow by transport operators in the UK. Section 2.4 illustrates the state-of-the-art in existing scour monitoring techniques by illustrating both direct and indirect scour measurement devices. Then, Section 2.5 illustrates the principal concepts of Bayesian logic and Bayesian Network, which are the probabilistic tool used to extend the piece of information collected by few scour monitoring systems to the unmonitored bridges. Finally, the SHM-based decision-making frameworks and procedures are reviewed in Section 2.6. The Chapter ends with a list of the key findings from the review in Section 2.7.

2.2 Bridge scour

Definitions of types of scour in the literature vary widely, and particularly the term *degradation scour*, is used with a range of different meanings by various author. For instance, Kirby *et al.* (2015) defines the scour process as:

> "the removal of material from the bed and banks of a channel and from around

structure foundations by the action of water."

The authors classify the scour process in compliance with the structures and circumstances that have caused it, and they report the following types of scour (Figure 2.3):

(i) *constriction scour* also known as *contraction scour*;

(ii) *local scour*;

(iii) *degradation scour*[1].

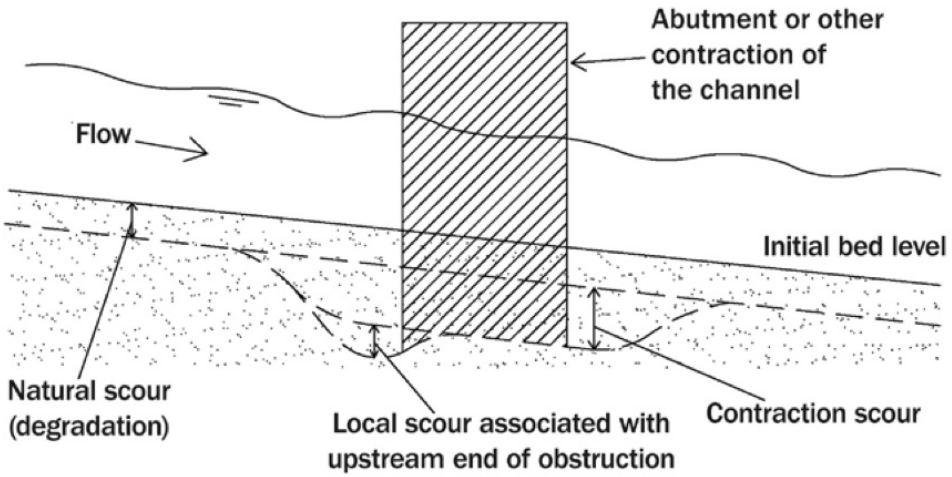

Figure 2.3: *Schematic illustration of total scour (Kirby* et al.*, 2015)*

Scour occurs naturally, and it may be caused by variations of flow in the riverbed, as part of river morphological evolution, or because of human activity, e.g., the construction of structures in the watercourse (Melville and Coleman, 2000). The different types of scour events can be classified depending on their nature, but, although triggers are different, they can occur at the same location and in the same time frame. The first two types of scour, i.e., local scour and constriction scour, are related to the existence of a bridge or hydraulic structures, whereas degradation scour is attributable to natural variations in the

[1]In certain literature, degradation scour is called general scour, and in others this term also includes the constriction scour. To avoid potential confusion, the term general scour is avoided in this thesis, and the term constriction scour is used hereinafter.

flow, irrespectively of the presence of a river crossing. These are the main mechanism, but other types of scour exist, such as debris flow scour or boat scour, but they occur in more specific cases and situations (Kirby *et al.*, 2015).

Bridge scour is indeed a fluid-soil-structure interaction phenomenon (Hamill, 1999). Thus, the river crossing failures under scour conditions are related to geotechnical, hydraulic and structural conditions. The hydraulic conditions consist of scour types, scour depths and flow characteristics; geotechnical conditions embrace all soil characteristic of the riverbed and of the bridge site; and, finally, the last ones refer to structural parameters and variables of bridges or any hydraulic structure.

Scour initiates when the shear stresses at the water-bed interface is higher than the critical ones corresponding to the initiation of motion of the soil particles. The type of bed material also plays an essential role in the scour process as the critical shear stress is peculiar to it. For example, the critical shear stress is lower for sand than for limestone (Pizarro *et al.*, 2020; Sheppard and Renna, 2005). This phenomenon poses a significant risk to bridges crossing rivers and channels, reducing the load-bearing capacity of foundations and causing the bridge to fail and collapse, often without any warning (Michalis *et al.*, 2015). Thus, monitoring and detecting scour at early stages of development is of paramount importance to ensure the operability and safety of bridges.

The main scour mechanisms listed above work cumulatively to produce total scour (Figure 2.3), and a bridge may collapse because of a combination of the individual scour types.

Constriction scour

Constriction scour affects all or most of the channel bed in the vicinity of a bridge or other hydraulic structure, and it is the outcome of confining the river channel, for instance between bridge piers and abutments. This type of scour occurs when there is sudden

increase in flow velocity, which causes an increase in shear stress, as a result of a reduction of channel cross-sectional area at the bridge location (Briaud *et al.*, 1999).

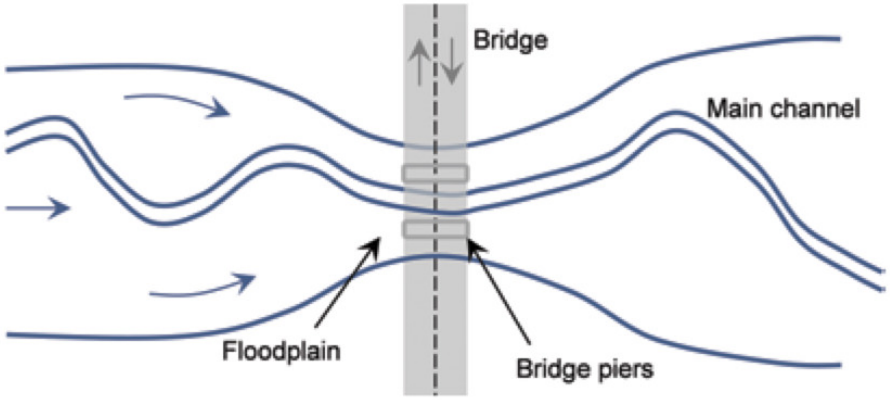

Figure 2.4: *Flows join the main channel because of the presence of a bridge, from Kirby* et al. *(2015)*

The phenomenon happens because the approach embankments to a bridge causes the flows to pass through the bridge opening by joining the main channel (Figure 2.4). The contraction of the channel width leads to an increase of the river flow velocity through the contraction. Hence, the increase in velocity results in additional shear stress on the riverbed surface, causing an increase in scour in the area of constriction (Umbrell *et al.*, 1998). The erosion of sediments starts when the shear stresses exceed the threshold value of the bed material (i.e., the value of shear stress below which scour does not occur) (Kirby *et al.*, 2015).

In general, the smaller the opening ratio, defined as the ratio between the bridge (or contracted) and the approach (or uncontracted) width, the larger the flow velocity and the greater the potential for scour (Hamill, 1999). Other factors that can generate constriction scour are ice formations or jams, natural stream constrictions, debris, and vegetative growth in the channel or floodplain.

Local Scour

Local scour is caused by the interference of individual structural elements, such as piers or abutments, with the flow and it is characterised by the formation of scour holes only in the immediate vicinity of those elements (Lauchlan and Melville, 2001). The basic local scour mechanism at piers or abutments is the development of vortices in the surrounding of their base. Figure 2.5 shows the formation of these horseshoe vortices at a cylindrical pier. The creation of the vortices around the element is due to the upstream accumulation of water and subsequent flow acceleration around the obstacle's nose. (Breusers *et al.*, 1977). This action removes bed material at the pier base.

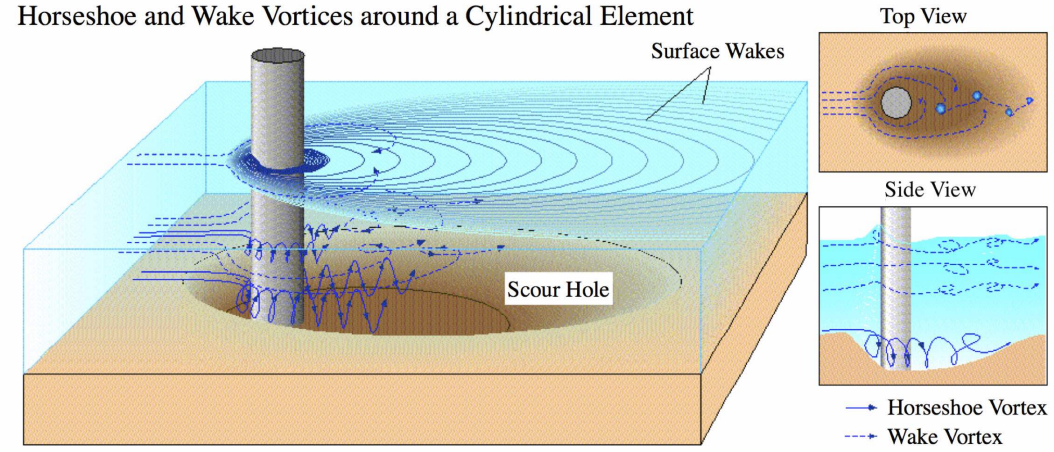

Figure 2.5: *Diagram of the formation of scour holes during a local scour process, adapted from United States Geological Survey (2016)*

In addition to the horseshoe vortex, there are vertical vortices downstream of the pier called wake vortex (Daraghi, 1990), as depicted in Figure 2.5. Both the horseshoe and wake vortices remove material from the pier base region. However, the greater the distance downstream of the pier the lower the intensity of wake vortices. Some of the factors that affect the extent of local scour depth are: the depth of flow at pier location, the velocity of the approach flow, the width and shape of a pier or abutment, the approaching flow angle between the structural element's axis (e.g., pier or abutment) and the flow direction, the

length of the pier if skewed to flow (Melville, 2008).

Local scour can be exacerbated by the presence of debris in the vicinity of the bridge pier (Parola *et al.*, 2000). Debris blockage increases the effective pier width and, therefore, reduces the channel width. The debris-induced constriction of the flow leads to an increase of water velocities in the surrounding of the pier, which in turn worsen scour (Benn, 2013; Lagasse *et al.*, 2010). Masonry bridges are more prone than other bridge types to risk of debris blockage since they usually have wider pier.

Few experimental studies were carried out to understand the effect of debris blockage on flow and pier scour. Early contributions considered circular or rectangular piers (Lagasse *et al.*, 2010; Melville and Dongol, 1992; Pagliara and Carnacina, 2011). The effect of debris accumulation on scour at the base of sharp-nose piers (i.e., typical foundation shape of masonry bridges) was studied by Ebrahimi *et al.* (2018) by performing a clear-water scour experimental study on a scaled model of a sharp-nose pier. These outcomes were lately used to develop the concept of "debris factor" in the evaluation of the local scour depth (Ebrahimi *et al.*, 2020), in replacing the equivalent pier diameter approach proposed in earlier studies.

Degradation scour

Degradation scour encompasses all scour processes that are not labelled as local scour or contraction scour. The erosion is due to the change of riverbed elevation that causes a lateral instability in the water flow. In a river, this is due to river flow changes, whereas, in the sea, it is because of the action of tidal currents and storm surges (Richardson and Davis, 2001). So, it is expected to occur at a site due to natural factors, without any additional effects produced by the presence of structures. Degradation scour includes aggradation of material at bends in the river, which can induce channel migration, bend scour (Figure 2.6), confluence scour and lateral migration through bank erosion (Kirby *et al.*, 2015). This type

of scour occurs within high flow periods characterised by a sufficient water energy to start the bed material movement.

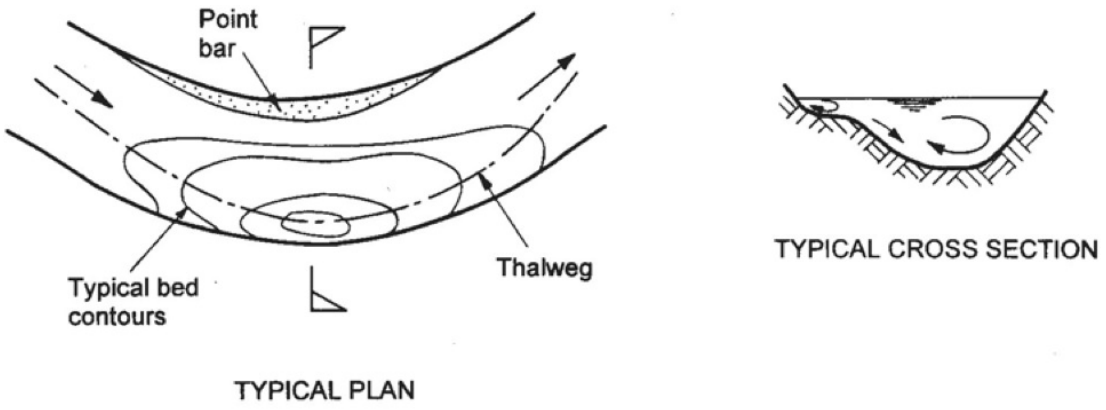

Figure 2.6: *Example of bend scour (Kirby* et al.*, 2015)*

2.2.1 Clear-water and live-bed scour

Overall, scour is a highly dynamic process that generally increases until an equilibrium value is attained (Hamill, 1999). However, at the end of a flood event the scour hole might have partly filled during the recession of the water level, thus making arduous capturing the maximum scour occurred during the event. Consequently, it is difficult to relate these maxima and equilibrium values with actual flood events at a bridge site since they are characterized by different hydrograph duration, magnitude and shape (Pizarro *et al.*, 2020). Moreover, a sequence of events occurs during the lifetime of the bridge, thus leading to accumulation phenomena.

Scour depends on the balance between riverbed erosion and sediment deposition (Brandimarte *et al.*, 2012). Many researchers have extensively studied the time evolution of the scour depth in the past decades, and the first articles that dealt with the development of scour process are from the 1950s. Two different regimes have been defined for scour: clear-water and live-bed scour (Chabert and Engeldinger, 1956), which depend on the

properties of the flow and of the bed sediment.

When the approach flow velocity is smaller than the sediment entrainment velocity, the bed material keeps static. However, especially under the effect of the horseshoe vortices mentioned in the previous section, the local velocity in the surrounding of the bridge piers increases. When the upstream flow velocity reaches the entrainment velocity, the bed material starts to move downstream, and a scour hole appears. At this stage, holes may occur only in relatively low flows leading to clear-water scour, which could be considered the initial scouring (Melville and Chiew, 1999). This type of scour occurs when the flow does not transport any sediment on the riverbed in the flow, or when the transportation rate of bed material in suspension through the scour hole is lower than the capacity of the flow (Melville, 1984). Clearly speaking, the scour hole is not refilled by the approaching sediment because the bed material is not transported from the upstream reach of the river.

The key parameters to distinguish the two different condition of scour are the mean velocity (v) of the flow upstream from the bridge and the scour-critical velocity (v_C) of the D_{50} sediment (i.e., mean diameter representative of the soil particle distribution), needed to move the bed material (Melville and Coleman, 2000). If $v \leq v_C$ the clear-water scour regime occurs because the flow does not contain any sediment and is "clear". Hence, the sediment removed from a scour hole is not replaced by bed material being moved by the approach flow. If the mean flow velocity remains below the limit value given by the scour-critical velocity, the maximum scour depth, in clear-water condition, is attained when the size of the scour hole leads to a localised reduction in velocity and the current can no longer erodes sediment from the area (Hamill, 1999).

Once the flow increases, there is then a supply of sediment from upstream to offset the local removal of material. This means that a local scour hole is continuously filled with the sediment transported by the approach flow. Scouring under these conditions is referred to as live-bed scour (Melville and Coleman, 2000). This happens when $v > v_C$.

The equilibrium value of scour depth under this scour regime is achieved when the bed sediment is transported into the pit at the same rate at which it is scoured. A scour hole is not just caused by live-bed condition in a uniform channel because of the continuous refilling from upstream. Therefore, in order to develop one some further increase in velocity is required (e.g., due to a contraction—natural or artificial—or a local obstruction, for instance, a bridge pier) (Hamill, 1999). For this reason, contraction and local scour may occur in both clear-water and live-bed conditions.

Figure 2.7 illustrates the scour depth development over time under stationary clear-water and live-bed scour regimes. The equilibrium scour depths under live-bed conditions is obtained rapidly for flow velocity v greater than the scour-critical velocity v_C (when sediment is generally in motion). Then, the depth of scour hole fluctuates around the equilibrium scour value because of the continuous refilling. Instead, scour pits develop more steadily under clear-water conditions (v is less than v_C). An equilibrium clear-water scour depth is achieved asymptotically more slowly than live-bed regime. Furthermore, the equilibrium clear-water scour depth is larger than that in live-bed condition and, for general practice, it is considered 10% greater than equilibrium live-bed scour depth.

Equations to estimate constriction scour and local scour in both clear-water and live-bed conditions could be found in the literature (Kirby *et al.*, 2015; Richardson and Davis, 2001). The value of the approach flow in the main channel discriminates between the two scour regimes and allows knowing if it is transporting sediments (i.e., live-bed condition, $v > v_C$) or is not (i.e., clear-water condition, $v \leq v_C$). Different equations have been proposed to determine the scour-critical velocity in the literature (Melville and Coleman, 2000), and most of them are based on the size of bed material and a given flow depth.

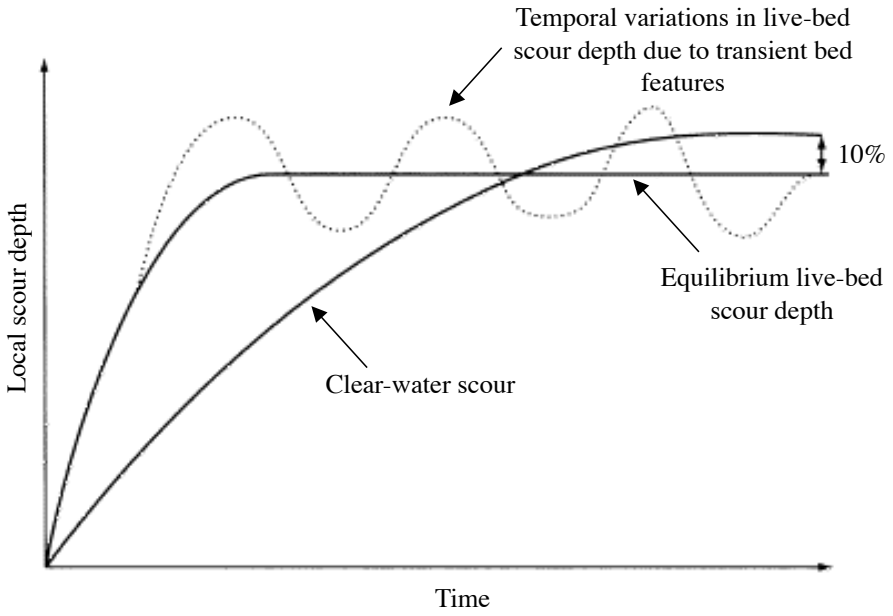

Figure 2.7: *Diagrammatic illustration of the increase in local scour depth with time for clear-water and live-bed conditions, adapted from Hamill (1999)*

2.2.2 Scour failure of bridges

Flood-induced scour is recognised as one of the most common causes of bridge failures worldwide. In the UK, there are more than 60,000 road and railway bridges crossing waterways (Clubley *et al.*, 2015) and around 95,000 bridge spans and culverts are susceptible to scour. Abutment and pier scour were identified as the most common cause of 138 rail bridge failures recorded in the UK during the period 1846–2013, which in terms of failure rate means 1 bridge every 2.44 years (van Leeuwen and Lamb, 2014). 15 fatalities have been directly imputed to bridge failures during flooding between 1846 and 1987 in the UK and Ireland (Rail Safety & Standards Board, 2005). Significant collapses due to scour in the UK include the Glanrhyd railway bridge disaster in 1987 in Wales (Cooksey, 1990), where a pier collapsed due to scour resulting in four death (Figure 2.8a).

Following record daily rainfall for the UK in November 2009, 20 road bridges in Cumbria

(a) **(b)**

Figure 2.8: ***(a)*** *Glanrhyd railway bridge disaster in 1987 in Wales (Huw Evans Agency, 1987) and* ***(b)*** *an aerial view of the destroyed Northside bridge in Workington (Cumbria) in 2009 (Byrne, 2009)*

were damaged or destroyed, including the Northside bridge (Figure 2.8b), which led to one death (Cumbria Intelligence Observatory, 2010). In December 2015, Cumbria was again battered by an extreme flood event as a consequence of Storm Desmond, which affected more than 130 bridges. The Pooley bridge was washed away, and one person died (Szoenyi *et al.*, 2015). The winter storms of 2015 resulted in serious damage/destruction to bridges across Scotland as well. This included the Lamington viaduct, which resulted in the closure of the West Coast mainline between Glasgow and London for nearly two months due to a scour failure at one of its piers (Rail Accident Investigation Branch, 2016).

In contrast, in the United States, it has been estimated that 22 bridges collapse or are closed due to scour every year on average (Briaud *et al.*, 2007). Moreover, a review of bridge collapses in the US in the 1990s carried out by Wardhana and Hadipriono (2003) shows that the 266 combined cases of flood and scour-related collapses constitutes the most dominant bridge failure cause (53% of the total cases of failures).

Imam and Chryssanthopoulos (2010) carried out a statistical analysis focused on failure/collapse cases of metallic bridges worldwide from the beginning of the 19th century up to 2010. The authors retrieved a total of 164 cases of failure of metallic bridges from

Table 2.1: *Modes of failures for metallic bridges worldwide in the last 150 years, adapted from Imam and Chryssanthopoulos (2010)*

Causes	% of failures
Scour	17.0
Buckling	16.0
Unknown	14.0
Fatigue	13.0
Vehicle impact	13.0
Other	13.0
Fracture	9.0
Overloading	5.0

Table 2.2: *Failure causes for all bridges in Imhof's database, adapted from Imhof (2004)*

Causes	% of failures
Natural hazard	40.0
Vehicle impact	25.0
Overloading	14.0
Poor knowledge	9.0
Design error	5.0
Deterioration	3.0
Human error	3.0
Vandalism	1.0

the literature. Table 2.1 shows that the most frequently encountered modes of failures for metallic bridges is scour of piers/foundations. Although the study was focused only on metallic bridges, flood-induced scour is the principal cause of failures. A similar review of worldwide steel bridge failures has shown an analogous trend in Biezma and Schanack (2007), where the authors pointed out scour as the principal cause for failure of the most collapsed steel bridges spanning rivers.

Imhof (2004) has established a large database of worldwide bridge failures as part of his PhD thesis. He found and collected from the literature 347 bridge collapses during the period between 1813 and 2004. The database includes road as well as railway and pedestrian bridges. The analysis of the database has shown that natural hazards along with ship and vehicle impacts are the common causes to collapses. Table 2.2 depicts the statistics for the most important factor involving failures for in-service bridges, omitting collapses at the construction stage in the analysis. Natural hazard is the most important failure cause if all recorded failures are considered. Table 2.3 shows instead the percentages of failure, focusing on natural hazard alone as the cause of collapse. Of all them, the most frequent was flooding, which induces scour, followed by earthquake. These outcomes demonstrate that every type of bridge could be subjected to failure because of pier or abutment scour.

Table 2.3: *Bridge failures caused by different types of natural hazards, from Imhof (2004)*

Causes	**% of failures**
Flooding	61.0
Earthquake	14.0
Fire or explosion	6.0
Storm	5.0

It is noteworthy that the threat of scour is expected to increase as a consequence of the worldwide climate changes and the upward trend in precipitation, especially in flood prone areas. The UK Climate Change Risk Assessment (CCRA) identified road and rail bridge failures due to scour as one of the main climate change risks in the transport sector (DEFRA, 2012; Thornes *et al.*, 2012). In the UK, and Scotland in particular, there is a clear upward trend in heavy rainfall and, more in general, in winter precipitation (Lowe *et al.*, 2019). It is therefore expected that climatic changes will cause an increase in frequency and magnitude of flood flows. River flow is logically the natural hazard contributing to scour risk, and CCRA, backed up by other research, has assessed increases in river flow as a consequence of climate change in Scotland. The predictions for a medium emissions scenario show flow increases of 5–10% by the 2020s, reaching up to 20–30% by the 2080s (Kay *et al.*, 2011). It is therefore likely that climate changes will lead to higher scour risk in the future, specifically for bridges designed in accordance with older standards and codes (i.e., higher scour demands than the ones they were originally designed for).

This has recently been highlighted by some studies demonstrating that climate change has the potential to re-classify the bridge to a higher scour risk level, thus leading to changes in transport agencies' long-term risk management (Ekuje, 2018). Although much uncertainty still exists about climate change modelling (Dikanski *et al.*, 2016), it has been noted that in some cases, hydraulic or bridge-related uncertainties (e.g., unknown foundation condition) might affect even more the scour assessment (Dikanski, 2018).

2.3 Scour risk assessment

Risk can be defined as the probability of suffering damage, loss and negative consequences from a hazardous event (Brooks, 2003). In the context of management phase, there is a clear relationship between the hazard in a given area to a specific element at danger (Downing *et al.*, 2001) and the probability of expected losses or damaging consequences. Nevertheless, risk cannot merely be associated to a source of hazard and to the possibility of damage since the reaction of elements to a particular hazard is always different. For this reason, the concept of vulnerability comes into play. Consequently, two distinctive factors describe the risk for a certain system, such as a civil infrastructure network or even a city: *(i)* a potentially damaging event, phenomenon or man-made activity, which is constituted by likelihood of occurrence, intensity, frequency and location and *(ii)* the vulnerability, which characterizes the degree of susceptibility of the elements exposed to that particular event and therefore manifests the relationship between the degree of exposure to the hazard and the degree of damage (Geiß and Taubenböck, 2012). Therefore, current frameworks of risk models calculate potential losses by integrating hazard parameters, hazard-exposed components and their assessed vulnerability.

First examples of such risk frameworks were developed in the field of seismic engineering (Porter, 2003), followed by frameworks for floods and costal hazards (FEMA, 2005) as well as hurricane hazards (Barbato *et al.*, 2013). The scour risk assessment is a crucial component of any bridge management system. This evaluation should combine information on the hazard, the bridge vulnerability, and the consequences of failure. However, the application of risk framework to the problem of scour so far has been limited (Pearson *et al.*, 2002; Tubaldi *et al.*, 2017, 2018).

In general, the vulnerability of a structural system such as a building or a bridge can be expressed employing fragility functions or hazard indexes (Calvi *et al.*, 2006). Fragility

curves for bridges exposed to scour hazard are less common than for earthquake hazard, and most of the works in the literature deal with the problem of combined scour and earthquake hazard (Alipour *et al.*, 2013; Roca and Whitehouse, 2012; Tanasić *et al.*, 2013). Few studies have analysed the vulnerability of bridges to scour, and in the literature, it is possible to find three different approaches:

(i) numerical approaches involving finite element analyses to model the interaction between all the components and mediums included (deck, pier, foundation, soil and water) (Hung and Yau, 2014; Klinga and Alipour, 2015; Tubaldi *et al.*, 2018);

(ii) analytical approaches considering the reduction of load-bearing capacity of bridge foundations due to scour (Federico *et al.*, 2003). In fact, in case of severe scour, the bearing capacity of the foundation-ground system can dramatically reduce, and significant amount of displacements and rotations of foundation can be induced;

(iii) empirical approaches based on a scour vulnerability index (SVI), typically expressed as the ratio between the total scour depth at the base of the pier, D_T, and the foundation depth, D_F (Barbetta *et al.*, 2015). The employment of this performance parameter has led researcher to proposed methodologies to compute a vulnerability index, allowing to classify the damage of structures after a hazardous event.

Finally, it is worth noting that the choice of the scour vulnerability approach to use depends on the type of foundations. For instance, the methodologies based on geotechnical analysis and performance parameter (i.e., the second and third approach) are suitable for shallow foundation alone, while numerical analyses can be employed with both types of foundations, e.g., deep foundation in Hung and Yau (2014) and Klinga and Alipour (2015); shallow foundation in Tubaldi *et al.* (2018).

2.3.1 Scour risk management

In the UK, Network Rail (NR) owns and operates around 19,000 underline bridges nationally: 8,700 of these structures are held within a National Scour Database. For the Scotland Route only, 1,750 structures are routinely inspected for scour, and 58 are considered to be at high risk. Transport Scotland (TS) is responsible for the Scottish trunk road network including 2,029 bridges or culverts over water. Of these, around 8% (or 168 bridges) are currently classified at risk of scour and needing detailed consideration, including possible monitoring and scour protection measures.

National transport agencies in the UK, such as TS or NR, carry out the assessment of the scour risk at highway and railway structures in accordance to the Procedure BD 97/12 (Highway Agency, 2012) and the EX2502 Procedure (HR Wallingford, 1993), respectively. These procedures provide the estimation models for scour depths before a flood-induced scour event and the scour ranking process to categorise the bridge asset. Each agency therefore defines a plan describing the actions to be taken during or after the occurrence of a flood event and furnishing a systematic and structured approach to how to respond to the threat of adverse weather. The two plans are the "Scour Management Strategy and Flood Emergency Plan" (Transport Scotland, 2018) and the "Scotland Adverse and Extreme Weather Plan" (Network Rail, 2017), used for TS's road bridges and NR's rail bridges, respectively. The purpose of these documents is to provide a framework that defines when an action needs to take place, what that action will be and who will implement it.

The two procedures (Highway Agency, 2012; HR Wallingford, 1993) provide a bridge scour risk classification through a SVI. The input parameter in TS's classification (Figure 2.9a) is the relative scour depth D_R, that is, the ratio between the total scour depth D_T and the foundation depth D_F. The total scour depth D_T is defined as the sum of constriction, D_C, and local scour depth, D_L, of which the BD97/12 provides the estimation

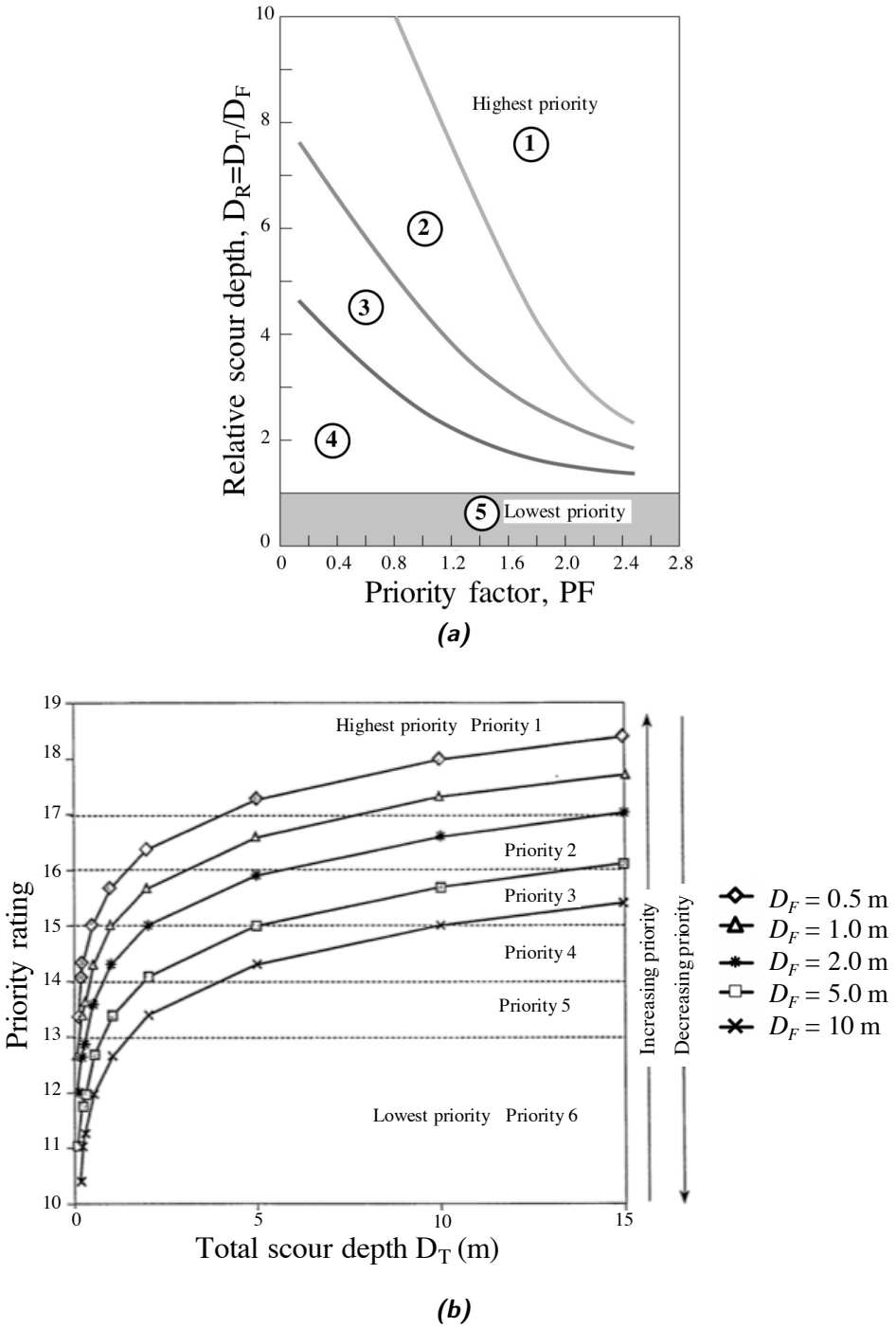

Figure 2.9: *Scour risk classification performed by* ***(a)*** *TS, and* ***(b)*** *NR*

formulas starting from an assessment flow (i.e., the flow corresponding to a return period of 200 years). Furthermore, a priority factor PF enters the risk rating to account for several

factors, such as the history of scour problems, the type of foundation and the importance of the bridge (i.e., vehicle traffic volume). For instance, if $PF = 2$, the scour risk classes are defined by the value of D_R as follows: Class 5 for $D_R \leq 1$, Class 4 for $1 < D_R \leq 1.8$, Class 3 for $1.8 < D_R \leq 2.3$, Class 2 for $2.3 < D_R \leq 3.5$, and Class 1 for $D_R > 3.5$.

The scour risk classification carried out by NR is performed according to the graph depicted in Figure 2.9b. It shows different curves according to the foundation depth D_F, consequently, even if the graph's axis related to scour depth is flipped with respect to TS chart, the two classification methods are equivalent because both transport agencies use D_R to categorise the bridge risk of scour. TS classification consists of five classes while NR method has six classes, and bridges with the highest priority fall into class 1 in both procedures. When a bridge is categorised into category 1 or 2, it is considered at high scour risk for both agencies.

The actions to be taken by TS and NR during a flood event are defined by their action plans (Transport Scotland, 2018; Network Rail, 2017). Both the schemes identify triggers that determine what actions needs to take place, with a "visual" decision scheme based on water level markers placed on the bridge upstream surface. When the water exceeds the levels shown on these markers, specific actions must be taken. For example, one action could be the closure of the bridge to traffic. Following the closure, inspection of the structure, including underwater parts and the riverbed, is undertaken as soon as it is safely practicable to do so, and the bridge may be re-opened to traffic once water levels have reduced sufficiently and only if there are no visible signs of deformation or structural distress. No direct or indirect measure of the actual scour depth enters the decision process until water levels have receded so that inspectors can safely carry out checks.

TS's structures vulnerable to scour are provided with two different marker plates, the Flood Level Marker (FLM) plate that corresponds to the 1 in 200 year flood level according to the BD97/12 (Figure 2.10a). The Red Plate is installed at the level of the bridge soffit

in those structures where the 1 in 200 year flood level is higher than this (Figure 2.10b). This marker is installed as a warning for deck uplifts (Transport Scotland, 2018).

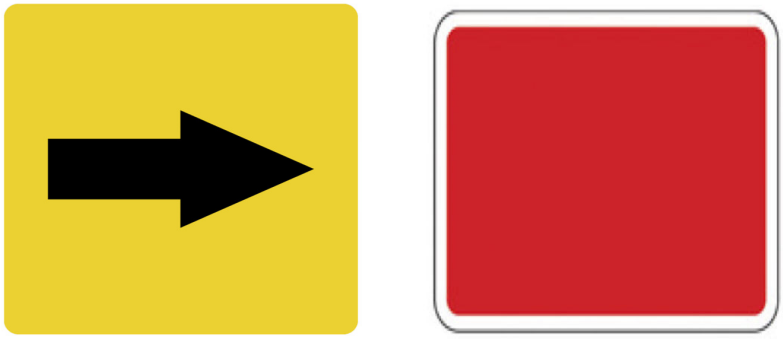

(a) ***(b)***

Figure 2.10: ***(a)*** *The Flood Level Marker plate and* ***(b)*** *the Red Plate*

NR decision process (Network Rail, 2017) is based on water level markers too. The red marker is established on a case-by-case basis based on scour assessments and engineering judgement, depending on several factors such as the type of structure, foundation, or river. However, the red marker is usually fixed in correspondence of the water level leading to a bridge classification in Priority class 2 (i.e., when the Priority rating is higher than 16). NR also define a yellow mark that triggers the appointment of a watchman to visually

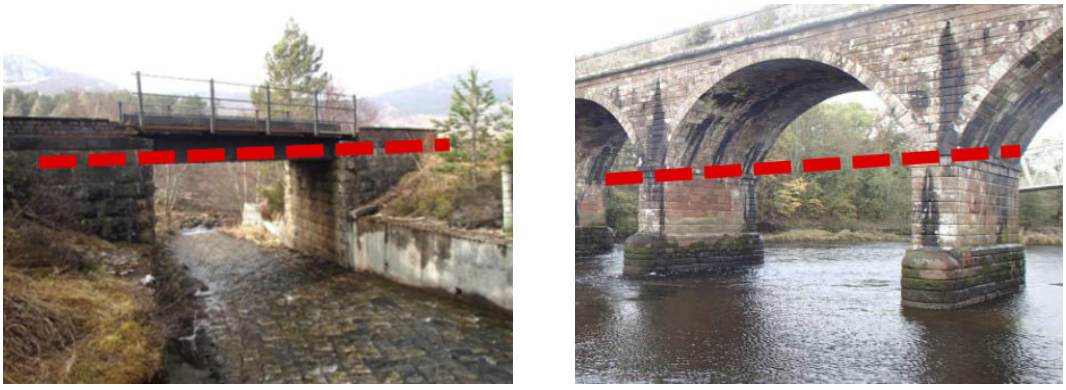

(a) ***(b)***

Figure 2.11: *Triggering water level for structure without red or yellow marks:* ***(a)*** *girder bridge and* ***(b)*** *arched bridge (Network Rail, 2017)*

observe and report the water level at the structure. If a structure experiencing flooding does not have a predetermined marker, the soffit on a girder bridge (Figure 2.11a) or springer level on an arched bridge (Figure 2.11b) are considered as the trigger for the decision plan. Table 2.4 summarises the action to undertake for the structures managed by NR.

Table 2.4: *Water level safety actions for structures managed by NR (Network Rail, 2017)*

Markers	**Water level**	**Action**
Yes	Below the yellow mark	Carry out observations
	At the yellow mark, or between the yellow and red marks	Post watchman with shelter and means of communication
	At the red mark or above it	Close structure
No	At or above soffit of girder bridge	Close structure
	At or above springer level of masonry bridge	Close structure

It can be observed that both transport agencies rely on visual inspections to identify the bridges that may be at risk of scour, to supplement the scour risk assessment provided by their procedures and to manage their bridge asset through their "visual" decision schemes. The inspections are carried out at regular intervals or after major flood events, by involving the use of scuba divers for underwater inspections of bridge foundations.

Although they are the predominant non-destructive evaluation technique used in bridge management to check the bridge condition (Moore *et al.*, 2001), visual inspections have clear disadvantages. Several elements might affect their reliability such as subject factors (e.g., visual acuity), environmental factors (e.g., lighting and background noise), or organizational factors (e.g., number of inspectors and provided equipment) (Megaw, 1979). In fact, they often involve basic instrumentation to identify structural irregularities and their outcomes are often subjective, depending on the inspector's experience (Moore *et al.*, 2001). And above all visual inspections are in general expensive and time-consuming. Furthermore, focusing on the scour evaluation, it is too dangerous to carry out underwater inspections

during peak flood events with high velocity (i.e., the maximum scour hole may have partially refilled at the end of the event).

These action plans specify that any bridge at high-risk ought to be closed when the water level attains a critical threshold at which the structure is considered to be at risk of scour. The threshold's choice is conservative by nature in order to ensure road users safety by closing the bridge before the water rises to a level at which serious scour is expected to occur. However, these plans do not consider the complexity in the temporal evolution of the scour process. For instance, in the case of live-bed regime, soil material may be partially redeposited in the scour hole at the end of the flood (Hamill, 1999). Thus, measurements of scour carried out at the end of a flood may not capture the maximum scour that occurred during the event as the scour hole might have partly filled during the recession (Melville and Coleman, 2000).

Furthermore, scour depth formula are based on lab experiments and the assumption that the designed flood acts over an infinite duration (Pizarro *et al.*, 2020), while real flood events are characterised by different hydrograph duration and magnitude. Thus, high-flow events (i.e., corresponding to a high-water level) may not necessarily result in the development of a significant scour hole, especially if they have a short duration. Moreover, bridges are exposed to sequences of events, each potentially contributing to scouring. Thus, their safety could be jeopardized by the progressive accumulation of the excavations under multiple events with low return period (i.e., water levels below the FLM) occurring in sequence, as was the case of the Lamington viaduct (Rail Accident Investigation Branch, 2016).

Flint *et al.* (2017) outlined that the risk of failure due to scour cannot be directly related to only one designed flood scenario and its corresponding return period T_R. Their review of 35 historical bridge collapses in the US (16 failure due to scour) shows highly dispersed flow return periods for scour-induced collapses, ranging between one to more than 1,000 years. Interestingly, the majority of analysed bridge collapsed under events with T_R lower than

200 years, i.e., the return period usually adopted for scour bridge design, thus highlighting the problem of accumulation of scour over a number of floods (Flint *et al.*, 2017).

Therefore, using the water level only to trigger decisions ensures that the bridge is not inundated or possibly struck with floating debris whilst open to traffic, but it does not allow the directly control of scour risk under floods with return periods different than the one considered for defining the fixed flood level marker. For these reasons, the water level can be considered only a very rough indicator of the scour risk, also considering that no measurement of scour enters the action plan until the river flow and level are considerably reduced, thus allowing the diver teams to safety check the bridge foundations.

2.4 Scour monitoring techniques

A way to overcome the limitations of visual inspections is to install Structural Health Monitoring (SHM) systems, which are methods aiming to provide, in near-real time, a reliable diagnosis of the "state" (i.e., condition) of structural components or the whole structure (Balageas *et al.*, 2006). In contrast to visual inspection, the main benefits of deploying SHM systems are their capacity to provide objective and quantitative information about the monitored structure, and to furnish continuous data about the structural state, even under an extreme event, such as an earthquake or flood (Farrar and Worden, 2007).

The last three decades have seen a growing trend towards the development of sensor technologies, data transmission and processing for the assessment of the performance of civil infrastructure under environmental conditions. These developments have resulted in more and more structures equipped with SHM systems (Brownjohn, 2007), and by far the infrastructure that has experienced the greatest growth in the application of SHM is bridges (Bakht and Jaeger, 1990; Betti *et al.*, 2016; Brownjohn *et al.*, 2016; Heywood *et al.*, 2000; Wang *et al.*, 2003). On-site campaigns aiming to continuously monitor real-time scour are

Table 2.5: *Most widespread scour monitoring techniques and their working principle for direct and indirect measurement devices.*

Direct scour measurement devices	
Scour Monitoring Techniques	**Working principle to detect scour**
[(1)]Pulse or radar devices	Measure of changes in property of the medium
[(2)]Single-use or float-out devices	Devices float out when scour depth is reached
[(3)]Fiber–Bragg grating systems	Strain measure of a cantilever rod buried into the riverbed
[(4)]Sounding or driven rod systems	Gravity-based probe moves downward as scour develops
[(5)]Sound wave devices	Measure of travel time of sound waves
[(6)]Electrical conductivity devices	Measure of electrical properties of the medium
[(7)]Dielectric probes	Measure of dielectric permittivity of the medium
Indirect scour measurement devices	
Scour Monitoring Techniques	**Working principle to detect scour**
[(8)]Tilt sensors	Monitoring of bridge/pier movement until a threshold angle
[(9)]Accelerometers	Changing in dynamic response of bridge/pier
[(10)]GPS and [(11)]satellite	Monitoring of bridge deformation from satellite images

still scarce due to accessibility issues under flood events, likelihood of damage, their cost, and their inherent imprecision. Still, a wide range of techniques has been developed in the last decades for monitoring bridge scour (Prendergast and Gavin, 2014). However, there are few examples of scour monitoring system installations, especially in bridges experiencing significant scour in the past.

Many of these monitoring techniques provide a direct measurement of the scour depth at a bridge pier, whereas other techniques provide information on the effects of scour on the bridge. Table 2.5 shows the most widespread scour monitoring techniques, based on both direct and indirect measurement of scour, and Figure 2.12 illustrates a bridge pier equipped with some of these techniques. After a brief description of each device, the section also introduces the advantages and disadvantages of the scour monitoring systems and highlights the importance of the proposed scour detection technology.

2.4.1 Direct scour measurement devices

Direct scour measurement devices provide a direct scour depth measurement at bridge piers or abutments. They are illustrated in Table 2.5 and described separately in the following sub-sections.

Pulse or Radar devices detect changes between two medium interfaces, such as sediment and water. Examples of radar and pulse devises are the ground-penetrating radar (GPR) and the time-domain reflectometry (TDR). GPR devices propagate electromagnetic pulses through water until they reach the streambed. The GPR can thus obtain the geophysical profile of the riverbed thanks to the energy that is reflected and returns to the receiver (i.e., the magnitude and the arrival time of the reflected signal are recorded by the receiver). The geophysical map is therefore used to detect the areas where the soil was eroded and provide the scour depth (Anderson *et al.*, 2007; Clubley *et al.*, 2015; Deng and Cai, 2010; Forde *et al.*, 1999). The method can provide detailed information about the surface condition of the ground but, being a portable device, it cannot be deployed as a continuous monitoring system, especially during during heavy-flood events where the risk of scour occurring is higher (Anderson *et al.*, 2007). TDR also operates by generating electromagnetic pulses and can detect the depth of scour by measuring the time taken by the reflected wave to reach back the TDR unit (where the wave is generated, and the reflected wave is monitored). A TDR monitoring system generally consists of a pulse generator and sampling oscilloscope, a connection cable, and a probe, which is the waveguide carrying the electromagnetic signal propagating through layers having different dielectric permittivity. Thus, differently from GPR devices, the probe provides localised scour estimates (Yu and Yu, 2009). The device works based on the principle that, when a fraction of the pulse returns to the receiver, the reflection is caused by a change in the permittivity (e.g., the sediment-water interface), thus providing information on the riverbed elevation (Fisher *et al.*, 2013; Hunt, 2009; Yu and

Yu, 2009). The principal advantages of TDRs are their capacity to monitor in real-time and to detect the scour depth development in time (Wang *et al.*, 2017). The key limitation of this monitoring technique is the length of the probe and the cable that could lead to excessive costs associated with installation and the cost of the TDR unit (including the step pulse generator and the sampling oscilloscope).

Single-use devices are float-out transmitters, which are buried in the riverbed at known depths in locations prone to scour. Once the riverbed is scoured from above the device, the sensor will float to the water surface. Its transmitter is activated by its change in the orientation from vertical to horizontal and starts emitting its unique signal, indicating that the scour has reached the depth where they are located (Hunt, 2009; Zarafshan *et al.*, 2012). These devices are easy to install, reliable due to their easiness of use, and they can indicate the presence of a scour hole based on their point of installation. However, the maintenance costs are high because they need to be re-buried every time scour occurs (Hunt, 2009; Prendergast and Gavin, 2014).

Sound wave devices operate on the same principles as radar but utilising acoustic waves (Prendergast and Gavin, 2014). Examples of these devices are the sonic fathometers, which are fixed to the bridge, or portable probes such as reflection seismic profilers and echo sounders. The former is installed on piers or abutments with the transmitter facing the waterline. The transmitter emits an acoustic wave that, when it encounters an object on its path, is reflected and recorded by the receiver. The distance between the transmitter and the riverbed is then established using the travel time of the wave in water, thus providing a continuous streambed profile, tracking scour and sediment deposition processes over time (Briaud *et al.*, 2011; Wang *et al.*, 2017). Unfortunately, this device can only be employed at specific depths (i.e., it has a limited depth tolerance), and the results can be affected by errors due to water salinity and temperature variations, presence of debris or water turbulence during high flows (Fisher *et al.*, 2013).

Fiber–Bragg Grating (FBG) sensors are devices that can operate for real-time and continuous scour monitoring. These sensors are installed in a cantilever rod embedded in the riverbed (Prendergast and Gavin, 2014), and they provide scour measurement according to two different approaches. The first one consists of the strain measurement along the fixed rod that bends under the hydrodynamic forces of the water flow when it is partially exposed due to scour. The higher the number of sensors, the higher the resolution of the scour measurement. Instead, for the second method, a single FBG sensor is placed on the embedded rod to determine its vibration frequency. Depth of scour can be detected using the inverse relationship between the length of the vibrating embedded rod and its fundamental frequency, given that the former increases when the rod is exposed due to scour (Lin *et al.*, 2006). FBG devices are a simple technique for scour monitoring; however, the system is highly susceptible to vibrations of the support structure caused by, e.g., traffic, thus affecting the accuracy of the measurement (Zarafshan *et al.*, 2012).

Sounding or driven rod systems are gravity-based physical probes positioned in the riverbed and moved downward due to the scour hole development. An example of these devices is the magnetic sliding collar device. The magnetic sliding collar (MSC) monitoring device consists of a rigid rod fixed to the bridge pier and embedded into the riverbed. The MSC is installed by sliding it down the rod and placed on the streambed surface. The rod is equipped with a number of magnetically activated switches spaced at known intervals of the rod; when the riverbed erodes, the collar slides down the rod and closes the magnetic switches, thus detecting the depth of scour at that particular location (Hunt, 2009; Zarafshan *et al.*, 2012). Although they are inexpensive and easy to operate, the MSC devices have several disadvantages. Scour depth detection is very localised, because it can only be measured in the vicinity of the device. The record of the global effect of scour on a bridge pier requires a number of devices. Moreover, the device uses a gravity sensor, and when the collar reaches the lowest switch on the rod, the device must be reset, which

can be time-consuming and expensive. Furthermore, the MSC devices cannot provide any information about the process of scour holes refilling (Prendergast and Gavin, 2014; Wang *et al.*, 2017).

Electrical conductivity devices use the difference of electrical conductivity in various surrounding media such as soil, water or air, to identify them (Hayes and Drummond, 1995). In particular, these systems measure the electric current between two electrodes, and they are able to detect changes in conductivity values due to increasing concentration of ions in the solution, based on the principle that current flows by ion transport. When there is a change in the material around the electrodes, the conductivity changes, therefore, these devices can detect any erosion in the riverbed by exploiting the difference of conductivity

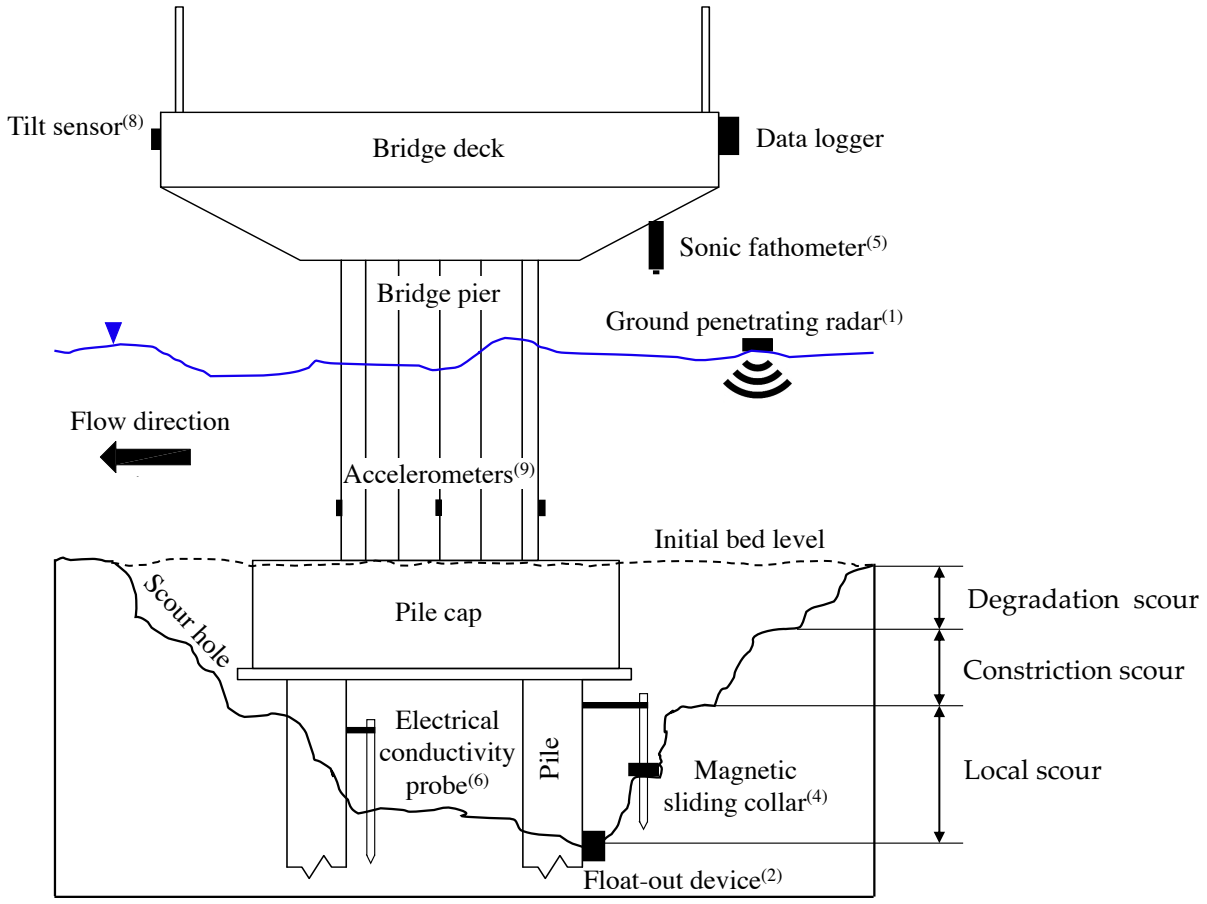

Figure 2.12: *Bridge scour monitoring devices. The techniques are numbered according to Table 2.5*

of the riverbed and the flowing water (Hayes and Drummond, 1995). In contrast to TDR monitoring systems, electrical conductivity devices are a multi-point measurement technology, i.e., several sensors can be mounted on a probe in order to provide measurements of electrical conductivity at different depths along the rod's height.

Dielectric probes, such as the ones used in the monitoring system whose deployment is described in Chapter 3, are multi-point measurement devices as well. These probes consist of a series of capacitive sensors installed on a rod, which measure the permittivity of the encompassing medium. Since the permittivity is an indicator of a material's water content, the sensors can discriminate between pure water and sediment (Michalis *et al.*, 2015). The principal advantages of dielectric probes are their capacity to continuously monitor the scour depth, including the capability to track the refill (deposition) process, but the scour detection is quite localised (i.e., the sphere of influence is about 14 cm from the external surface of the probe). However, they are one of the few devices allowing for recording during an extreme flood event. The technology is frequently deployed in agriculture to measure the soil water content, thus assisting with irrigation scheduling (Davey & Maynard Agricultural Consulting, 2001). Dielectric probes are usually preferred to the electrical permittivity devices because their measurements are much less sensitive to ion concentration.

2.4.2 Indirect scour measurement devices

Indirect scour measurement sensors provide information on the effects of scour on the bridge and its components; however, this leads to their main drawback. Since these devices only detect change in the structural response (e.g., modifications in bridge's dynamic properties or inclination of piers due to a certain level of scour), they typically recognised the presence of a scour hole when it is so critical to affect the structural stability. The most common ones are listed in the second part of Table 2.5 and described hereinafter.

Tilt sensors (or tiltmeters) measure the inclination of a bridge pier, abutment or deck

along two directions in a field of measurement of ±90°, i.e., parallel and perpendicular to the direction of traffic. The monitoring system based on these sensors are able to detect abnormal rotations induced by the settlement of the foundations (Tubaldi *et al.*, 2018) and can send an alert message when these rotations exceed a given threshold. The main drawback of this monitoring system is that it is difficult to establish the critical threshold since bridge components do not behave rigidly and their movement can be caused not only by scour but also by many other (and often concurrent) actions, such as traffic, wind or temperature (Hunt, 2009; Prendergast and Gavin, 2014; Wang *et al.*, 2017). Furthermore, it is worth noting that most tilt sensors are accelerometers estimating pitch and roll angles with respect to the direction of gravity (Maroni, 2015).

Accelerometers provide the measurement of structural behaviour in response to a modification in boundary conditions. Several authors have explored the suitability of using dynamic measurements to observe the existence of a scour hole beneath bridge foundations (Briaud *et al.*, 2011; Elsaid and Seracino, 2014). These approaches are based on the detection of changes of modal properties (e.g., natural frequency, modal shapes) that can be attributed to scour. Besides the use of accelerometers, they often involve the development of numerical models of the bridge (Foti and Sabia, 2011; Scozzese *et al.*, 2019). The problem is however very complicated because the dynamic properties are also influenced by many other actions.

Two modern *geodetic techniques*, namely the Global Positioning System (GPS) (Hofmann-Wellenhof *et al.*, 1992) and Interferometric Synthetic Aperture Radar (InSAR) (Bamler and Hartl, 1998), have revolutionized the way land and hydrographic surveys are performed, and they started to play an essential role for monitoring dams, buildings, bridges and many civil engineering infrastructures. The working principle of the two techniques is similar since both use electromagnetic waves to provide the precise distance between the satellites and ground targets. Thanks to their resolution, they both able to detect if a structure has drifted even a few centimetres. Considering bridge monitoring specifically, GPSs have been

used for dynamic displacement measurements for long-span bridges (Çelebi and Sanli, 2002) whereas the InSAR has been used to monitor bridge movements to ascertain structural behaviours and deformations (e.g., thermal expansion) (Fornaro *et al.*, 2012; Sousa *et al.*, 2014) and bridge pier settlements (Del Soldato *et al.*, 2016). Thanks to their capacity to measure displacements and deformations, the technologies might be promising applications in the context of early warning systems for scour failure (Selvakumaran *et al.*, 2018).

2.4.3 Comparison of scour monitoring methods

To be effective, bridge scour monitoring should provide continuous real-time data with a good resolution, especially during a peak flood event. Detecting the presence of redeposited soil can also deliver beneficial information about the foundation bearing capacity. Table 2.6 reviews the scour monitoring techniques based on the features that quantify their reliability and define their field of application. Among those, the table outlines the ability of the devices to provide a continuous monitoring, their usefulness in identifying and monitoring the scour depth development during high flows as well as the capability to track the refill (deposition) process. Furthermore, the scour measurement resolution of each sensor is highlighted, where "High" defines a resolution better than 10 cm whereas “Low” means “order of tens of cm”. This property is not quantifiable for the indirect scour monitoring devices because they only detect change in the structural response (e.g., pier inclination or changes in bridge’s modal properties due to a certain level of scour), and typically recognised the presence of scour when it is so critical to affect the structural stability. The last column provides an estimation of costs for the deployment of the monitoring technique (i.e., including installation costs), where "High" indicates costs greater than £25,000, "Medium" defines the range £5,000–10,000 while "Low" means costs lower than £3,000.

In summary, few technologies are able to make a scour detection with a resolution better

Table 2.6: *Comparison of the advantages and disadvantages of scour monitoring techniques*

	Continuous monitoring	Measurement during extreme events	Scour depth resolution	Detection of refill	Costs
Direct Scour Measurement Devices					
[(1)]Pulse or radar devices	✓	✓	High		Medium
[(2)]Single-use or float-out devices			Low		Medium
[(3)]Fiber-Bragg grating systems	✓	✓	Low		Low
[(4)]Sounding or driven rod systems	✓	✓	Medium		Medium
[(5)]Sound wave devices	✓		High	✓	High
[(6)]Electrical conductivity devices	✓		High	✓	Medium
[(7)]Dielectric probes	✓	✓	High	✓	Medium
Indirect Scour Measurement Devices					
[(8)]Tilt sensors	✓	✓			Low
[(9)]Accelerometers	✓	✓			Low
[(10)]GPS	✓	✓			Medium
[(11)]Satellite	✓	✓			Low

than 10 cm while at the same time are able to separate the redeposited soil and saturated soil. Among these, the dielectric probes are the only ones which allow for recording during an extreme event and thus can be used for an early warning system. Although very appealing to date, this class of sensors has only been tested in the laboratory.

2.4.4 Bridge scour monitoring installations

Despite the development of the sensors mentioned above, practical applications aiming to monitor real-time bridge scour are very limited because of accessibility issues under flood events, damage, their cost and their inherent imprecision. However, there are few examples

of scour monitoring systems installation, especially in bridges experiencing significant scour in the past and even nearly scour failure. The following paragraphs concern scour installations in the UK, a country whose bridges have been affected significantly by scour in recent years and where the use of scour monitoring sensors is increasing fast.

Cumbria, a non-metropolitan county in North West England, has been particularly battered by storms and flood events in the last decade. Following record daily rainfall for the UK in November 2009, 20 road bridges were damaged or destroyed, including the Northside bridge, which led to one death (Cumbria Intelligence Observatory, 2010). In December 2015, Cumbria was again hit by heavy flooding as a result of Storm Desmond (i.e., it broke the United Kingdom's 24-hour rainfall record, 341.4 mm of rain falling at Honister Pass in Cumbria (Marsh *et al.*, 2016)), which affected more than 130 bridges. The Pooley bridge was washed away, and one person died (Szoenyi *et al.*, 2015). In order to respond to the region of Cumbria proneness to flashing flood event and the consequences that these have on bridges, the Cumbria County Council, in partnership with Department

Figure 2.13: *Bridgecat technology for bridge inspection (PCSG, 2019)*

of Transport and Gaist Solutions, developed 'BridgeCat' technology to check flood-hit bridges for damage more quickly (Tritech, 2018). The system allows for monitoring and inspecting hard-to-reach areas of the bridge, including the underwater parts of piers without involving divers. The solution consists of vehicle featuring a hydraulic arm equipped with a mechanical scanning sonar, a high-resolution camera able to provide imagery of foundations beneath the water, and a digital altimeter measuring height off the riverbed (Figure 2.13).

The winter storms of 2015 resulted in serious damage/destruction to bridges across Scotland as well. This included the Lamington viaduct, which resulted in the closure of the West Coast mainline between Glasgow and London for nearly two months due to a scour failure at one of its piers (Rail Accident Investigation Branch, 2016). Following the incident, scour countermeasures have been undertaken to increase the resistance of the bed to scour (i.e., rock armouring has been placed below the riverbed) and monitoring systems have been installed at the viaduct.

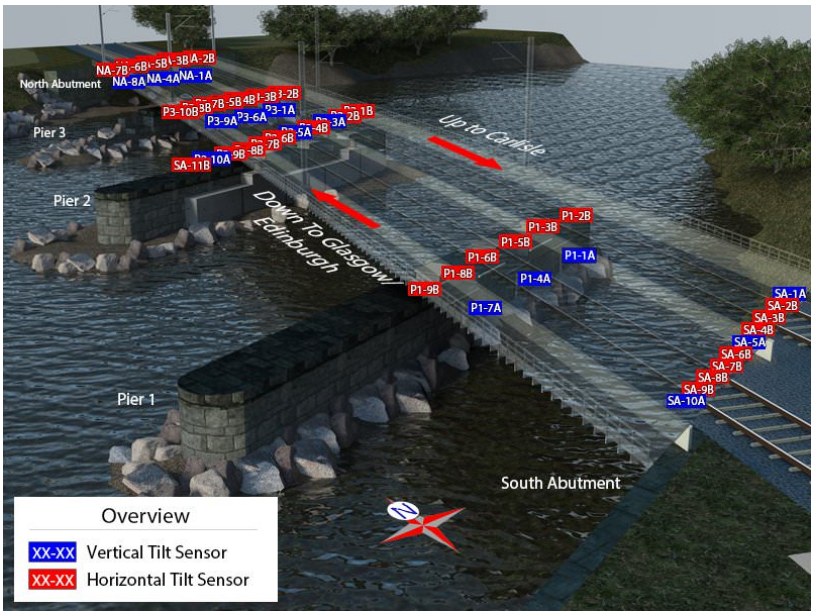

Figure 2.14: *Layout of the SHM system installed at the Lamington viaduct (courtesy of Network Rail)*

The first system measures the water level at the upstream region of the Lamington viaduct over time. The second is an SHM system consisting of a network of tilt sensors

for detecting structure movement caused by scour. The monitoring system includes 48 inclinometers (i.e., 33 of them measure the inclination along the horizontal direction and 15 along the vertical direction) installed throughout the bridge covering both abutments and the three piers. A schematic layout of the SHM system is depicted in Figure 2.14. The instrumentation is able to measure very small movements, has a battery life of several years and uses wireless technology.

An additional scour monitoring system involving indirect measurement of scour has been presented in Kariyawasam *et al.* (2019), where a vibration-based scour detection system was deployed for five months at the Baildon bridge in Bradford, UK. The monitoring system consisted of ten 3-axis accelerometers installed on the two piers and the superstructure. The BridgeCat mobile inspection system described above was used to scan the riverbed before and after the installation of the sensors and it detected the presence of scour holes. Analysing data measured on-site through the frequency domain decomposition (FDD) method, the authors showed the potential of alternative structural response parameter (i.e., spectral density and mode shape) as scour detection parameters, rather than using natural frequency alone.

2.5 Bayesian statistical inference

For a long time, bridge SHM has relied on deterministic approaches based on the development of finite element (FE) models of the monitored bridges and FE updating techniques for damage identification (Doebling *et al.*, 1998; Kessler *et al.*, 2002; Koh and Dyke, 2007; Fan and Qiao, 2010). However, models are just the analytical representation of a real structure and, obviously, they are not expected to reproduce perfectly the full behaviour of the real-life structure. In addition to the simplifications introduced in modelling the problem, neglecting the many uncertainties inherent to the monitoring and modelling

process (e.g., environmental noise, uncertainty inherent to the parameters and errors in models employed for data analysis) (Zonta, Glišić and Adriaenssens, 2014) can lead to misidentification of structural damage. Any SHM method should account for the uncertainties that arise in the definition of the problem and in the estimation model by employing a probabilistic approach to study how much they affect the damage identification or estimation of the structural condition (Vanik *et al.*, 2000). Using a probabilistic approach, the benefit of the SHM data can be quantified by the uncertainty reduction in the estimates of the structural condition.

Statistical inference can be defined as the process to draw a conclusion, that is, appraising the value of an uncertain random variable, using data or evidence (Bolstad, 2004). There are two primary approaches concerning statistical inference: the frequentist and the Bayesian approach. The former approach is based on the frequency notion of probability. Unfortunately, in many branches of risk assessment against natural hazards, the available data and observation will scarcely create a sufficiently large sample. Instead, Bayesian statistical methods are generally more robust in cases of data shortage (Bensi *et al.*, 2011).

Bayesian inference provides a general, rational, and robust approach for evaluating the structure condition (e.g., damaged or undamaged) or judge sensor and model performances, by taking into account all the sources of uncertainty relevant to the problem. Usually, information about a monitored structure might come from different sources, such as observations collected by sensors, design documentation of the structure, inspections and test reports or engineering judgement (Cappello, 2017).

The inverse problem of estimation of the parameters of a model is tackled by treating them as uncertain and using available data to update their probabilistic distribution. Hence, this approach constitutes an accumulation of knowledge (Bolstad, 2004). Equation (2.1) illustrates the Bayes' theorem, attributed to the 18th century mathematician and philosopher

Thomas Bayes, for the problem of updating of state variables distribution:

$$p(state|data) = \frac{p(data|state) \cdot p(state)}{p(data)} \tag{2.1}$$

where the probability $p(state)$ is called prior probability and represents the perspective of the state prior to the collection of data. The probability $p(data|state)$ is called likelihood of the observed data. Analogously, $p(state|data)$ is called the posterior probability of the state because it is the updated belief after new information is gained through observed data. The dominator $p(data)$ is a normalising factor called evidence, which must be calculated by integrating over the parameter space through application of the Total probability theorem.

Bayesian methods have received increased attention across a number of disciplines in recent years; in particular, they have been successfully implemented in SHM problems where information of structure's state is evolving, as in the case of a real-time monitoring system (Cappello *et al.*, 2015; Enright and Frangopol, 1999; Sohn and Law, 1997; Vanik *et al.*, 2000). Consequently, there has been an increased interest in the use of graphical models, such as Bayesian networks, to enable Bayesian model updating in complex and large-scale problems.

2.5.1 Bayesian networks

Although the technologies described in the previous section offer the possibility to assess in real-time the scour depth at bridge foundations, monitoring an entire infrastructure network is not economically sustainable, and for this reason scour sensors may be installed only at few critical bridges. The term "critical" refers to either bridges at high risk of scour (i.e., detecting scour with an SHM system would be more probable) or the most representative ones (e.g., bridges designed with the same static scheme or built over the same river might have stronger correlation). The correlation existing between the scour

depths at different locations within the same bridge, or even within the bridges of the same network, can be exploited in order to extend information on scour from the monitored to the unmonitored locations, thus allowing a more confined estimate of the scour risk. This relation between the monitored and the unmonitored locations and the updating process from the former to the latter can be described using the concept of Bayesian Network.

A Bayesian network (BN), developed by Judea Pearl in 1985, is a graphical model using a directed acyclic graph to represent a set of random variables (RVs) and their conditional dependencies (Jensen and Nielsen, 2007). Each RV, which can be discrete or continuous, is depicted by a node and the probabilistic dependency between two variables is represented by a link (Figure 2.15).

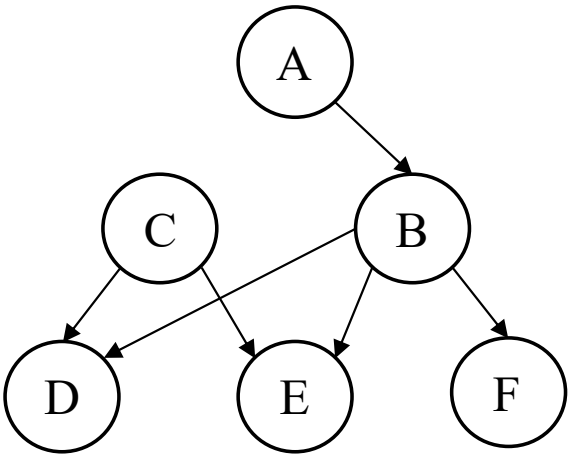

Figure 2.15: *A simple Bayesian network*

In BN terminology, it is unequivocal to refer to specific nodes as parent or child, since a directed acyclic graph represents a hierarchical arrangement. Any node extending from another one is denoted as a child, while the inverse relationship defines a parent node. Nodes without parents are known as root nodes and are described by their probability density function, which, in Bayesian terms, can be understood as their prior probability density function (pdf).

Two forms of probabilistic inference can be carried out in BNs: predictive analysis that

is based on evidence (i.e., information that the node is in a particular state) on root nodes, and diagnostic analysis, also called Bayesian learning, where observations enter into the BN through the child nodes (Ben Gal, 2007). The child node pdfs can be estimated from the roots' pdfs by performing predictive analysis, whereas Bayesian learning allows updating root node pdfs when new information enters into the BN through a child node.

When evidence enter into the BN, the piece of information is spread inside the network to update variable's probabilities through one of the two forms of inference mentioned above. In particular, the second approach, the Bayesian learning, is attractive when the analysed system is based on constantly evolving information, as in the case of a real-time monitoring system. Furthermore, BNs are well suited for representing knowledge under uncertainty. Uncertainties from variables, measurements and model itself can be implemented into the BN such as components of the model or even as an updatable node. For these reasons, BN framework can be merge with monitoring systems in order to continuously update the state of bridges (i.e., including their risk of failure following an extreme event) in an infrastructure network.

In recent years, there has been an increasing amount of literature on the use of BNs. Although BN were first implemented in the context of the artificial intelligence community (Korb and Nicholson, 2010), they have become quickly popular in every field of study thanks to their excellent performance and suitability for dealing with a broad range of problems that involve probabilistic reasoning and uncertainty quantification.

BNs started to be used for Bayesian modelling in engineering risk analysis due to their ability to manage many dependent RVs. One of the earliest works dealing with risk assessment through the use of BNs was carried out by Friis-Hansen (2000). After that, several works on the employment of BN for risk assessment have been proposed starting from the paper by Faber *et al.* (2002) where BNs were utilised for assessing the risk related to the decommissioning of offshore facilities. Following examples have been focused on the

natural hazard risk assessment (Straub, 2005; Straub and Der Kiureghian, 2010*a*,*b*; Vogel *et al.*, 2014), damage detection (Addin *et al.*, 2007; Naidu *et al.*, 2006; Nguyen *et al.*, 2004), optimal sensor placement (Malings and Pozzi, 2015) and structural deterioration due to metal corrosion and fatigue using an extended version of BN that includes time-variant parameters (i.e., Dynamic BNs) (Straub, 2009; Luque and Straub, 2015).

The applications in seismic risk are many (see for instance Bayraktarli *et al.*, 2005) and they address different topics such as the reliability analysis of critical infrastructures in the aftermath of a hazardous event (Pozzi and Der Kiureghian, 2013; Tien and Der Kiureghian, 2017) or bridge asset management (Bensi *et al.*, 2011; Yue *et al.*, 2012). BNs have been also used to evaluate multi-hazard risk (Gehl and D'Ayala, 2016; Liu *et al.*, 2015; Marzocchi *et al.*, 2012).

2.6 SHM-based decision making

Despite differences of opinion, there appears to be some agreement in the research community that SHM should help to identify the optimal decisions concerning structural management, such as the assessment of a structural state. There is a large amount of published studies describing the role of SHM in decision-making processes, especially in the field of civil engineering. Some studies have been focused on quantifying the benefit of SHM on decision-making (Bolognani *et al.*, 2018; Mussi, 2004; Pozzi and Der Kiureghian, 2011; Thöns and Faber, 2013; Zonta, Glišić and Adriaenssens, 2014) or the optimal sensor placement (Flynn and Todd, 2010*a*,*b*; Flynn *et al.*, 2011).

Although these studies have recognised the benefit of SHM campaigns, asset owners and managers are still doubtful about the benefit of the deployment of SHM systems because they have a cost that does not enhance the performance of the monitored structure. Therefore, they may prefer to undertake retrofitting work instead of investing on these

systems, especially if they have a limited budget. Moreover, although the interest in the use of SHM for the structural state prediction is growing thanks to the progress in technologies, it is still unclear how an asset manager is supposed to make SHM-based decisions (Cappello *et al.*, 2016). The reasons are mainly two: first, the managers tend to act based on their experience because, as said above, they question SHM benefits; second, and it might explain why they are sceptical, SHM outputs are affected by several and severe uncertainties, which are often hard to quantify Verzobio *et al.* (2018).

A common solution adopted by infrastructure operators consists of sending inspectors to the structure to collect more information about its true state or to reduce the uncertainties of information provided by SHM system. However, the more the uncertainty about the structure or river condition (e.g., bridge geometry or hydraulic parameters of rivers), the higher the number of inspections over time, the greater the cost for asset operators. Accordingly, operators spend a big part of their budget every year to manage and inspect their asset (Dalton, 2008), and this is no longer economically feasible for several of them.

Along with the deployment of SHM systems, it is therefore necessary to establish new strategies to make optimal decisions for bridge management based on the sole monitoring data, with inspectors sent to the structure only when it is strictly necessary. Thus, SHM-based decision-making approaches could help operators in optimising the management of structures and correctly allocating the resources needed to keep them in a safe condition.

A typical workflow to decision-making based on SHM is: *(i)* sensors and data transmission units are deployed on the structure; *(ii)* the SHM data are analysed; *(iii)* an algorithm recognises potential damage, ascertains its position, and supplies information on performance and structural health; *(iv)* the manager in charge makes the decision to whether mend the structural damage or not. SHM consists of the first three steps, while step four refers to decision-making (Cappello *et al.*, 2016). Indeed, SHM should not be merely viewed as the use of sensors and a monitoring system; it includes the data acquisition through sensor

devices and also encompasses the analyses performed to assist the engineer managing the monitored structure (Cappello, 2017; Lynch, 2007).

The approach presented above can easily lead to the error of considering the decision-making process as an output of structural health monitoring, but SHM and decision-making are two distinct processes regardless of their connections. Monitoring concerns obtaining data and information, and not making decisions. In contrast, decision-making deals with ascertaining and selecting the optimal action to undertake based on the structural state assessed in the SHM process (Cappello *et al.*, 2016).

The three steps of the SHM process are usually performed using the Bayesian logic, which provides a rational, and robust approach for estimating the structure condition from monitoring data. As mentioned in Section 2.5, the Bayesian approach allows considering different source of information about a monitored structure, and every time a new observation becomes available, the structure state is updated regardless the input order, thus accumulating the knowledge about the monitoring structure (Bolstad, 2004).

Decision-making process occurs downstream of the acquisition of monitoring data; however, only part of the SHM data is normally used in the decision process. SHM-based decision support systems are frameworks aiming to provide suggestions for the structure management by taking the SHM data as an input and converting them into information for the manager (Wenzel, 2008). The SHM-based decision support system is usually based on a decision model considering the structural models and the probability of damage/failure provided by the Bayesian inference as well as the costs and, above on that, the consequences that might result from the structure downtime or even its collapse. In fact, the expression "optimal action (or decision)" generally indicates the financially optimal choices from operators' perspective (Cappello, 2017), where the term 'financially' includes all the costs incurred by operators, from the management to direct and indirect costs involved in using the structure.

Expected utility theory (von Neumann and Morgenstern, 1953) and prospect theory (Kahneman and Tversky, 1977) are decision theories widely utilised in economy and finance that allow taking optimal decisions considering the condition of the monitored structure and the cost incurred by the realisation of each possible state. Cappello *et al.* (2016) and Bolognani *et al.* (2017) show two applications to decision problem based on SHM observation of these two decision theories, respectively.

Expected utility theory can be used to quantify the benefit (or the value) of an SHM system using the concept of the Value of Information (VoI) (DeGroot, 1984). In this context, the VoI is expressed as the difference between the expected utilities of operating the structure with or without the SHM system (Bolognani *et al.*, 2018; Pozzi and Der Kiureghian, 2011; Zonta, Glišić and Adriaenssens, 2014). It is worth noting that both utilities are computed before receiving any information from the monitoring system because the VoI is the metric that can drive the manager's decision on whether or not to monitor a structure. Therefore, the VoI provides an economic evaluation of the impact of monitoring on bridge management before its adoption, thus quantifying how useful these systems are at assisting decision-making. The application of VoI framework for assessing the benefit of scour SHM system so far has been limited (Giordano *et al.*, 2020).

2.7 Conclusions

This Chapter presented a literature review of the assessment and how it is currently managed the bridge scour risk for road and railway bridges. The key findings from the review are the following:

- Scour, the erosion of sediment around bridge foundations due to flowing water, is recognised as one of the most common causes of bridge failures worldwide in the last century. The problem of scour is also exacerbated by climate changes.

- The scour risk assessment is a crucial component of any bridge management system; however only few studies have analysed the vulnerability of bridges to scour.

- Transport agencies' scour risk management relies on:

  (i) visual inspections at regular intervals to identify the bridges at risk of scour;

  (ii) bridge scour risk classifications through a scour vulnerability index;

  (iii) "visual" decision schemes based on water level markers placed on the bridge upstream surface.

  Visual inspections are in general expensive and provide unreliable estimates of scour while triggering bridge closures according to flood level markers does not allow the directly control of scour risk under floods. Furthermore, the many uncertainties affecting the problem might lead to an overestimation of scour depths that might cause a misclassification of the bridge scour risk and bring to unnecessary bridge closure. In essence, visual inspections and water levels are very rough indicators of bridge scour risk.

- A wide range of techniques has been developed in the last decades for monitoring bridge scour; however, on-site campaigns aiming to continuously monitor real-time scour are still scarce due to accessibility issues under flood events, their cost, and their inherent imprecision.

- To be effective, bridge scour monitoring should provide continuous real-time data with a resolution better than 10 cm (especially during a peak flood event) and track the presence of redeposited soil. Among the range of scour detection techniques, the dielectric probes are the only ones presenting these three features altogether.

- Although sensor technology offers in principle the possibility to install a scour device at each pier of a bridge network, monitoring an entire infrastructure system is not

economically feasible. A way to overcome this limitation is to install scour monitoring systems at critical or representative bridge locations, and then extend the piece of information gained to the other assets exploiting the correlations present in the system. The relation between the monitored and the unmonitored locations and the updating process from the former to the latter can be described using the concept of Bayesian network, i.e., a statistical tool becoming more and more popular in the last decades. The use of BNs is indeed attractive to continuously update the state of bridges (i.e., including their risk of failure following an extreme event) in an infrastructure network when new information comes from an SHM system.

- SHM-based decision support systems are frameworks aiming to provide suggestions for the asset management by taking the SHM data as an input and converting them into information for the manager. Thus, SHM-based decision-making approaches could help operators in optimising the decision about managing their asset and correctly allocating the resources needed to keep them in a safe condition. Although there is a large amount of published studies describing the role of SHM in decision-making processes, asset owners and managers are still doubtful about the benefit of the deployment of these systems.

In conclusion, the analysis of the current literature has highlighted that new systems for scour risk management require to be introduced. Thus, there is a need of a system that, during and after an extreme weather event, is capable not only of monitoring the evolution of scour at bridge foundations, but also of providing transport operators with clear and direct information about scour and bridge state to support risk mitigation strategies and decision-making processes under flood events.

CHAPTER 3

Electromagnetic sensors for underwater scour monitoring

Abstract

Scour jeopardises the safety of many civil engineering structures with foundations in riverbeds and it is the leading cause for the collapse of bridges worldwide. Current approaches for bridge scour risk management rely mainly on visual inspections, which provide unreliable estimates of scour and of its effects, also considering the difficulties in visually monitoring the riverbed erosion around submerged foundations during peak flood events with high velocity. Thus, there is a need to introduce systems capable of monitoring the evolution of scour at bridge foundations during and after extreme weather events. This Chapter illustrates the development and deployment of a scour monitoring system consisting of smart probes equipped with electromagnetic sensors. This is the first application of this type of sensing probes to a real case-study for continuous scour monitoring. Designed to observe changes in the permittivity of the medium around bridge foundations, the sensors allow the detection of scour depths and the assessment of whether the scour hole has been refilled. The monitoring system was installed on the A76 200 Bridge in New Cumnock (south–west Scotland) and has provided a continuous recording of the scour for nearly two years. The scour data registered after a peak flood event (supported by the actual

measurement of scour during a bridge inspection) show the potential of the technology in providing continuous scour measures, even during extreme flood events, thus avoiding the deployment of divers for underwater examination.

3.1 Bridge scour

Scour is a soil-structure interaction phenomenon that is defined as the erosion of riverbed material surrounding foundations of structures immersed in water (Hamill, 1999). This phenomenon poses a significant risk to bridges crossing rivers and channels, reducing the load-bearing capacity of foundations and causing the bridge to fail and collapse, often without any warning (Michalis *et al.*, 2015). Thus, monitoring and detecting scour at early stages of development is of paramount importance to ensure the operability and safety of bridges.

Scour initiates when the shear stresses at the water-bed interface is higher than the critical ones corresponding to the initiation of motion of the soil particles. The type of bed material also plays an essential role in the scour process as the critical shear stress is peculiar to it. For example, the critical shear stress is lower for sand than for limestone (Sheppard and Renna, 2005; Pizarro *et al.*, 2020).

Three types of scour generally occur: degradation scour, constriction (or contraction) scour and local scour. When scouring occurs in a bridge, the total scour is the resultant of these three types of scour working simultaneously (Kirby *et al.*, 2015; Pizarro *et al.*, 2020):

(i) *Degradation scour*: the erosion is due to the change of riverbed elevation that causes a lateral instability in the water flow. In a river, this is due to river flow changes, whereas, in the sea, it is because of the action of tidal currents (Richardson and Davis, 2001). Degradation scour includes aggradation of material at bends in the river, which can induce channel migration.

(ii) *Constriction (or contraction) scour*: this type of scour occurs when there is sudden increase in flow velocity, which causes an increase in shear stress, as a result of a reduction of channel cross-sectional area at the bridge location (Briaud *et al.*, 1999). The erosion of sediments starts when the shear stresses exceed the threshold value of the bed material (i.e., the value of shear stress below which scour does not occur) (Kirby *et al.*, 2015).

(iii) *Local scour*: it is due to the flow, acting at the upstream end of bridge piers, that results in the creation of vortices, which lead to further development of scour holes (Hamill, 1999).

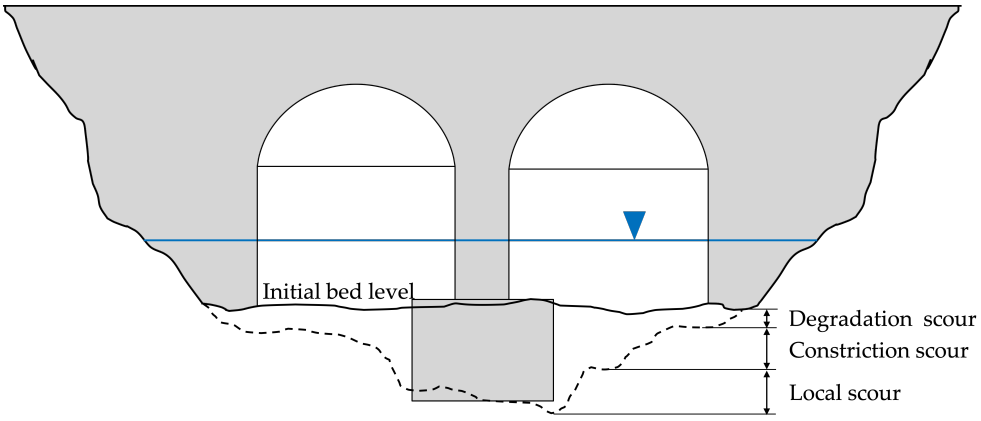

Figure 3.1: *Schematic illustration of total scour*

Figure 3.1 shows the different types of scour that can occur at a bridge and its piers, considering degradation, constriction, and local scour. The three scour types are also summarized in Table 3.1.

Table 3.1: *Types of scour*

Types of scour	**Cause of occurrence**
Degradation Scour	Change in riverbed elevation
Constriction Scour	Higher velocity and shear stress due to channel narrowing
Local Scour	Downward flow at upstream end of bridge pier

Flood-induced scour is recognised as one of the most common causes of bridge failures worldwide. For example, 15 fatalities have been directly imputed to bridge failures during flooding and scour between 1846 and 1987 in the UK and Ireland (Rail Safety & Standards Board, 2005). At least 138 railway bridge failures occurred due to scour between 1846 and 2013 in the UK, which in terms of failure rate means 1 bridge every 2.44 years (van Leeuwen and Lamb, 2014). In contrast, in the United States, it has been estimated that an average annual rate of 22 bridges collapse or are closed due to scour (Briaud *et al.*, 2007). Moreover, a review of bridge collapses in the US in the 1990s carried out by Wardhana and Hadipriono (2003) shows that the combined figure of 266 flood/scour-related cases constitutes the most dominant bridge failure cause (53% of the total cases of failures).

3.1.1 Current scour risk assessment

Current practice for assessing the scour risk of bridges relies on visual inspections at regular intervals, which can involve the use of scuba divers carrying underwater inspections of bridge foundations. During an extreme weather event, transport operators make decision to close the bridge to traffic by visually comparing the water level with a fixed flood level marker (Network Rail, 2017; Transport Scotland, 2018). For example, for the bridges managed by Transport Scotland, the marker indicates the design 200-year flood level calculated based on the scour risk assessment procedure of BD97/12 (Highway Agency, 2012). No direct or indirect measure of the actual scour depth enters the decision process until water levels have receded so that inspectors can safely carry out checks.

Visual inspections are in general expensive, time-consuming, and the outcomes are often subjective, depending on the inspector's experience. In fact, they often involve basic instrumentation to identify any structural irregularities such as deterioration of structures, cracks and direct measurement of the depth of scour. Underwater inspections carried out by divers are even more expensive and have limitation in terms of the quality of data

collected, the efficiency of the process and the risk to the individual inspector. It is indeed too dangerous to carry out these inspections during high-flow events flood peak, but the probability to experience the maximum scour hole is higher (i.e., it might have been refilled when the flooding event is over). Furthermore, using the water level only to trigger decisions ensures that the bridge is not inundated or possibly struck with floating debris whilst open to traffic, but it does not allow the direct control of scour risk under floods with return periods different than the one considered for defining the fixed flood level marker.

Overall, scour is a highly dynamic process. Under steady conditions, such as those created in laboratory experiments, the scour depth increases until a maximum equilibrium value is attained. At the end of the flood, the scour hole may be partially refilled in the case of live-bed conditions (Hamill, 1999). Thus, measurements of scour carried out at the end of a flood may not capture the maximum scour that occurred during the event as the scour hole might have partly filled during the recession (Melville and Coleman, 2000). In reality, flood events at a bridge site are characterized by different hydrograph duration, magnitude and shape. Moreover, a sequence of events occurs during the lifetime of the bridge, thus leading to accumulation phenomena. For these reasons, a very intense flood with a high-flow rate (thus corresponding to a high-water level) does not immediately mean the development of a significant scour hole at the pier if the duration of the flood event is short. At the same time, the safety of a bridge could be jeopardized by the progressive accumulation of the excavations under multiple events with low return period (i.e., corresponding to water levels below the marker) occurring in sequence, as was the case of the Lamington viaduct in south–west Scotland (Rail Accident Investigation Branch, 2016).

In summary, visual inspections and the water level are very rough indicators of the scour risk. Thus, there is the need to introduce Structural Health Monitoring (SHM) systems that, during and after an extreme weather event, are capable of detecting scour depth at bridge foundations, providing quantitative information about the structure condition

to be used in the process of risk evaluation and supplementing the flood level threshold after which a bridge is closed. Many different types of sensors can significantly help to achieve this goal, by allowing more precise measurements of the extent of scour at bridge foundations and the relevant effects on the performance of bridge components.

This Chapter describes the concept, installation and functioning of a pilot scour monitoring system based on the use of smart electromagnetic probes and installed on the A76 200 bridge over the River Nith in New Cumnock, UK. Section 3.2 outlines a review of existing scour monitoring techniques by showing both direct and indirect scour measurement devices. The in-depth description of the devices is presented in Chapter 2, precisely in Section 2.4. Section 3.3 illustrates the sensors and components used to develop the pilot scour monitoring system, by providing information on their working principle and on how the sensors readings are converted into permittivity measurements and into scour depth estimates. Section 3.4 describes the case study, the A76 200 Bridge over the river Nith, and the pilot sensing system installed there, consisting of two probes. Section 3.5 presents the results obtained by post-processing the data recorded from the probes since their deployment. Section 3.6 discusses the study outcomes and the comparison with results obtained from bridge visual inspections. The Chapter ends with a conclusion and future research section.

3.2 Scour Monitoring Techniques

A wide range of techniques has been developed in the last few decades for monitoring bridge scour (see Prendergast and Gavin (2014) for a state-of-the-art review). Many of these techniques provide a direct measurement of the scour depth at a bridge pier, whereas other techniques provide information on the effects of scour on the bridge. Table 2.5 has showed the most widespread scour monitoring techniques, based on both direct and indirect measurement of scour, and Figure 3.2 illustrates a bridge pier equipped with some of these

techniques.

Direct scour measurement devices provide a direct scour depth measurement at bridge piers or abutments while indirect scour measurement sensors provide information on the effects of scour on the bridge and its components. Both monitoring techniques and the corresponding developed devices are described in details in Section 2.4).

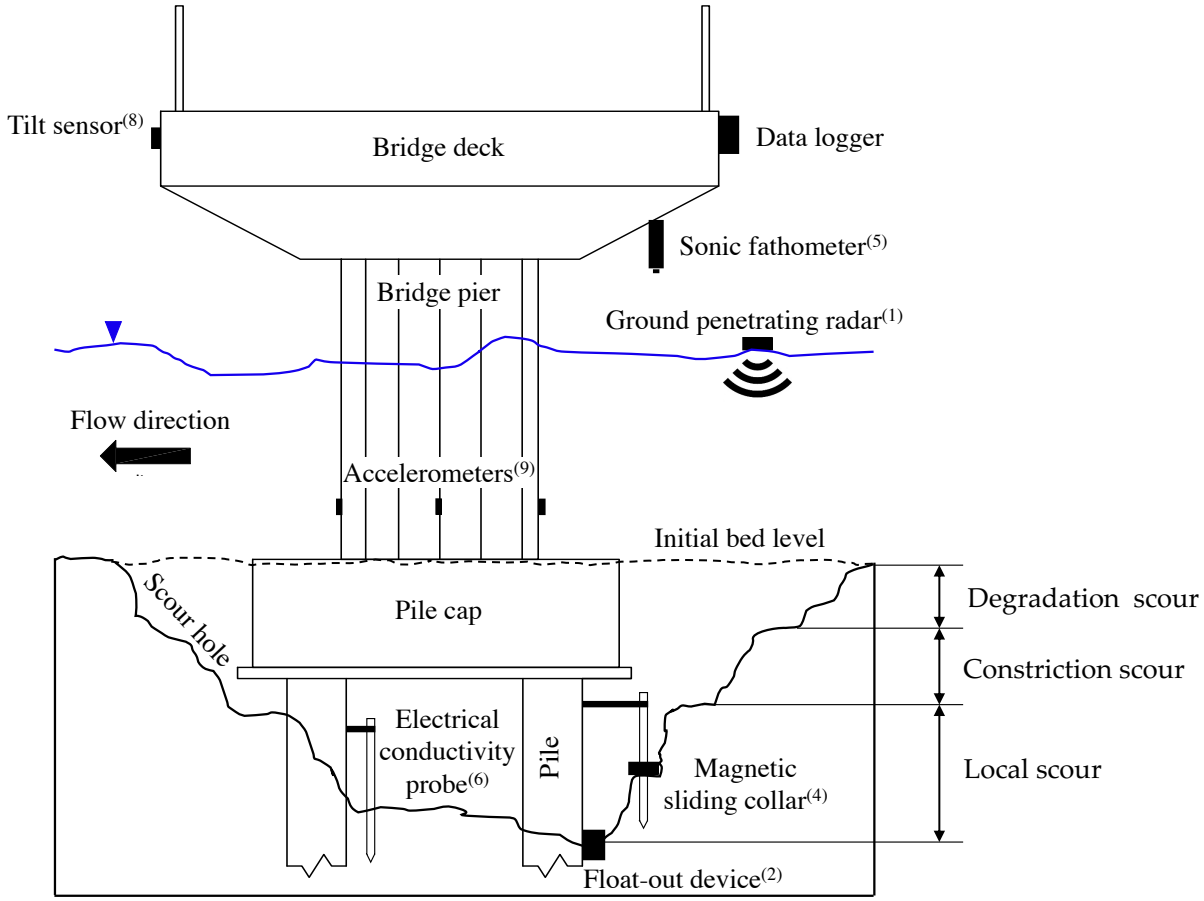

Figure 3.2: *Bridge scour monitoring devices. The techniques are numbered according to Table 2.5*

3.3 Pilot scour monitoring system

The sensing system described in this Chapter is based on the use of a dielectric probe equipped with capacitive sensors, which represent one of the techniques available

for measuring electromagnetic properties of the soil (Schwank *et al.*, 2006). The term "capacitive" refers to the working principle of the electric device, which can be exemplified by considering an LC circuit (L= Inductor, C= Capacitor) (Schwank *et al.*, 2006). The resonant frequency of the LC circuit depends on the dielectric permittivity of the medium interposed between the two capacitor conductors.

Each sensor is formed by an electrode pair (i.e., the two capacitor ring conductors) which transmits an electromagnetic fringing field that penetrates the external surrounding medium (see Figure 3.3). Since the two electrode rings have diameter greater than their spacing, the capacitance is not only affected by the medium directly between the conductors (as is the case of the infinite conductors) but also on the medium surrounding the electrodes laterally. Since the configuration and geometry of the probe remain constant, any change in capacitance only depends on the dielectric property of the surrounding soil. The capacitor made of the two ring conductors is inserted into an LC-type circuit. The capacitance

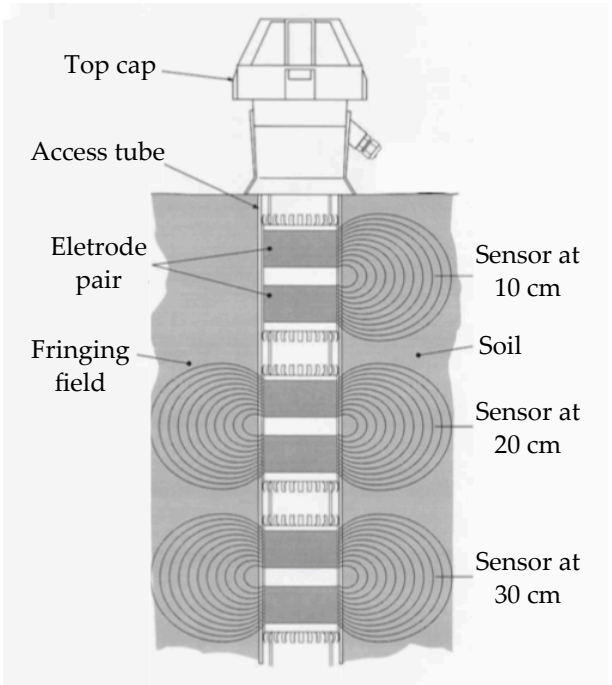

Figure 3.3: *Schematic of the dielectric probe equipped with electromagnetic sensors.*

and, hence, the dielectric permittivity of the surrounding soil, is measured by the resonant frequency of the circuit via an oscillator inserted into the LC circuit as discussed by Tarantino *et al.* (2008). The term "electromagnetic sensor" is used hereinafter to refer to these smart probes, since they are used in this context to measure the dielectric permittivity (i.e., a soil electromagnetic property) to detect a scour hole.

The dielectric permittivity can therefore be measured if a calibration function is established to convert the resonant frequency read by the sensors into a permittivity value, which differs between the soil in the riverbed and the water (Michalis *et al.*, 2015). The system is calibrated to detect erosion and deposition of riverbed sediment in different soil types and under temperature that would commonly occur in a real case-study scenario (Michalis *et al.*, 2015). It also allows distinction between in-situ and re-deposited bed material, providing useful information about the load-bearing capacity of bridge foundations. It is noteworthy that although smart sensing bars with electromagnetic devices have already been proposed and studied (Michalis *et al.*, 2015), to the authors' knowledge, this is the first time they have been applied to a real case study for the continuous monitoring of scour at a bridge location.

The electromagnetic device installed in the A76 200 bridge is the EnviroSCAN probe (Figure 3.4a), developed by Sentek sensor technologies (Sentek technologies, 2017) and provided by Soil Moisture Sense in the UK. The probe is different from the one used by Michalis *et al.* (2015) since Soil Moisture Sense was the only supplier providing a be-spoke version (i.e., customisable length) of the sensing bar. However, these two probes share similar working principle. Every component of sensing bar is described in the following sections, including the experiments performed in the laboratory to calibrate each electromagnetic sensor and to test the smart probe's functioning in a real-case scour scenario. The laboratory tests have been carried out an improved version of the protocols used in Michalis *et al.* (2015) to calibrate and test a similar capacitance probe.

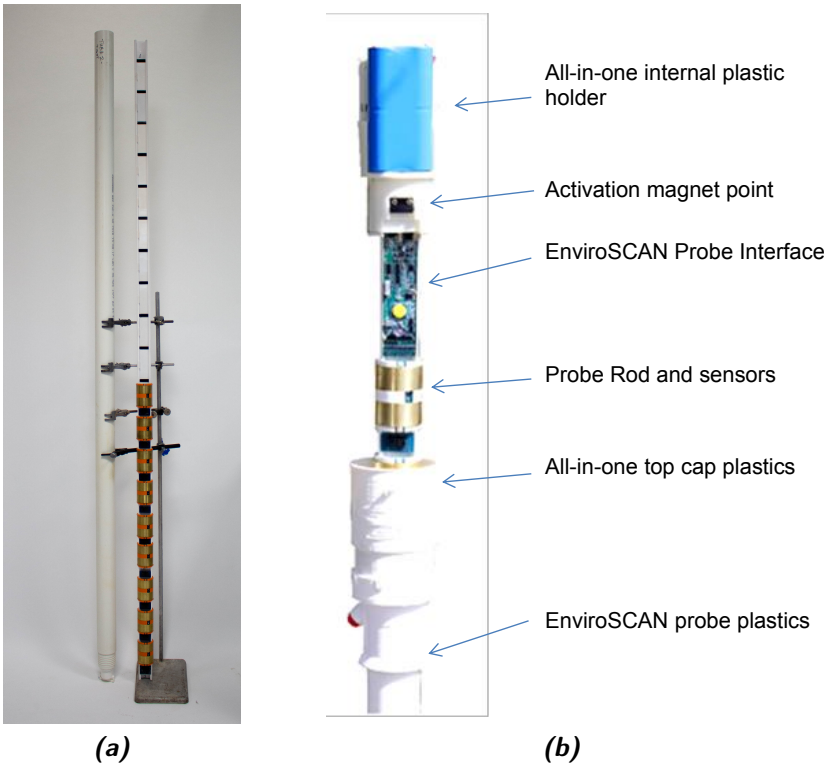

Figure 3.4: ***(a)*** *The EnviroSCAN probe; and* ***(b)*** *probe's components (Sentek technologies, 2015)*

The specifications of the off-the-shelf version of the probe are depicted in Table 3.2. The probe consists of a plastic rod equipped with multiple sensors, installed every 10 cm along the rod height. Therefore, the monitoring system has a resolution of 10 cm. The standard version is 50-cm long and is equipped with maximum 5 sensors, but the seller also offers a bespoke versions of the probe with a customisable length of the plastic rod. However, the EnviroSCAN probe is supplied with a maximum of 16 sensors, regardless the length of the rod, because its mainboard has 16 channels. Therefore, being the sensors removable, their arrangement is customisable since the plastic rod has several slots (at 10 cm to each other) where to insert a sensor. This feature makes the probe very versatile because different configurations can be achieved, such as a probe with 1.60-meter-long monitoring part with 10-cm resolution (i.e., 16 sensors installed without empty slots among them) or with a 3.20-meter-long monitoring part with 20-cm resolution (i.e., an empty slot

Table 3.2: *Specifications of the off-the-shelf EnviroSCAN probe (Sentek technologies, 2015)*

Feature	**EnviroSCAN Probe**
Maximum cable length to logger or third party device	60 m (200 ft)
Maximum sensors per standard probe	16
Sensor Measuring Principle	High frequency capacitance
Output Options	SDI-12
Protocol options	SDI-12
Interface Measuring Principle	16 Bit pulse count
Output Resolution	16 Bit
Output Method	Serial data
Current Consumption	250 μA @ Sleep 66 mA @ Standby 100 mA @ Sampling
Reading range	Water Content/Salinity 0 to $\approx$ 65%/0 to 17 dSm^{-1}
Temperature effects	$\pm$3% 5°C to 35°C
Operating temperature range	$-$20°C to +75°C
Time to read one sensor	1.1 seconds
Sphere of influence	99% of the reading is taken within a 14 cm radius from the outside of the access tube
Sensor diameter	50.5 mm
Access tube diameter	56.5 mm
Probe length	50 cm (20 inches)

after each sensor). Therefore, the more extended is the monitoring part, the lower is the resolution of the system. Figure 3.4b shows the components of the scour probe, which includes a battery, an electronic board (which is the EnviroSCAN Probe Interface), a GPRS modem, and the electromagnetic sensors. The probe has an extended access tube made of plastic which protects the components of the probe (as shown in Figure 3.4a) from water damage and debris when it is installed in wet environments for monitoring purposes.

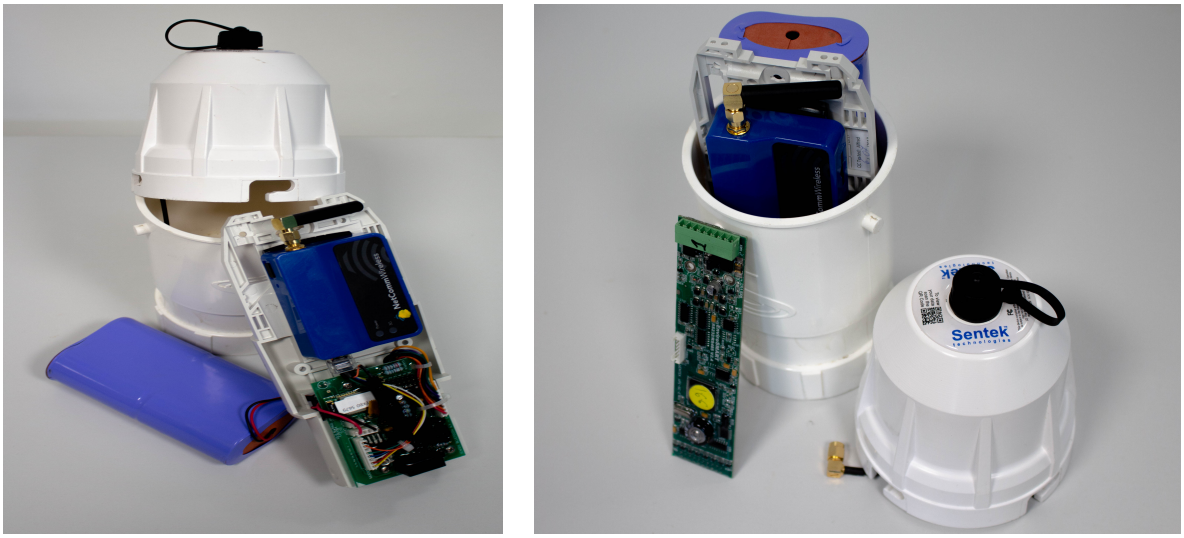

(a) *(b)*

Figure 3.5: ***(a)*** *The modem and battery; and* ***(b)*** *the plastic holder and the electronic interface board.*

Figure 3.5a shows the GPRS 3G modem along with an electronic board, the battery and the internal antenna, while Figure 3.5b shows the plastic holder protecting the battery and the EnviroSCAN Probe Interface electronic board. The components shown in Figure 3.5a compose the Data Transmission Unit (DTU), called Sentek PLUS All-in-One. The sensor data can be stored into the probe, but they can also be sent to an ftp server thanks to the 3G modem the DTU is equipped with. The probe uploads a .esp file at every reading, and then the data are converted in .csv/.xslx format through a dedicated software provided by the Soil Moisture Sense.

The DTU is also equipped with a Bluetooth module that is used for wireless testing and configuration, using a laptop with the Probe Configuration Utility (i.e., the Sentek probe configuration app). The data logger is also equipped with a high-capacity Lithium battery (14V 14 Ah), which provides energy supply to the probe and to the DTU for every data uploading. It generally lasts 12 months when using Sentek's standard configuration (five sensors sampling every 30 minutes and upload interval of three hours) (Sentek technologies,

Figure 3.6: *The electromagnetic sensors*

2015). Figure 3.6 shows the electromagnetic sensors that measure the frequency of the surrounding medium.

The EnviroSCAN probes forming the scour monitoring system deployed at the A76 200 bridge have been developed and tailored to the case-study. The bespoke version consists of a 4-meter-long plastic rod equipped with 16 equally spaced sensors installed at the bottom part of the rod. This constitutes the sensing segment that will be insert into the riverbed to detect the scour hole. Instead, the part emerging from the riverbed will be well secured at the bridge to prevent any movement and to ensure stability during a flood event. A detailed description of the pilot scour monitoring system is provided in Subsection 3.4.

3.3.1 Permittivity of Soil

The permittivity of a material (ε), defined as its capability to polarize when exposed to an electrical field, is a dimensionless variable (Whalley *et al.*, 1992). Average values of the (static) dielectric permittivity of water, solids, and air are respectively $\varepsilon_{\mathrm{w}} \approx 78$, $\varepsilon_{\mathrm{s}} \approx 3$–$5$, and $\varepsilon_{\mathrm{a}} \approx 1$. The bulk permittivity of soil ε_{s} depends on the dielectric permittivity of its constituents (free water, bonded water, solids, and air) and their volume fraction (represented

by the dry density, volumetric water content, and surface area). Since the dielectric permittivity of free water depends on temperature, ion concentration, and electromagnetic frequency, so does the bulk dielectric permittivity of the soil. However, the parameter that has the most substantial influence on ε_{s} is the volumetric water content θ, as can be seen comparing the dielectric permittivity values of water and dry solid particles mentioned above. Furthermore, one of the most efficient method for determining the volumetric soil water content θ is based on field measurement of dielectric properties of wet soils, such as the dielectric permittivity (Topp *et al.*, 1980; Robinson *et al.*, 2005; Roth *et al.*, 1992). It is worth noting that the term "permittivity" will hereinafter refer to the dimensionless "relative dielectric permittivity" ε_{r}, which is the permittivity of a material relative to vacuum permittivity.

A three-phase model can be used to define the bulk permittivity (ε_{m}) of a soil mixture having negligible amount of bonded water (i.e., negligible fraction of active clay) (Roth *et al.*, 1990):

$$\varepsilon_{\mathrm{m}}^{\alpha} = \theta \times \varepsilon_{\mathrm{w}}^{\alpha} + (1 - \eta) \times \varepsilon_{\mathrm{s}}^{\alpha} + (\eta - \theta) \times \varepsilon_{\mathrm{a}}^{\alpha}, \tag{3.1}$$

where:

- θ is the volumetric water content;
- η is the porosity;
- α is a dimensionless coefficient ranging from $+1$ to -1, which is positive when the electric field is perpendicular to the soil layer and negative when the electric field is parallel to the soil layer.

The volume fraction that corresponds to the solid phase is $(1 - \eta)$, whereas $(\eta - \theta)$ is the volume fraction that corresponds to the air phase. When the soil is saturated ($\eta = \theta$),

Equation (3.1) reduces to the following one:

$$\varepsilon_{\mathrm{m}}^{\alpha} = \eta \times \varepsilon_{\mathrm{w}}^{\alpha} + (1 - \eta) \times \varepsilon_{\mathrm{s}}^{\alpha}. \tag{3.2}$$

It is instructive to calculate the soil bulk dielectric permittivity using Equation (3.2) for the cases where the electromagnetic sensor is surrounded by *(i)* in-situ soil sediment (pre-scour), *(ii)* water (soil washed away due to scour), and *(iii)* redeposited soil sediment having higher porosity (post-scour). These are given in Table 3.3 assuming $\alpha = 0.50$, $\varepsilon_{\mathrm{s}} = 4$, and $\varepsilon_{\mathrm{w}} \approx 78$ and porosities in the range $\eta = 0.4$–0.5 for the original riverbed soil before scouring and $\eta = 0.5$–0.6 for the redeposited sediment.

The significant dissimilarity in bulk permittivity before, upon, and post scouring is used to detect scour and bed material deposition processes surrounding the foundations. An example of the time history of the permittivity values before, during and after a scouring

Table 3.3: *Values of calculated permittivity during scouring process*

Soil Condition	**Porosity (η)**	**Permittivity (ε_{m})**
Pre-Scouring (Saturated Soil)	0.40–0.50	23–30
Scouring (Soil is washed away)	1	78–80
Post Scouring (Re-deposited Soil)	0.50–0.60	30–38

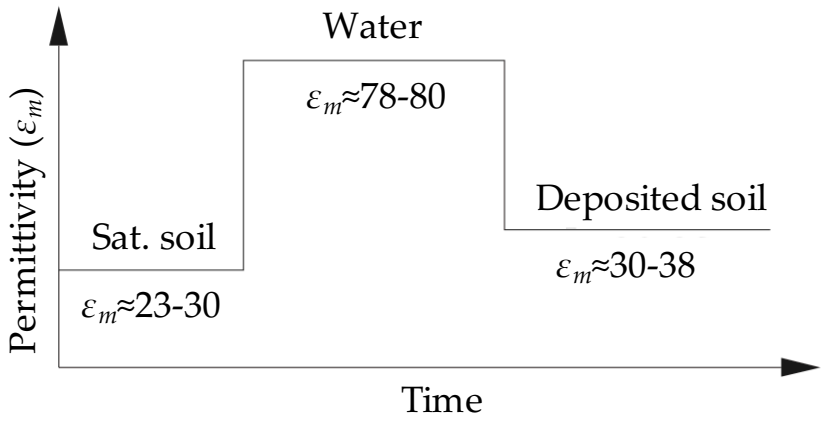

Figure 3.7: *Variation of permittivity over time during scouring action*

process is shown in Figure 3.7. It can also be observed that the pre-scour and post-scour conditions correspond to quite different permittivity values, which is useful to identify whether the scour hole has been refilled.

There is a clear agreement that the temperature affects the dielectric permittivity of water and soil (Baumhardt *et al.*, 2000; Chanzy *et al.*, 2012; Or and Wraith, 1999). However, the significant drift occurs comparing the permittivity at very low temperature (e.g., 0°C, or even below zero) and at high temperature (e.g., 65°C-90°C). Instead, looking at the seasonal range of temperature of a river (e.g., −5°C–35° C) for both fresh water and soil, the permittivity values are less sensitive to temperature changes. Both fresh water and soil permittivity decrease when the temperature increases, but the decrease is in the order of 3% for saturated soil (i.e., considering $\varepsilon_{\mathrm{m}} = 25$ at 0°C) (Or and Wraith, 1999) and 10% for fresh water (i.e.,$\varepsilon_{\mathrm{m}} = 90$ at 0°C) (Michalis *et al.*, 2015). Considering that the scour detection technique is based on the significant difference between the permittivity values during the soil conditions (as shown in Table 3.3), this negligible effect of temperature was not studied during the calibration tests shown in the next paragraph and the recorded permittivity of the scour monitoring system was not compensated over temperature. In fact, in Michalis *et al.* (2015), their study of a similar dielectric probe for scour detection resulted in the conclusion that these devices provide an accurate measurement in the range ε_{m} =1–80.46, regardless temperature or salinity effects.

3.3.2 Scaled frequency N

As mention before, the electromagnetic sensor provides information on the permittivity of the medium around it by measuring the resonant frequency. The EnviroSCAN probe retunes the resonant frequency of the surrounding medium in terms of scaled frequency that depends on the frequency of water and air (Sentek technologies, 2011). The scaled frequency

N^k (for the $k = 1, 2, \ldots, N$ sensor) is evaluated according to the expression below:

$$N^k = \frac{R^k_{\mathrm{A}} - R^k_{\mathrm{E}}}{R^k_{\mathrm{A}} - R^k_{\mathrm{W}}} \tag{3.3}$$

where:

- R^k_{A} is the resonant frequency of air read by the kth sensor;
- R^k_{W} is the resonant frequency of water read by the kth sensor;
- R^k_{E} is the resonant frequency of the field read by the kth sensor.

N^k is a dimensionless number that varies depending on the dielectric permittivity of the medium surrounding the sensors (with $N^k = 0$ when the sensor is in air and $N^k = 1$ when it is submerged in pure water).

3.3.3 Calibration of scour probe

A calibration is required to establish the correlation between the bulk permittivity of the soil mixture (ε_{m}) to the scaled frequency (N^k) collected by the sensors of the EnviroSCAN probe. The calibration study was conducted in the geomechanical laboratory located at the University of Strathclyde, Glasgow, prior to installation in the bridge site, by exposing the probe to various media using different chemicals of known dielectric permittivity and by measuring the corresponding sensor readings (Michalis *et al.*, 2015). The scaled frequency N^k corresponding to each chemical is calculated with Equation (3.3), where the values of R^k_{A} and R^k_{W} have been recorded in the laboratory during the calibration phase by submerging the probe in fresh water and air. The chemicals used for the experiment are Acetone, Acetonitrile and Methanol. The permittivity values of these above-mentioned chemicals are shown in Table 3.4, together with those of water and air.

Table 3.4: *Known values of permittivity $\bar{\varepsilon}_{\mathrm{m}}$ of different mediums*

Medium	**Permittivity ($\bar{\varepsilon}_{\mathrm{m}}$)**
Air	1.0
Acetone	20.7
Methane	32.6
Acetonitrile	36.0
Water	78.0

The calibration test consists in a 40-minute-long reading of the scaled frequency N for each chemical with a sampling interval of 30 seconds. The scaled frequency readings of the probe were plotted in a graph against the values of the permittivity of the considered chemicals and the following analytical relationship was fitted (Schwank *et al.*, 2006), consisting of a quadratic and an exponential factor:

$$\varepsilon_{\mathrm{m}}(N) = \left(a_0 + a_1 \times N + a_2 \times N^2\right) \times e^{k_1 N} \tag{3.4}$$

It is worth recalling that the scaled sensor reading has two extreme values, i.e., $N = 0$ when the sensor is in air, and $N = 1$ when it is in pure water. Thus, in accordance with the Equation (3.3), Equation (3.4) must fulfil two constraints: $\varepsilon_{\mathrm{air}}(N = 0) = 1$ and $\varepsilon_{\mathrm{water}}(N = 1) = 78.4$. Therefore, the values of the parameters a_0 and a_1 can be evaluated and Equation (3.4) can be reduced to:

$$\varepsilon_{\mathrm{m}}(N) = \left(\varepsilon_{\mathrm{air}} + \left(\varepsilon_{\mathrm{water}} \times \mathrm{e}^{-k_1} - 1 - a_2\right) \times N + a_2 \times N^2\right) \times e^{k_1 N} \tag{3.5}$$

Figure 3.8 shows the calibration curve obtained after conducting the experiment using the chemicals shown in Table 3.4. The green dots denote the values of the known permittivity of the chemicals plotted against the measured scaled sensor readings (N). Plotted in the same figure is the curve corresponding to Equation (3.5), with the parameters $a_2 = 1.2794$ and $k_1 = 6.6537$ fitted using least square method. The values of the permittivity estimated

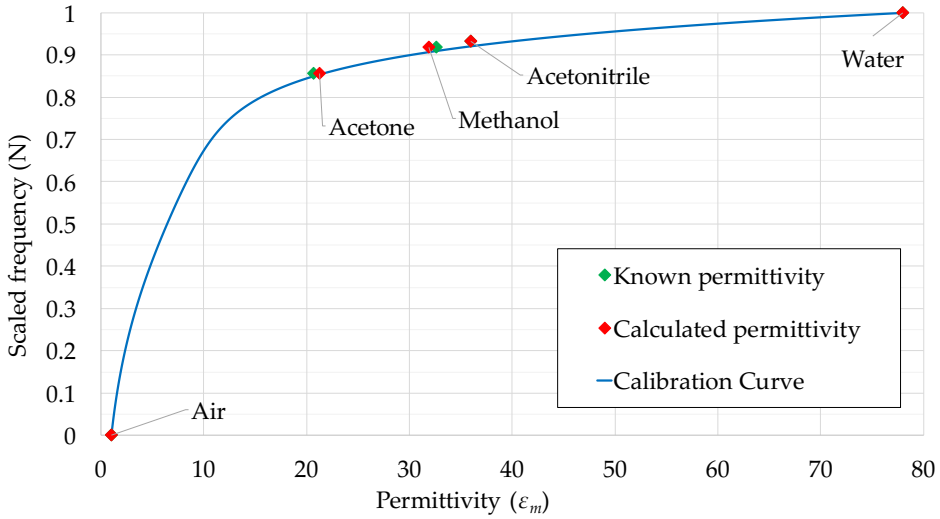

Figure 3.8: *Calibration curve from calibration tests*

by the proposed equations are very close to the known permittivity of the chemicals, as also shown in Table 3.5. The table also shows the mean value of the sensor reading N recorded during each test, and its standard deviation σ_N. Thus, Equation (3.5) can be used to convert the in-field scaled sensor readings N^k into values of permittivity using the fitted values of the parameters a_2 and k_1.

Table 3.5: *The values of known permittivity* $\bar{\varepsilon}_\mathrm{m}$ *and calculated permittivity* ε_m

Medium	$\boldsymbol{N}$	$\boldsymbol{\sigma_N}$	$\bar{\boldsymbol{\varepsilon}}_\mathbf{m}$	$\boldsymbol{\varepsilon}_\mathbf{m}$	$\boldsymbol{\sigma}_{\boldsymbol{\varepsilon}_\mathbf{m}}$
Water	1.0	-	78.4	78.4	-
Acetonitrile	0.93	0.0006	36.0	35.94	0.22
Methanol	0.92	0.0018	32.6	31.86	0.51
Acetone	0.86	0.0042	20.7	21.27	0.44
Air	0.0	-	1.0	1.0	-

Table 3.5 also shows the standard deviations of the sensor readings recorded during the tests and the permittivity calculated using Equation (3.5). Regarding the latter values, error bars are depicted in Figure 3.9 showing the region of interest of the calibration curve (i.e., the sensor readings of the chemicals range between 0.86–0.93). Standard deviations of

water and air readings are not quantifiable according to the way the scaled frequency N is calculated (i.e., whatever the sensor reading is, $N = 0$ when the sensor is in air and $N = 1$ when it is submerged in water) and Equation (3.5) is developed to fulfil two constraints: $\varepsilon_{\text{air}}(N = 0) = 1$ and $\varepsilon_{\text{water}}(N = 1) = 78.4$

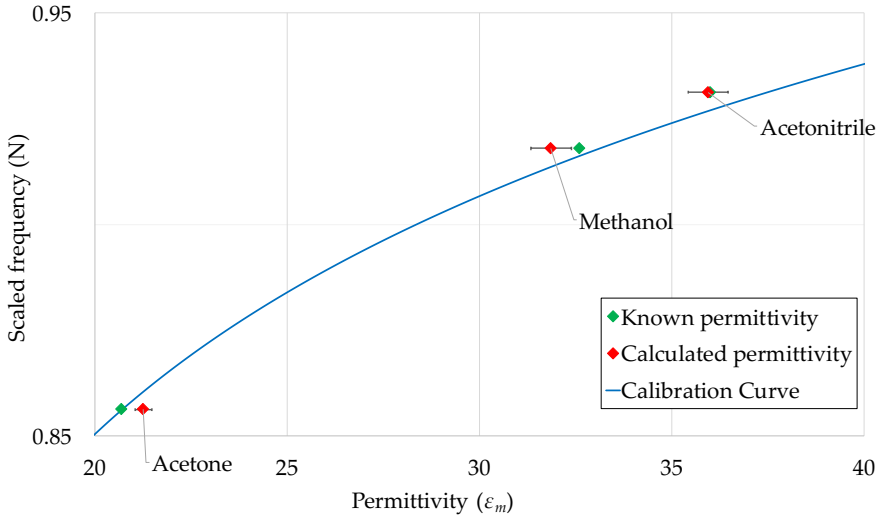

Figure 3.9: *Region of interest of the calibration curve after the tests of the chemicals*

3.3.4 Static scour test

A "static" scour test was performed in order to mimic probe functioning in a real-case scour scenario. Figure 3.10 depicts the schematic of the test setup used to record the probe response during a simulated scour event and the following deposition phase. The probe, equipped with nine electromagnetic sensors, was placed in the middle of a custom made cylindrical acrylic tank with diameter and height of 45 cm and 100 cm respectively. The initial setup consisted of three sensors in each medium, i.e., soil, water and air (Figure 3.10). The soil used for the experiment was silica sand of particle size of 1 mm.

The static scour test consisted of the removal of soil by hand in order to reproduce the scour process and, after recording the sensor response, of the manual refilling of the tank to simulate the deposition phase.

The test protocol expanded the one used by Michalis *et al.* (2015) by highlighting the capability of the sensor to monitor the scour hole refill process (i.e., step 6). It was articulated in the following steps:

1. The probe was placed in the centre of the acrylic tank and kept vertical with the help of supports.
2. The acrylic tank was filled with silica sand for 40 cm. Each time a 10-cm layer of sand was added, it was compacted using a proctor hammer and a square-shaped plywood piece to ensure even compaction.
3. The soil was saturated with fresh water, and the tank was filled with 30 cm of water above the sand surface to simulate a static soil-water interface, such as the riverbed condition (Figure 3.10a).
4. The probe recorded the sensors' response for ten minutes (i.e., "pre-scour condition").

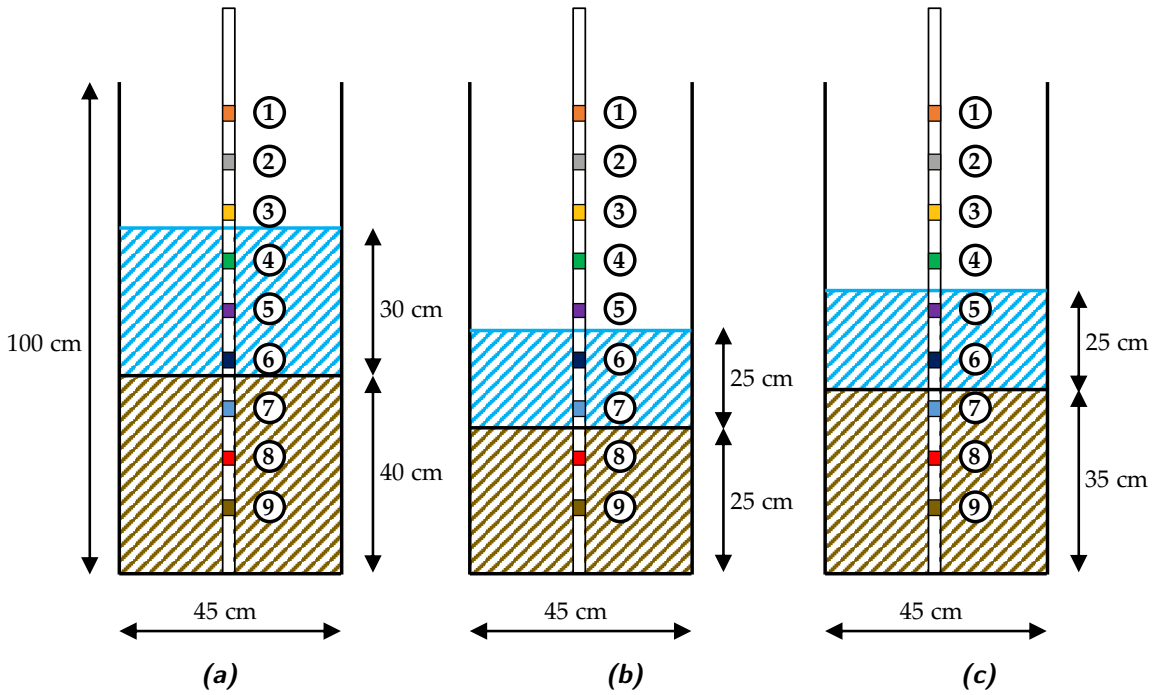

Figure 3.10: *Schematic of the experimental setup:* ***(a)*** *the pre-scour,* ***(b)*** *the scour, and* ***(c)*** *the deposition condition*

5. The scour process was started by manually removing a 15 cm layer of soil around the probe until a depth of about 25 cm was reached (Figure 3.10b). For this purpose, a small shovel was used. The "scour condition" lasted 20 minutes.

6. The deposition process was mimicked by partly refilling the layer of removed soil around the probe, reaching a total soil depth of 35 cm ((Figure 3.10c)). The response of sensors was recorded for ten minutes (i.e., "deposition condition").

During the experimental campaign, the influence of the water turbulence was not investigated since the sensors response is not affected by the dynamic effect of water (Tarantino, 2019) as suggested by the results shown in Michalis *et al.* (2015), i.e., the sensor behaviour is similar either during their static test or the flume experiment they performed.

Figure 3.11 shows the three conditions achieved during the test, e.g., pre-scour, scour and deposition period.

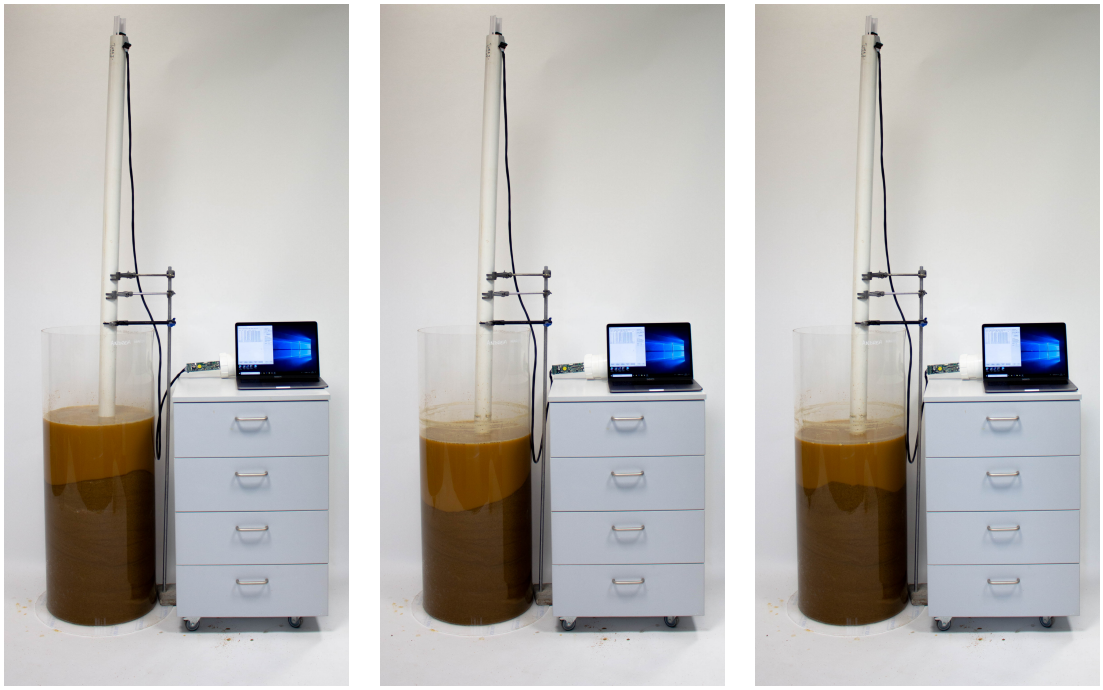

(a) ***(b)*** ***(c)***

Figure 3.11: *Static scour test showing* ***(a)*** *the pre-scour,* ***(b)*** *the scour, and* ***(c)*** *the deposition condition*

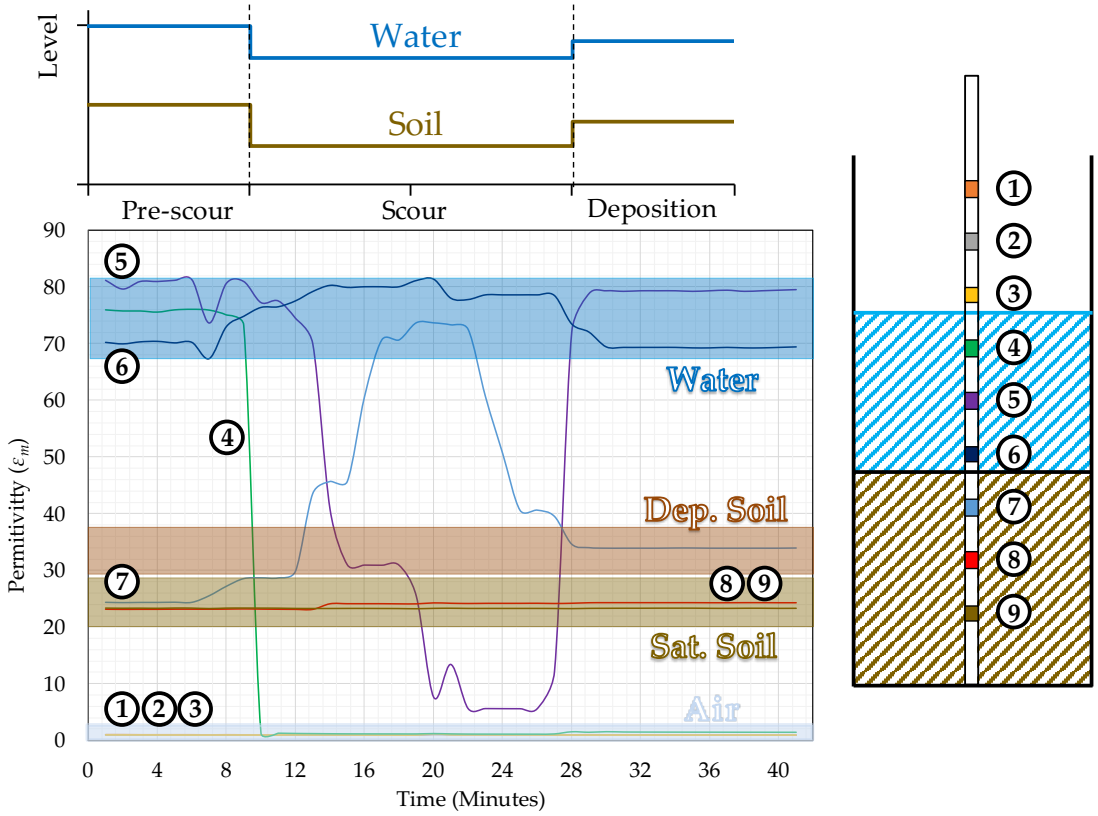

Figure 3.12: *Permittivity ε_{m} recorded by the nine sensors during the static scour test*

Figure 3.12 illustrates the time history of the permittivity values recorded during the test by the nine sensors in the probe. The values of permittivity shown in Figure 3.7 allows to identify four bands in the plot, separating the sensor reading associated to the permittivity of water ($\varepsilon_{\mathrm{m}} = 70$–$80$), saturated soil ($\varepsilon_{\mathrm{m}} = 23$–$30$), deposited soil ($\varepsilon_{\mathrm{m}} = 30$–$38$) and air ($\varepsilon_{\mathrm{m}} = 1$). The scouring and deposition process did not affect sensors 1, 2 and 3 because they were in air for all the duration of the test. This is confirmed by the value of the permittivity near one maintained throughout the experiment. Similarly, sensors 8 and 9 recorded a constant value of permittivity of about 23, i.e., the value of ε_{m} associated with saturated soil.

The response of sensor 4 shows a drop in the permittivity from 75 (i.e., water) to 1 (i.e., air) that can be explained by the fact that the water level dropped after the soil was

removed (see Figure 3.11b, c and the top graph of Figure 3.12). The initial value was not recovered after the scour hole was refilled by re-depositing sand. The recording of sensor 5 exhibits a similar behaviour: it starts in water, it is in air during the scour condition because the water level falls but, when the soil is refilled, the water level slightly rises, and the sensor is again submerged in water.

Sensor 6 stayed in water for all the test duration, and the recording of its permittivity is almost constant. Some noise and signal disturbances can be noticed during the scour condition due to the manual excavation and refilling (i.e., the mixture of water, soil and air bubbles might explain the fluctuations of the signal).

Sensor 7 is the sensor where the three different conditions simulated in the test can be observed. Initially, during the pre-scour period, the permittivity is around 23 (i.e., within the permittivity range of saturated soils). When the scour is simulated, the signal record starts increasing and reaches a value of 74, which falls in the water range. During the excavation actions, and when the soil is later filled as well, the sensor registers intermediate values of permittivity because when the soil is removed or repositioned, the surrounding medium is a mixture of water and soil. Finally, during the deposition period, the permittivity decreases to a value in the range of deposited soil (i.e., $\varepsilon_{\mathrm{m}} = 30$–$38$).

3.4 A76 200 Nith bridge

The A76 200 Nith bridge is a 3-span stone masonry arch carrying the A76 two-lane single carriageway over River Nith in the small village of New Cumnock in the south-west of Scotland (Figure 3.13a). The middle span is 10.70m long, whereas each of the approaching spans is 9.10m long. The span width is 8.5m between the outer faces of the spandrel walls. The arches are formed of ashlar stonework with punched face and chamfered edges (Figure 3.13b). Abutments and piers are all founded on spread footings on the natural

riverbed and based on previous inspections have experienced significant scour in the past.

3.5 meters upstream of the A76 200 bridge (Figure 3.13c) there is a pedestrian bridge. This is a single span, simply supported composite structure, with a clear span of 34m. The deck consists of precast concrete deck units supported on two I-beams at 1250mm centre-to-centre distance. The beams have a rectangular section, 920mm high and 350mm wide. The precast concrete deck units are formed with a slight up-stands, on which the pedestrian parapets are bolted (Figure 3.13d).

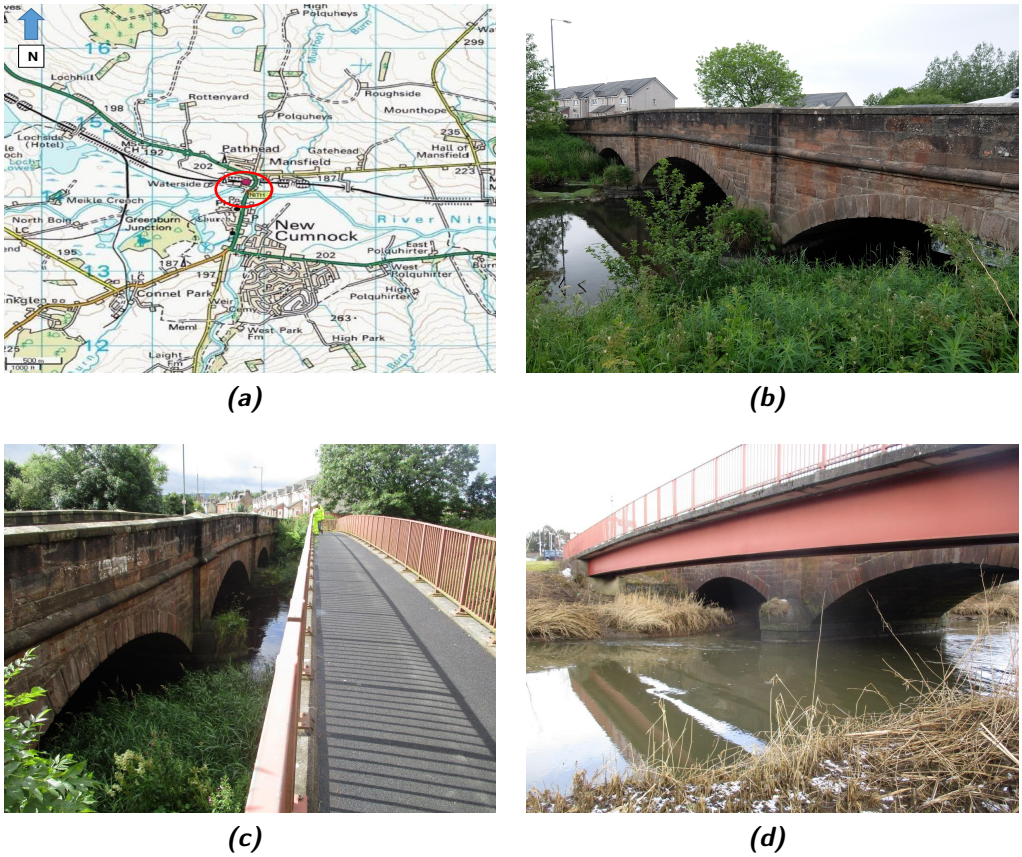

Figure 3.13: ***(a)*** *Location of the A76 200 Bridge;* ***(b)*** *Side view of the A76 200 Bridge;* ***(c)*** *The pedestrian bridge;* ***(d)*** *Side view of the two bridges*

The scour monitoring system consists of two 4-meters-long scour probes that are equipped with electromagnetic sensors installed along the plastic rod height. Therefore, there are sensors buried into the riverbed and others within or above the running water of River

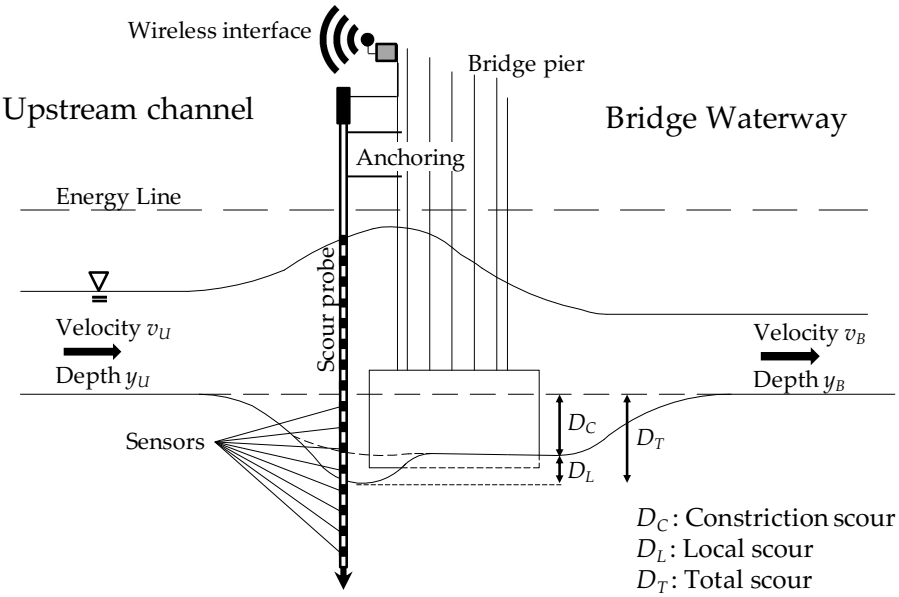

Figure 3.14: *Outline of the pilot scour monitoring system*

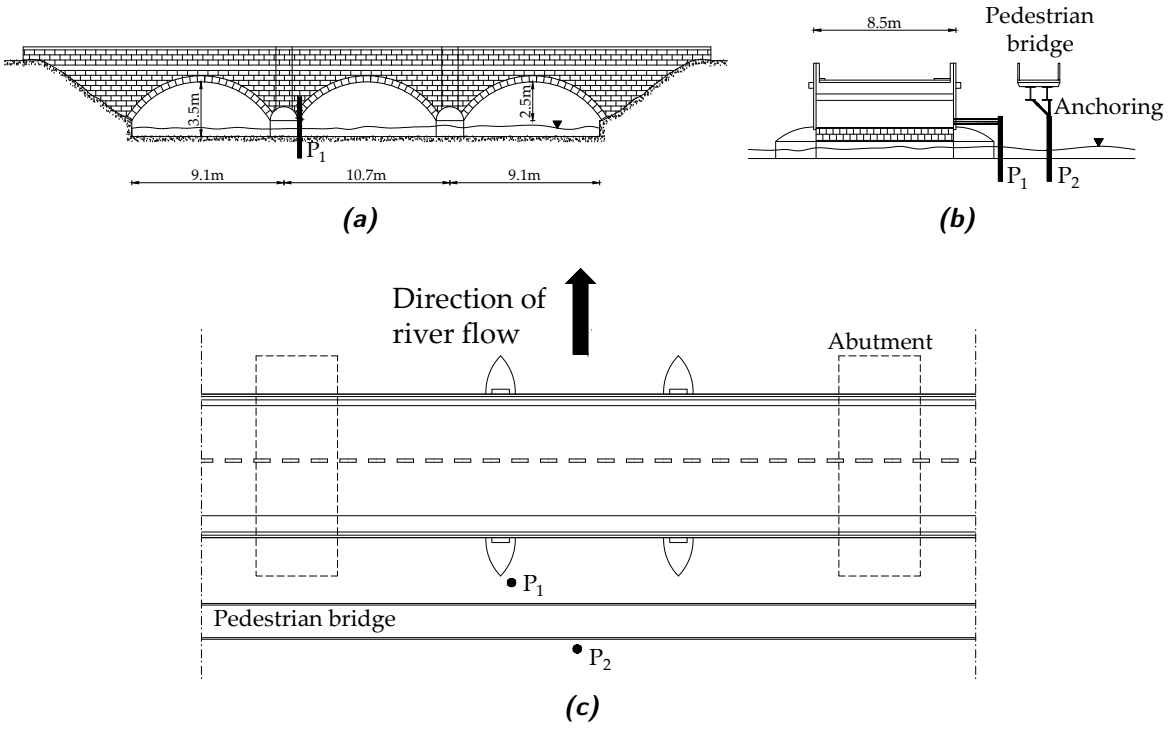

Figure 3.15: *Layout of the pilot scour monitoring system.* ***(a)*** *Side view;* ***(b)*** *Section view;* ***(c)*** *Plan view*

Nith. The former sensor can detect the scour depth, whereas the latter one, being able to discriminate the permittivity values between air and water, can be used to measure the water level (Figure 3.14). The smart probe is protected from water by a plastic tube. The probe and the tube are encased into a CHS metal tube, which is well secured at the top to the piers to prevent any movement and to ensure stability during a flood event.

One probe (P_1) is installed on the upstream face of a pier of the A76 200 bridge to detect total scour, whereas the other (P_2) is installed in the centre of the river to detect degradation and constriction scour, and is connected to the pedestrian bridge (Figure 3.15). Ideally, the locations of maximum scour depth would have been close to the sharp nose of the pier for the probe P_1 (i.e., maximum total scour depth) and below the masonry arch for the probe P_2 (i.e., maximum constriction scour depth). Unfortunately, these locations were constrained by practicality of installation (i.e., there did appear to be obstruction at close proximity to the cutwater, probably due to the spread footing of the pier foundation) or bureaucracy problem (i.e., the bridge is A-listed so installations on its arches and spandrel walls are limited).

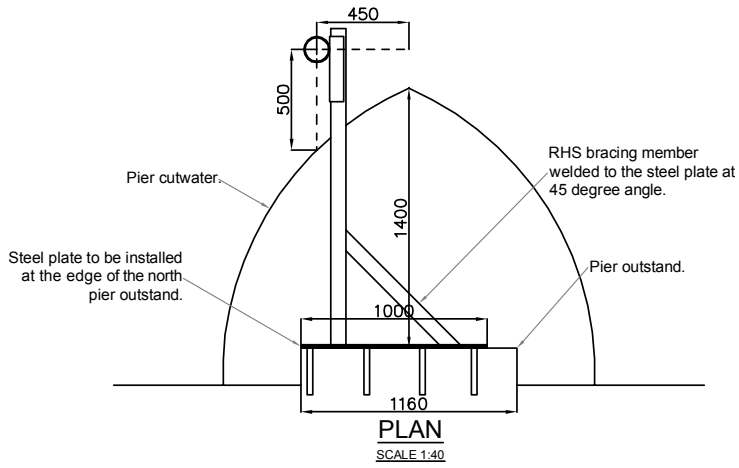

Figure 3.16: *Location of probe P_1 for detecting the total scour depth (not in scale)*

Therefore, probe P_1 was installed 450 mm x 500 mm far from the cutwater pier (Figure 3.16) and the for the installation of probe P_2 the presence of pedestrian bridge was

exploited. Figure 3.17 shows the details of the connections between the two probes and the bridges, ensuring their stability during a flood event. Probe P_1 is equipped with 11 sensors (4 sensors buried into the riverbed), whereas probe P_2 with 15 sensors (3 sensors into the riverbed). Probe P_1 is able to monitor up to 40 cm of scour depth, whereas probe P_2 can

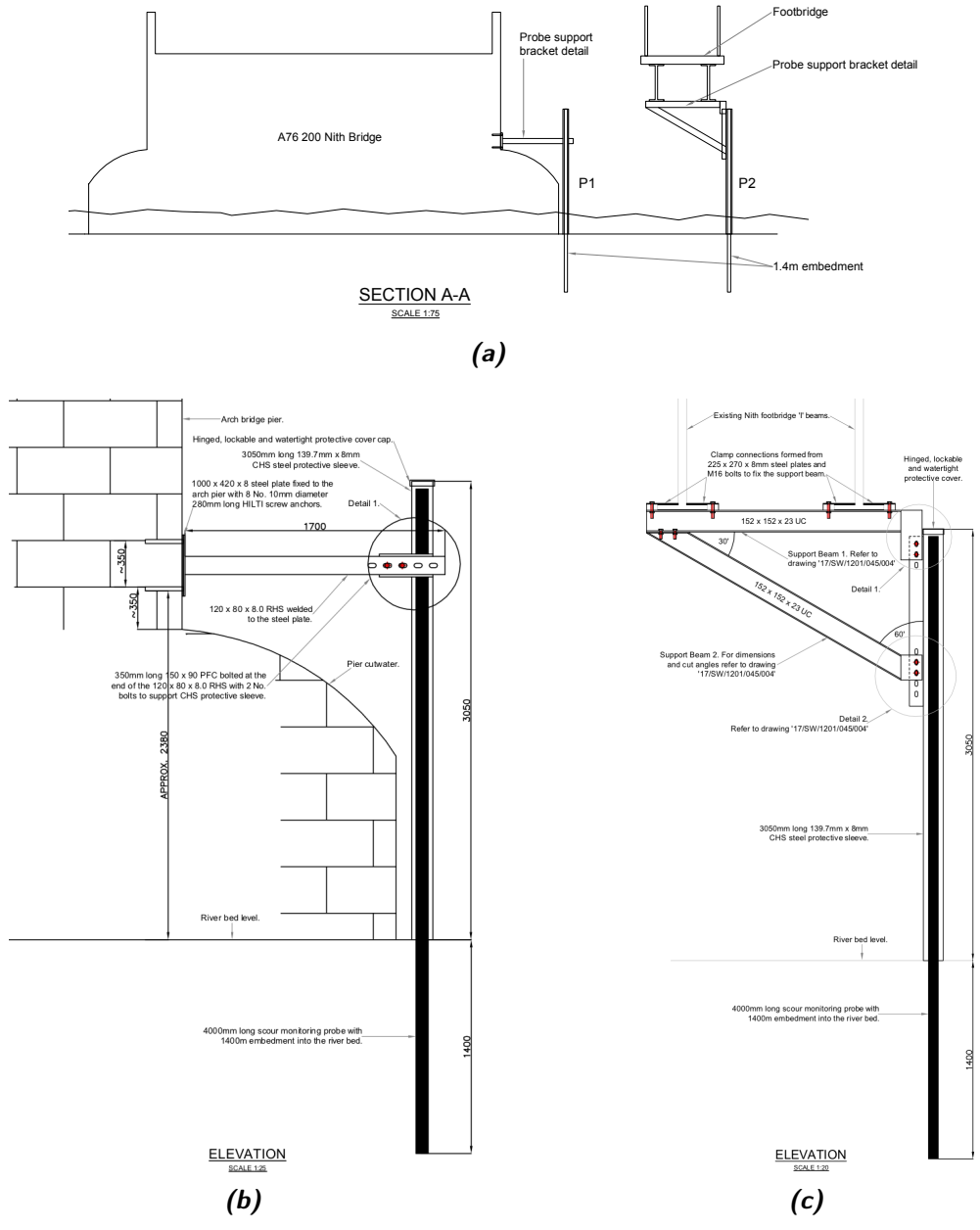

Figure 3.17: ***(a)*** *Anchorage system for the probes,* ***(b)*** *elevation of anchorage system for probe* P_1*, and* ***(c)*** *elevation of anchorage system for probe* P_2

detect a maximum scour depth of 30 cm.

The two probes were installed on the 4th of October 2018, and the monitoring of the scour depth started on the same day (Figure 3.18). In January 2019, the probes were equipped with an external antenna to improve the 3G modem signal for the uploading of the data. The battery of probe P_1 reached its end of life at the beginning of November, thus

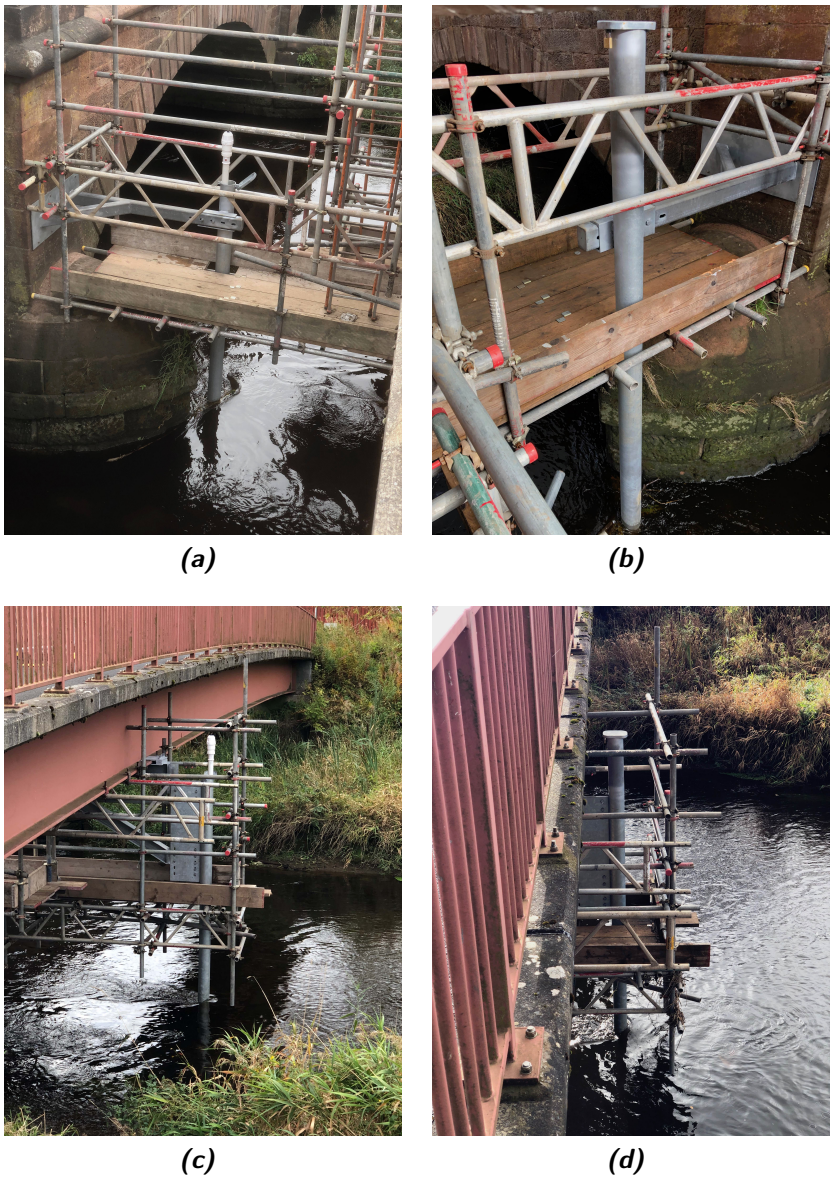

(a) ***(b)*** ***(c)*** ***(d)***

Figure 3.18: ***(a)*** *and* ***(b)*** *Probe* P_1*, and* ***(c)*** *and* ***(d)*** *Probe* P_2

exceeding the expected lifespan according to the DTU's user manual (Sentek technologies, 2015). Close to the end of its life, data were still recorded, but the battery voltage was not enough to transmit to the cloud. As a result, data from 7th November 2019 to 11th December 2019 were lost because the memory in the probe's motherboard has limited space (i.e., 2000 readings) and new readings overwrite the oldest reading first when the storage is full.

3.5 Scour data analysis

3.5.1 Probe P_2 in the middle of the channel

Figure 3.19 shows the sensors readings collected by probe P_2. According to the different values of permittivity shown in Figure 3.7, three bands can be identified, associated to the permittivity of water ($\varepsilon_m = 70$–80), saturated soil ($\varepsilon_m = 20$–27) and air ($\varepsilon_m = 1$).

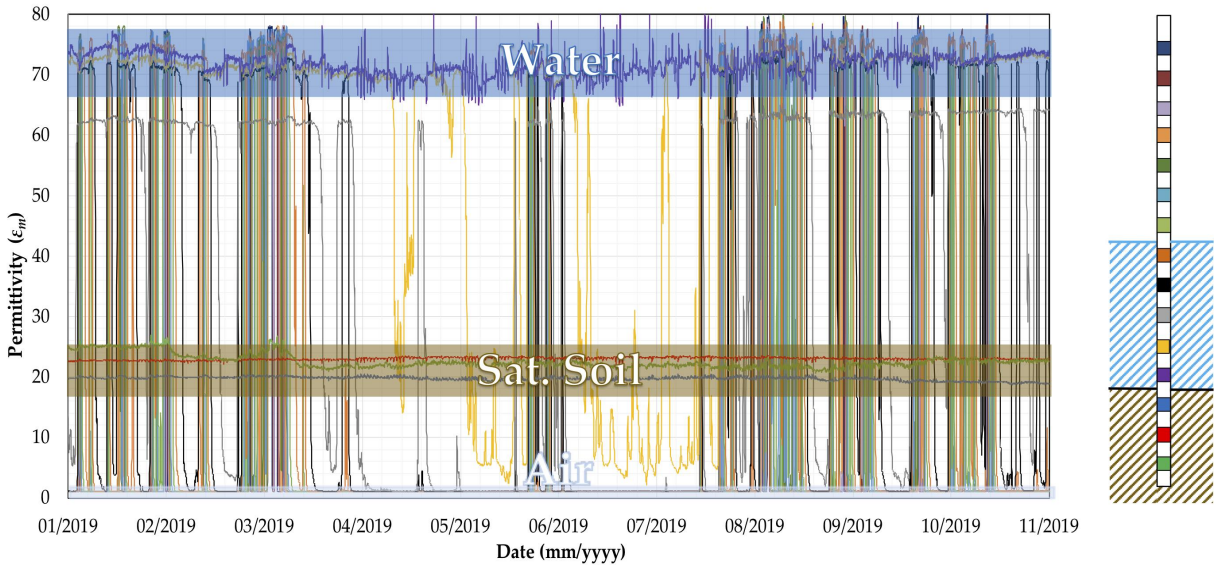

Figure 3.19: *Readings of the 15 sensors installed into probe P_2*

Thanks to the sensor capacity of reading the permittivity of water and air, it is possible to discriminate the status of a sensor between these two environments and, essentially,

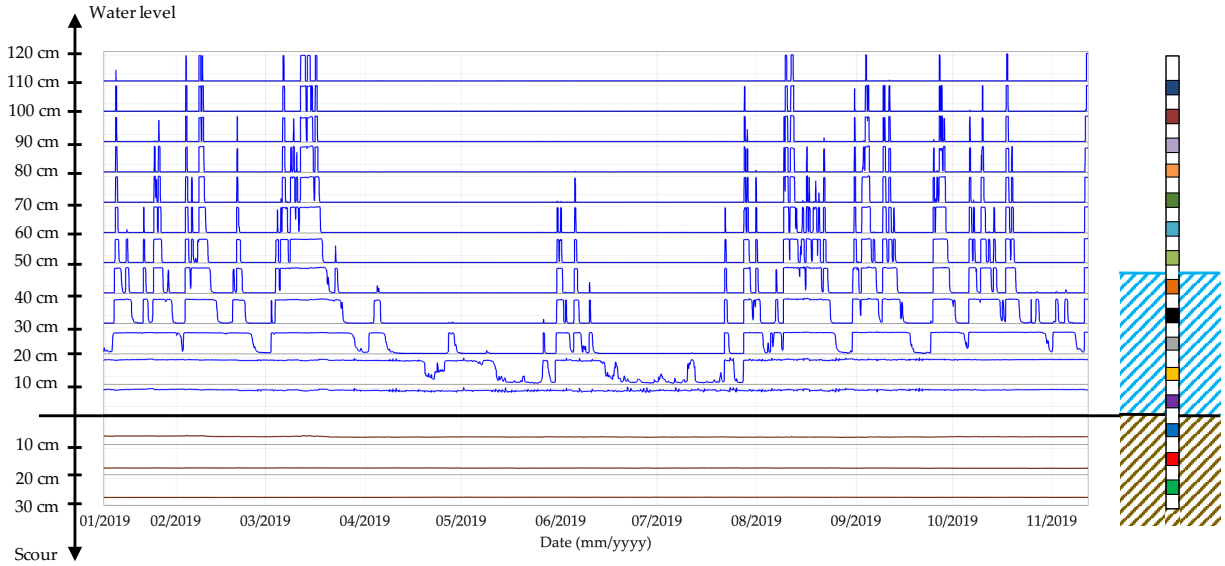

Figure 3.20: *Rise and fall of water detect by the sensors of probe P_2*

the probe can also be used as water level detector, as shown in Figure 3.20. The only drawback of this monitoring technique is the limited number of sensors involved for water level measurements; the main board of the probe has 16 channels, which poses a limit to the number of sensors that can be deployed. Considering that some of them are buried into the riverbed for detecting the erosion, only a few electromagnetic sensors can be employed

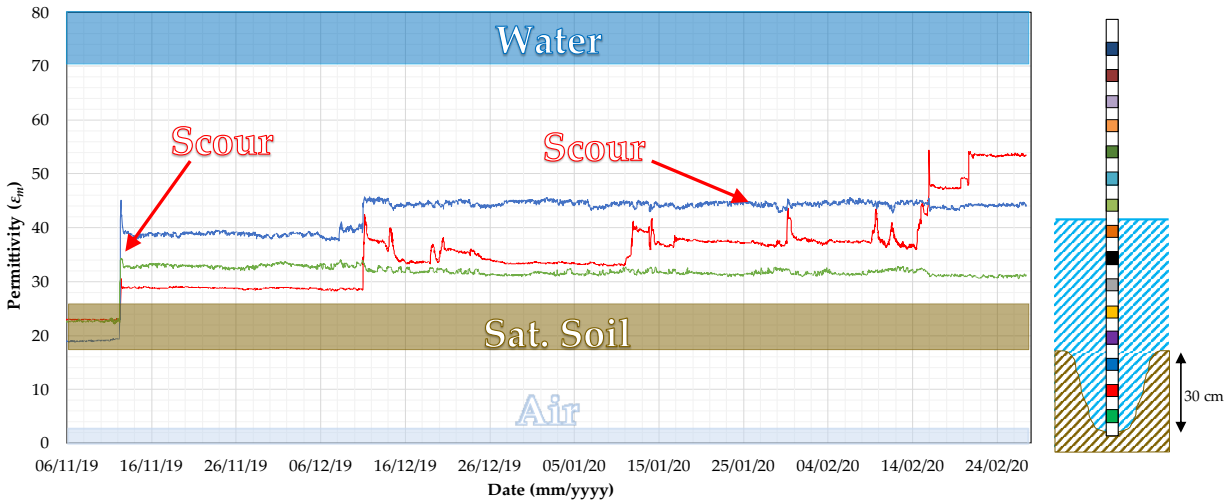

Figure 3.21: *Detection of scour hole by probe P_2*

to measure the rise and fall of river water. For instance, probe P_2 can measure a maximum water level equal to 120 cm.

On the 12th of November 2019 at 4 am, the three sensors of probe P_2 located into the riverbed registered a change in the value of permittivity. The jump of the three sensor readings (green, red and blue signal in Figure 3.21) indicates the presence of a scour hole of 30 cm (i.e., the spacing among sensors is 10 cm).

3.5.2 Probe P_1 at the bridge pier

The probe P_1 installed at the pier of the A76 200 Bridge has not recorded any scour. As observed in Figure 3.22, the signals of the last four sensors have never changed from the value of permittivity for saturated soil ($\varepsilon_m m = 20$–27). Unfortunately, the battery of

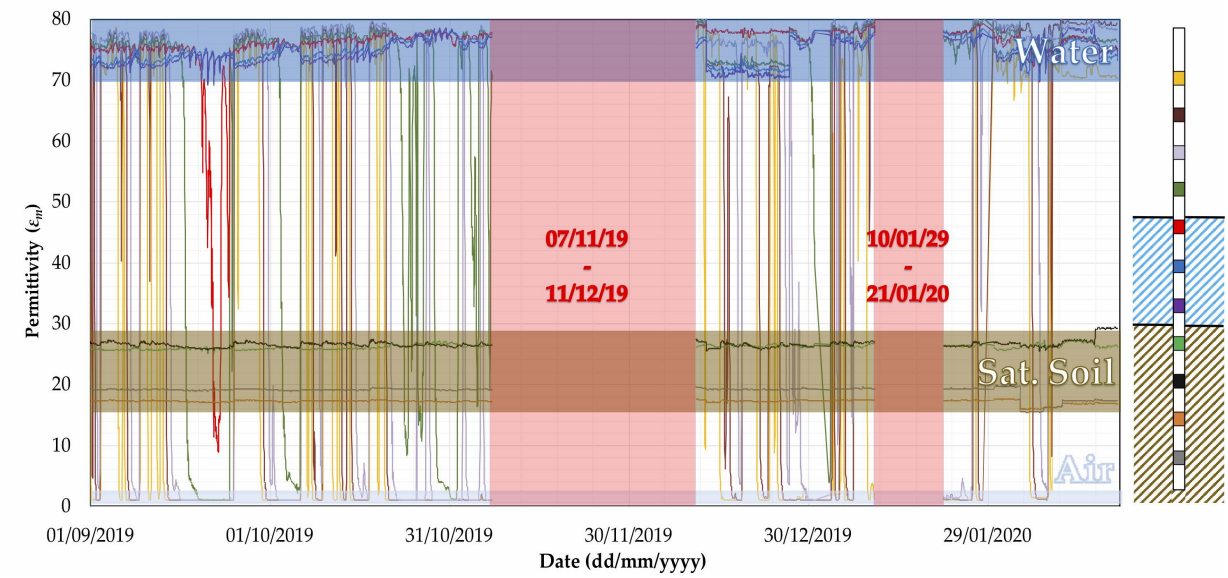

Figure 3.22: *Readings of the 11 sensors installed into probe P_1*

probe P_1 failed few days before the peak flooding event (12th of November), and there is a data loss of around one month but, once the battery was replaced most of the data were recovered, and it can be seen that the permittivity values are still very close to those recorded in November before the failure of the battery.

3.6 Discussion

Data concerning the maximum daily value of river stage provided by the Scottish Environmental Protection Agency (SEPA) show a peak in the water level of the river during the night before the 12th November, which could have caused the scour event registered by probe P_2.

Figure 3.23: *Map of SEPA gauging stations*

In particular, the gauging station located in Dalgig (upstream to the A76 200 bridge, see Figure 3.23) registered a value of water level equal to 1.883m at 3:15 am of the 12th November 2019, as shown in Figure 3.24a. The gauging station located in Hall Bridge (downstream to the A76 200 bridge, see Figure 3.23) registered a peak value of water level equal to 1.667m at the 6:45 am of the 12th November 2019, as shown in Figure 3.24b. Both values are the maximum values registered by the gauging stations since March 2019, as can be seen from the graph in Figure 3.24. Furthermore, the water levels recorded by the two gauging stations have been exceeded only ten times at Dalgig and 16 times at Hall bridge in the last six years.

It is worth noting that the water level profile shown in Figure 3.24a visually agrees with the water level provided by the probe P_2 (Figure 3.20) since the peaks of water level and its rise and fall during months occur during the same time-frames. It is hard to verify that and find a correlation between the two dataset because the gauging station is quite upstream

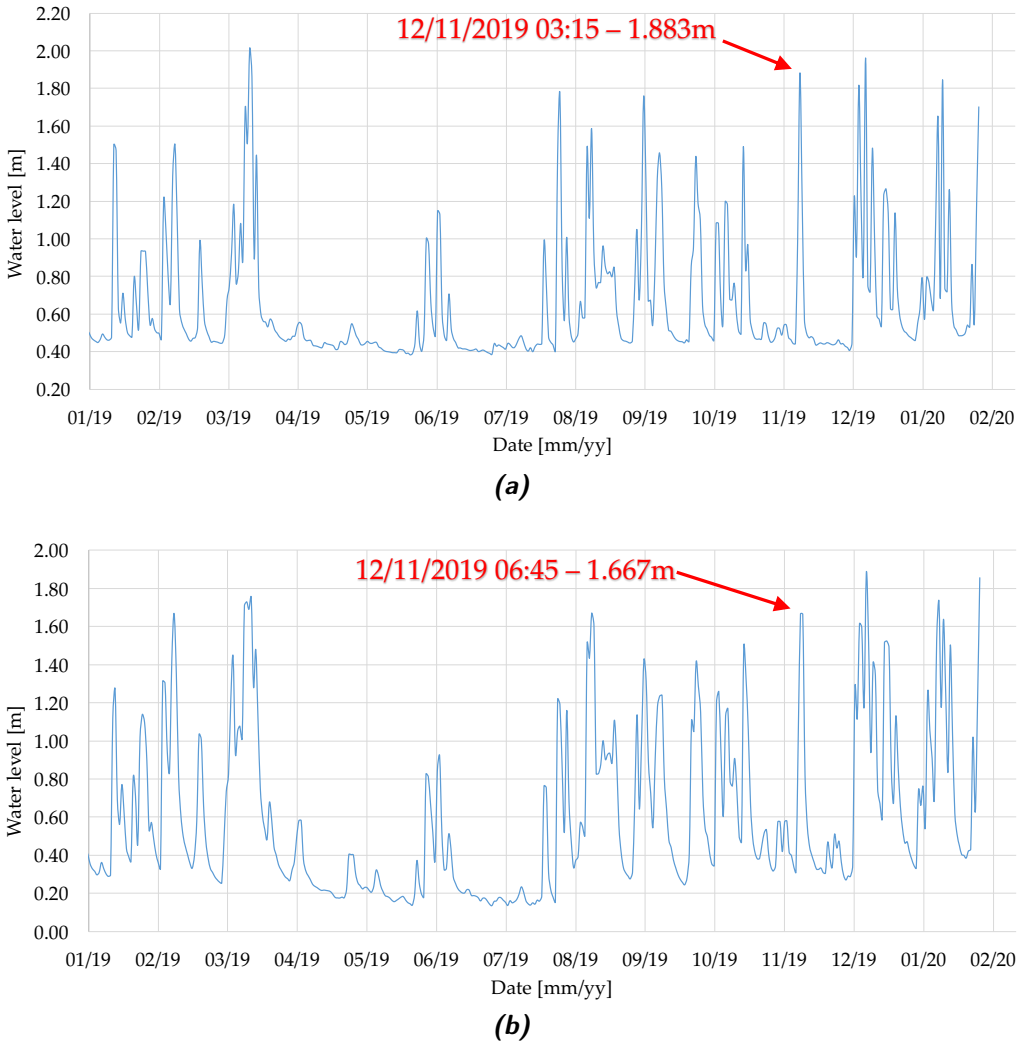

Figure 3.24: ***(a)*** *Water level time-history at Dalgig station; and* ***(b)*** *Hall Bridge station from January 2019.*

to the Nith bridge (i.e., several tributary rivers flow into the River Nith) and the probe can record 1.20 m as maximum value of river stage, so that, the water level values cannot match. However, the shapes of the two water level profiles match, thus providing a sort of verification of the water level measurements recorded by the probe.

3.6.1 Inspection and visual check at the bridge site

In order to verify the recorded data and check the scour recorded by the two probes, the A76 200 bridge was visually inspected and the riverbed depth was measured at the two probe locations. A 3.6-meter-long telescopic pole was used to evaluate the scour at the locations illustrated in Figure 3.25, based on the comparison between the initial river bed depth at the time of probe installation and at the time of the new measurement. During the installation of the probes, the steel protective tubes (3.05-meter-long) were laid on the riverbed before being connected to the bridges through the support brackets. Therefore, the telescopic pole was used to measure the current distance from the riverbed and the welding mark on the steel tube (i.e., the steel tube was extended in order to cover all the probes – there was problems with the driving of the access tube into the soil – so the welding mark is 3.05 meter high). The difference between the two reference points (i.e., one on the telescopic pole and the other on the steel tube) was then measured with a measuring tape, with a measurement precision of 0.5 mm. The measured values of the scour, referred to as d, are reported in Table 3.6.

Table 3.6: *Scour inspection – Locations and scour measurements d*

Location	**Description**	**Scour depth d**
P_1	Highly localised hole around the steel tube	0-10 cm
P_2	Large hole downstream the steel tube	30 cm
P_2	Hole upstream the steel tube	20 cm

The data obtained by the probe P_2 are supported by the actual measurement of scour in the vicinity of the steel tube and immediately downstream to it. Several measurements carried out around the metal tube provided the same value of scour depth (i.e., 30 cm). Figure 3.25 shows only five of them for not having a cluttered picture. Few measurements were taken upstream the tube, just over the scaffolding, and 20 cm of scour was recorded.

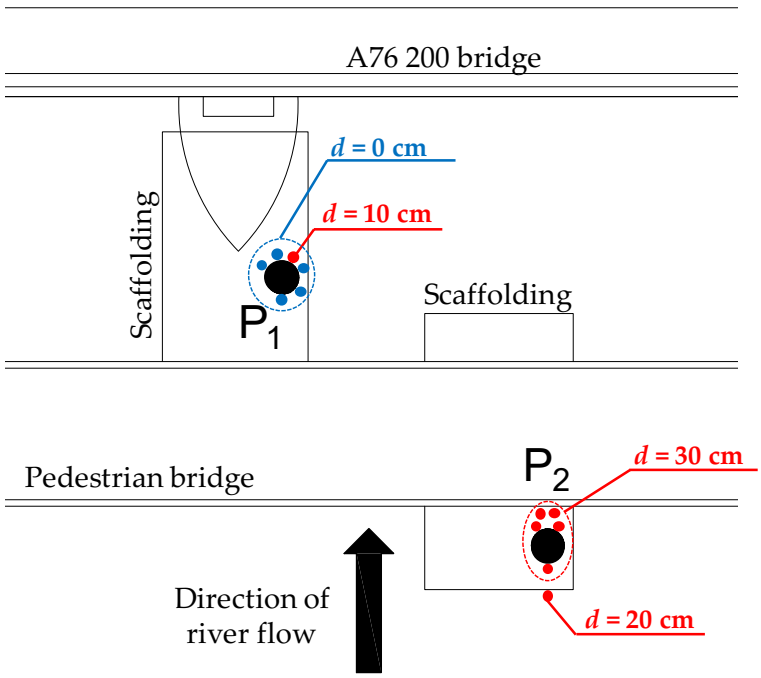

Figure 3.25: *Locations and scour measurements d carried out during the probe inspection*

The recorded scour might be the result of the turbulence of water around the steel pipe, since a circular tube inserted into the riverbed can induce local scour depths up to 2.5 times its diameter (Melville, 1997). The diameter of the tube is 139 mm, which therefore may lead to a scour depth of 35 cm. However, this pipe-induced scour does not invalidate the obtained results, and in fact, it has confirmed the probe capacity to detect scour.

Moreover, the abundant presence of debris and particularly of hay on the scaffolding and the steel tube (see Figure 3.26) may explain the recorded values of the permittivity of the last three sensors of P_2, which were around 50 (Figure 3.21) and did do not reach the water permittivity reference value ($\varepsilon_{\mathrm{m}}m = 70$–$80$). Nevertheless, this value is higher than the permittivity of the saturated soil, allowing the probe to detect the scour.

Finally, a small and highly localised scour hole (i.e., less than 5 cm of diameter) was found on the downstream side of the steel tube protecting probe P_1. This may be due to the local erosion induced by the turbulence of water around the steel pipe as well. However,

Figure 3.26: *Hay and debris on the probe P_2*

the remaining soil surrounding the tube was not found to be scoured, and this explains why the small hole did not influence the readings of probe P_1.

It is worth mentioning that using the formula of BD97/12 (Highway Agency, 2012), a total pier scour depth equal to 2.93 m is obtained under the discharge corresponding to the peak flood event registered in the early morning of 12th November. This outcome shows that empirical formulas embedded in current assessment procedures may result in over-conservative scour estimates. This is mainly because they are based on laboratory tests under controlled conditions that are not representative of real ones (see e.g., Pizarro *et al.*, 2020), and the key assumption of the procedure is that an equilibrium in scour depth is reached at a constant high-flood event (e.g., the water flow with a return period of 200 years), which leads to very high theoretical scour depths. However, these values of scour holes will never be achieved as the flooding event does not remain at its peak long enough to developed the full scour depth. Thus, information from scour monitoring at bridge

foundations could be very useful to reduce the bias and improve scour estimation models (Pizarro and Tubaldi, 2019).

3.7 Conclusions

This Chapter presents the concept, functioning and output of the pilot scour monitoring system installed on the A76 200 bridge over the River Nith in New Cumnock, UK. The scour monitoring system consists of a smart probe equipped with electromagnetic sensors designed to detect changes in the medium permittivity surrounding bridge foundations. The monitoring technique allows tracking the evolution of the scour depth and can also distinguish between air, water, saturated soil and deposited soil, which is useful to assess whether the scour hole has been refilled after the flood peak has receded.

After a brief review of the most diffused scour monitoring techniques, the Chapter introduces the principle of operation of the probe, together with the procedure implemented for calibrating and testing the sensors. The final part of the Chapter describes the pilot scour monitoring system installed in the A76 200 Bridge in New Cumnock (south–west Scotland). The system consists of two probes, one measuring the total scour at one pier (i.e., probe P_1) and one monitoring the constriction scour in the middle of the channel (i.e., probe P_2). After a peak flood event, the latter probe measured 30 cm of scour, and the recorded data are consistent with the actual measurement of scour in the vicinity of the probe carried out using a telescopic pole during a bridge inspection. This proves the potential of the technology in providing continuous scour monitoring, even during extreme flood events, thus avoiding the deployment of divers for underwater examination. Furthermore, it is noteworthy that the data collected by the scour monitoring system have shown that empirical formulas overestimate the scour depth, proving that several uncertainties affect scour models. Therefore, scour monitoring systems should be used to help in quantifying

the scour model errors and developing more precise scour estimation formulas.

As continuation of the work presented in this Chapter, a better characterisation of the sensor response could be proposed by including the study of the effect of temperature and investigating how long-term drift could impact the accuracy of the sensor.

Even though the recorded scour might be the result of the turbulence of water around the steel pipe, this pipe-induced scour does not invalidate the obtained results, and in fact, it confirms the probe capacity to detect scour. However, it raises a concern about the design of the protective system for the probe; an improved design must be pursued to have a system that protects the probe alone, and not induce the scour to be monitored. Shortening the steel protective tube and replacing its bottom part with a cage (e.g., wider than the tube diameter and welded at its bottom part) could be a starting idea to avoid (or at least highly reduce) water turbulence around the pipe. Furthermore, the response of the sensors in the presence of a very localised/non-uniform scour holes must be studied in laboratory.

The obtained data will be used to validate and improve current formulas for estimating the scour depth under transient flood conditions. Finally, these real-time measurements of scour depth will be used within a probabilistic framework for scour risk assessment to update in real-time the estimates of the scour depth at other locations of the bridge and other bridges.

Acknowledgements

The authors would like to acknowledge Derek McNee (Geomechanical Laboratory, University of Strathclyde) for his support during the lab experiments; Douglas Walker and Jim Brown (Transport Scotland), Iain Exley and Edgars Lode (Scotland TranServ), Sam Hunter, Gordon Gibney and Colin Pratt (Balfour Beatty) for their cooperation in

the design of the scour monitoring system, its installation and management; the Scottish Environmental Protection Agency for the flow and river stage data; Steve Roffe (Network Rail) for the information about the structural monitoring system installed on the Lamington Viaduct.

CHAPTER 4

Using Bayesian networks for the assessment of underwater scour for road and railway bridges

Abstract

Flood-induced scour is among the most common external causes of bridge failures worldwide. In the United States, scour is the cause of 22 bridges fails every year whereas, in the UK, it contributed significantly to the 138 collapses of bridges in the last century. Scour assessments are currently based on visual inspections, which are time-consuming and expensive. Nowadays, sensor and communication technologies offer the possibility to assess in real-time the scour depth at critical bridge locations; yet monitoring an entire infrastructure network is not economically feasible. A way to overcome this limitation is to install scour monitoring systems at critical bridge locations, and then extend the piece of information gained to the other assets exploiting the correlations present in the system. In this Chapter, we propose a scour hazard model for road and railway bridge scour management that utilises information from a limited number of scour monitoring systems to achieve a more confined estimate of the scour risk for a bridge network. A Bayesian network is used to describe the conditional dependencies among the involved random variables and to update the scour depth distribution using data from monitoring of scour and river flow

characteristics. This study constitutes the first application of Bayesian networks to bridge scour risk assessment. The proposed probabilistic framework is applied to a case study consisting of several road bridges in Scotland. The bridges cross the same river, and only one of them is instrumented with a scour monitoring system. It is demonstrated how the Bayesian network approach allows to significantly reduce the uncertainty in the scour depth at unmonitored bridges.

4.1 Introduction & background

4.1.1 Bridge scour

Flood-induced scour is among the main reason of bridge collapses, resulting in significant loss of life, traffic disruption and economic losses (Wardhana and Hadipriono, 2003). Scour is defined as the excavation of material around bridge foundations as a result of the erosive action of flowing water. The phenomenon is usually classified into three different types, namely degradation, constriction (or contraction), and local scour (Kirby *et al.*, 2015). While the first type is associated with the natural evolution of the riverbed, the two other types are related to the presence of a bridge. Constriction scour results from the increase of water velocity due to the reduction of the river channel width, caused by the presence of bridge abutments and piers. Local scour is due to the interference of individual structural elements, such as piers or abutments, with the flow, inducing the formation of vortexes at the base of this elements and the removal of sediments from the bed (Lauchlan and Melville, 2001). The aforementioned scour mechanisms work simultaneously to give the total scour. Scour events are expected to occur at most bridge structures with piers or abutments founded on the riverbed during their life span (Richardson and Davis, 2001). When the depth of scour develops significantly, the load-bearing capacity of bridge foundations may be

severely compromised, leading to structural instability and ultimately catastrophic failure (Tubaldi *et al.*, 2018).

In the UK, there are more than 60,000 highway and railway bridges crossing waterways (Clubley *et al.*, 2015) and almost 95,000 spans and culverts are susceptible to scour processes. According to van Leeuwen and Lamb (2014), abutment and pier scour were identified as the most common cause of 138 rail bridge failures recorded in the UK during the period 1846–2013. Reviews of 1,502 river crossing failures that occurred in the United States in the period 1966–2005 revealed flood and scour were the reason of 58% of the recorded collapses (Briaud *et al.*, 2007). Following record daily rainfalls for the UK in November 2009, 20 road bridges across Cumbria were damaged or destroyed (Cumbria Intelligence Observatory, 2010). Furthermore, the winter storms of 2015 resulted in severe damage/destruction to bridges across Scotland and the north of England (Department for Traffic, 2015). This includes the near failure of the Lamington viaduct, which resulted in the closure of the West Coast mainline between Glasgow and London for three months (Rail Accident Investigation Branch, 2016).

4.1.2 Scour risk assessment

The scour risk assessment is a crucial component of any bridge management system. This evaluation should combine information on the hazard, the bridge vulnerability, and the consequences of failure. The first examples of structural risk assessment frameworks were developed in the context of seismic engineering (Porter, 2003). However, their application to the problem of scour so far has been limited (Roca and Whitehouse, 2012; Tubaldi *et al.*, 2017).

Vulnerability (or fragility) analysis is an essential component of any structural risk assessment because it determines how likely a structure is to fail given the occurrence of a hazardous event (Roca and Whitehouse, 2012). In general, the vulnerability of a structural

system such as a building or a bridge can be expressed employing fragility functions or hazard indexes (Calvi *et al.*, 2006). Few studies have analysed the vulnerability of bridges to scour, and in the literature, it is possible to find three different approaches to that in the literature:

(i) numerical approaches involving finite element analyses of the soil-foundation-bridge components (Hung and Yau, 2014; Klinga and Alipour, 2015; Tubaldi *et al.*, 2018);

(ii) analytical approaches considering the reduction of load-bearing capacity of bridge foundations due to scour (Federico *et al.*, 2003);

(iii) empirical approaches based on a Scour Vulnerability Index (SVI), typically expressed as the ratio between the total scour depth at the base of the pier, D_T, and the foundation depth, D_F (Barbetta *et al.*, 2015).

Regardless of the approach employed, an accurate estimation of the scour hole at the foundations of bridge piers and abutments is at the base of any scour vulnerability and risk assessment.

In the UK, Network Rail (NR) owns and operates around 19,000 underline bridges nationally: 8,700 of these structures are held within a National Scour Database. For the Scotland Route only, 1,750 structures are routinely inspected for scour, and 58 are considered to be at high risk. Transport Scotland (TS) is responsible for the Scottish trunk road network including 2,029 bridges or culverts over water. Of these, around 8% (or 168 bridges) are currently classified at risk of scour and needing detailed consideration, including possible monitoring and scour protection measures.

TS and NR assess the risks associated with scour on road and railway bridges using the Procedures BD 97/12 (Highway Agency, 2012)and EX2502 (HR Wallingford, 1993), respectively. Both these procedures rely on visual inspections, carried out at regular intervals or after major flood events, to identify the bridges that may be at risk of scour. More

detailed assessments are then carried out for these bridges, and a SVI is used to rate them and prioritise scour risk mitigation interventions.

Underwater visual inspections have many limitations and drawbacks. First of all, they are time-consuming, and depend heavily on the surveyor's experience, thus providing subjective outcomes. Furthermore, they are expensive. For example, the total NR Scotland Route expenses on scour assessments in 2017 were approximately £450,000. Similarly, TS spends annually £2m on routine inspections of bridges, and around one-third of its total assets are inspected each year. Finally, visual inspections cannot be carried out during the peak of the flood, when the risk of scour is highest, but only after the flood has receded and the scour hole may have been refilled.

Nowadays, a wide range of sensor and communication technologies offer the possibility to assess in real-time the scour depth at bridge foundations (see for instance Anderson *et al.*, 2007; Lin *et al.*, 2006; Michalis *et al.*, 2015; Prendergast and Gavin, 2014; Yu and Yu, 2009). This could help to overcome the limitations of visual inspections, by increasing the identification of the bridges most at risk of scour. However, monitoring an entire infrastructure network is not economically sustainable, and for this reason scour sensors may be installed only at a few critical bridges.

This Chapter illustrates a probabilistic framework for the assessment of the scour hazard of bridges in a network, which is capable of using the data from scour monitoring systems installed only at critical bridge locations to improve the assessment of the scour in the other assets. In particular, the proposed framework is based on a Bayesian network (BN), which describes the conditional dependencies among the random variables (RVs) involved in the scour depth assessment at different bridges. Once a new observation on the scour depth or the flow discharge is available at a location, the BN is exploited to estimate and update the scour depth at unmonitored locations. This work constitutes the first application of BNs to bridge scour risk management.

The rest of the Chapter is organized as follows: Section 4.2 outlines the principal concepts of the Bayesian logic and BN, i.e., the probabilistic tool used for the scour hazard model. The in-depth review of past application of BN framework is presented in Chapter 2, precisely in Section 2.5. Section 4.3 illustrates the developed BN, the involved RVs, and the models employed to describe their conditional dependency. The section also explains how the BN is fed with observations from various monitoring systems and how this new information updates the variables of the network. Section 4.4 briefly describes the numerical algorithm employed to solve the BN and update the variables involved in the scour estimation. In section 4.5, we present and describe the case study used to demonstrate the functioning of the BN, consisting of bridges managed by TS in south–west Scotland. These bridges cross the same river, and the scour monitoring system is installed only on one of them. The outcomes of the application of the proposed framework to the case study are shown in Section 4.6. The Chapter ends with a conclusions and future works section.

4.2 Bayesian statistical inference and model updating

Bayesian inference provides a general, rational, and robust approach for evaluating the structure condition or judge sensor and model performances, by taking into account all the sources of uncertainty relevant to the problem. Usually, information about a monitored structure might come from different sources, such as observations collected by sensors, design documentation of the structure, inspections and test reports or engineering judgement (Cappello, 2017).

The inverse problem of estimation of the parameters of a model is tackled by treating them as uncertain and using available data to update their probabilistic distribution. Hence, this approach constitutes an accumulation of knowledge (Bolstad, 2004). Equation (4.1) illustrates the expression of the Bayes' theorem for the problem of updating of state variables

distribution:

$$p(state|data) = \frac{p(data|state) \cdot p(state)}{p(data)}, \tag{4.1}$$

where the probability $p(state)$ is called prior probability and represents the perspective of the state prior to the collection of data. The probability $p(data|state)$ is called likelihood of the observed data. Analogously, $p(state|data)$ is called the posterior probability of the state because it is the updated belief after new information is gained through observed data. The denominator $p(data)$ is a normalising factor called evidence, which must be calculated by integrating over the parameter space through application of the Total probability theorem.

4.2.1 Bayesian network

A Bayesian network, developed by Judea Pearl in 1985, is a graphical model using a directed acyclic graph to represent a set of RVs and their conditional dependencies (Jensen and Nielsen, 2007). Each RV, which can be discrete or continuous, is depicted by a node and the probabilistic dependency between two variables is represented by a link (Figure 4.1).

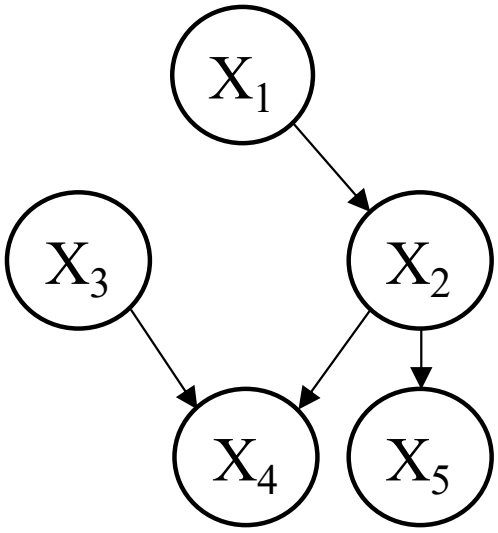

Figure 4.1: *An example of a Bayesian network*

In BN terminology, any node extending from another one is denoted as a child, while

the inverse relationship defines a parent node. Nodes without parents are known as root nodes and are described by their probability density function (pdf), which, in Bayesian terms, can be understood as their prior pdf.

Two forms of probabilistic inference can be carried out in BNs: predictive analysis that is based on evidence (i.e., information that the node is in a particular state) on root nodes, and diagnostic analysis, also called Bayesian learning, where observations enter into the BN through the child nodes (Ben Gal, 2007). The child node pdfs can be estimated from the roots' pdfs by performing predictive analysis, whereas Bayesian learning allows updating root node pdfs when new information enters into the BN through a child node.

When evidence enter into the BN, the piece of information is spread inside the network to update variable's probabilities through one of the two forms of inference mentioned above. In particular, the second approach, the Bayesian learning, is attractive when the analysed system is based on constantly evolving information, as in the case of a real-time monitoring system. Furthermore, BNs are well suited for representing knowledge under uncertainty. Uncertainties from variables, measurements and model itself can be implemented into the BN such as components of the model or even as an updatable node.

4.3 Bayesian network for scour estimation

This section illustrates the probabilistic framework used to update the scour depths at any location of a bridge network given the data from sensors monitoring scour only at critical locations. The rationale of this framework is the following: a scour monitoring system measures the scour depth at the pier of one bridge, and the piece of information is then extended to the other piers and the unmonitored bridges by exploiting the conditional dependence between the scour depths at different locations, as described by a BN.

The developed BN is based on BD 97/12 (Highway Agency, 2012), which is the procedure

followed by TS to assess the scour risk of their road bridges. This procedure can be divided into four steps: *(i)* assessment of the flow hydraulic properties; *(ii)* estimation of the constriction scour; *(iii)* estimation of local scour; and *(iv)* estimation of total scour. In particular, starting from the river flow characteristics (such as river flow Q), different models are applied to estimate the depth of flow upstream of the bridge y_U, and the two components of scour, constriction scour (D_C) and local scour (D_L), whose sum is equal to the total scour depth D_T. For the purpose of developing the BN, model uncertainties are added to each model to describe the randomness of the estimation processes. Thus, each formula is structured in the following way:

$$x = f_x\left(y_1, \ldots, y_N\right) \cdot \left(1 + e_x + {}^{(j)}\, e_x\right), \tag{4.2}$$

where the model f_x estimates the variable x through the dependent variables $y_1, \ldots, y_N$, and e_x and ${}^{(j)}e_x$ are the two model uncertainties: the first one represents the random error of the equation, the second an additional error that is associated with the specific jth location (e.g., pier or bridge). Both type of model uncertainties embraces the uncertainty of individual parameters involved (e.g., hydraulic parameters or bridge and pier geometry) so that defining a single error node (i.e., one correlated and j uncorrelated) for each uncertain model. Every RV representing model uncertainty is set to be a root node of the BN, and thus is described by assigning to it a prior pdf. These pdfs are expressed as Normal distributions with zero mean and a standard deviation (SD). The RVs ${}^{(j)}e_x$ are assumed to be independent and identically distributed for the different piers. The values of SD are assumed by considering previous work found in the literature; however, a sensitive analysis demonstrates that the results are not affected by initial parameter values (e.g., the changes are within a ±3–5% range). In fact in Bayesian statistic, the effect of the chosen prior is always small compared to the data (Bolstad, 2004).

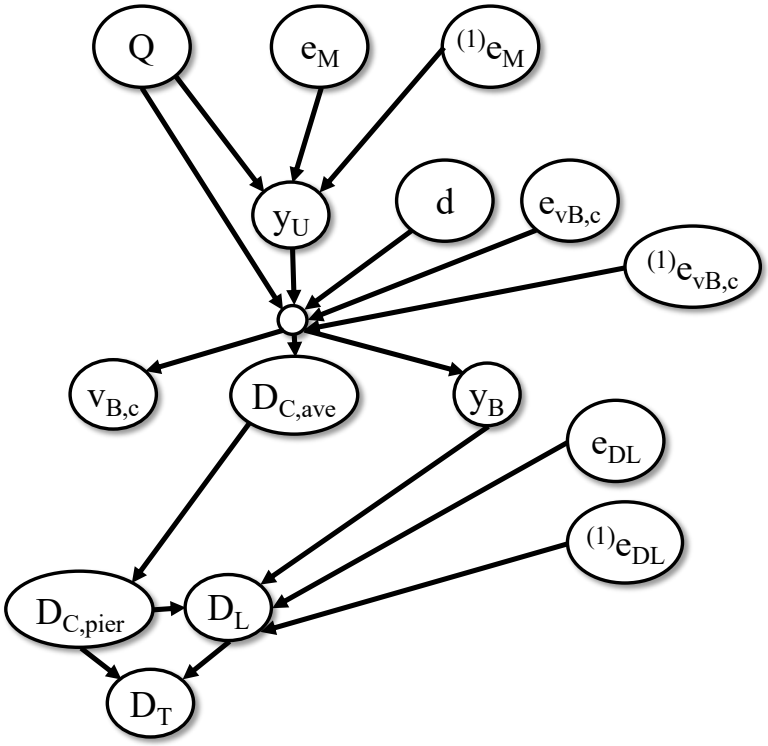

Figure 4.2: *BN for scour estimation at a single bridge location. Q: water flow; y_U: depth of flow upstream the bridge; $v_{B,C}$: scour threshold velocity; d: bed material grain size; $D_{C,\text{ave}}$: average depth of constriction scour; y_B: depth of flow below the bridge; $D_{C,\text{pier}}$: depth of constriction scour at the pier; e_x and ${}^{(j)}e_x$: model uncertainties applied to the estimation models*

Figure 4.2 illustrates the BN for the problem of scour assessment at a single bridge pier. The models employed in the four steps of the assessment procedures are described more in detail in the following subsections.

Flow analysis

Manning equation (Equation 4.3) is used to describe the relationship between Q and y_U.

$$y_U = \left(\frac{Q\, n}{B_B\, s^{1/2}} \right)^{3/5} \left(1 + e_M +^{(j)} e_M\right), \tag{4.3}$$

where n is the Manning coefficient; B_B is the channel width at bridge opening and s is the channel slope. Two model uncertainties are employed: e_M is the correlated model error of the Manning equation and ${}^{(j)}e_M$ is the uncorrelated model error in the jth bridge. The SD of each error is chosen equal to 0.10 in order to define a total SD corresponding to 0.15, as shown in the work presented in Tinkler (1982).

Constriction scour

The reduction of channel width due to the presence of bridge piers or abutments leads to an increase of the water velocity v_B. When the velocity reaches the critical value $v_{B,c}$ (i.e., threshold velocity below which scour does not occur), the erosion of the riverbed starts. The equilibrium (i.e., the final scour hole) is reached when the increase in cross section area of flow for constriction scour is such that $v_B < v_{B,c}$.

A nonlinear system of three equations in three variables is developed to estimate the constriction scour depth. Q, y_U and the bed material grain size d are the input parameters of the system that enable us to evaluate the average constriction scour $D_{C,ave}$, the water level through the bridge y_B, and the threshold velocity $v_{B,c}$. The nonlinear system consists of the Colebrook–White equation, (Equation 4.4.a) (Kirby *et al.*, 2015), the conservation of fluid mass (Equation 4.4.b), and the Bernoulli equation (Equation 4.4.c):

$$\begin{cases} v_{b,c} = -\sqrt{32}\, v_0(d) \cdot \log_{10}\left(\dfrac{d}{12\ y_0} + \dfrac{0.222\ \nu}{y_0 \cdot v_0(d)}\right)\left(1 + e_{v_{B,c}} +^{(j)} e_{v_{B,c}}\right) & (4.4.a) \\ Q = v_{B,c}\ y_0\ B_B & (4.4.b) \\ y_U + \dfrac{(Q/y_U\ B_U)^2}{2\ \mathrm{g}} = y_B + \dfrac{v_{B,c}^2}{2\ \mathrm{g}} & (4.4.c) \end{cases}$$

where y_0 is the local flow depth including the constriction scour depth (i.e., $y_0 = y_B + D_{C,ave}$), $v_0(d)$ is the shear velocity at the threshold of movement and ν is the kinematic viscosity of water (Kirby *et al.*, 2015). The nonlinear system is represented through an empty node (see

Figure 4.2), thus avoiding showing all the intermediate nodes for the sake of visualisation.

The last two equations are considered deterministic; therefore, the model errors are added to the Colebrook–White equation alone: the correlated, $e_{v_{B,c}}$ (i.e., it is the bias of the Colebrook–White equation) and the uncorrelated error, ${}^{(j)}e_{v_{B,c}}$ (i.e., it is the error in the estimation in the jth bridge). The total SD is set equal to 0.15 — following the analysis carried out in Johnson *et al.* (2015) — and it is split equally between the two types of model uncertainties meaning that their SDs are equal to 0.10 each.

Table 4.1: *Constriction scour distribution factor F_S (Highway Agency, 2012)*

Location	**Outside of bend**	**Centre of channel**	**Inside of bend**
On or downstream of sharp bend	2	1.25	1
On or downstream of moderate bend	1.5	1.25	1
On straight reach	1.25	1.25	1.25

The previous step of the BN provides the average value of the constriction scour $D_{C,ave}$; this value is then multiplied by a factor F_S to obtain the constriction scour depth along the channel width. Table 4.1 provides the values of F_S according to the shape of the river and Figure 4.3 shows the two scenarios described in the table. In order to include all the cases of Table 4.1, we define the constriction scour depth at the pier $D_{C,pier}$ or, generally, the constriction scour at every location of the river as:

$$D_{C,pier} = D_{C,ave}\left(1 + e_{F_S} + e_{D_{C,ave}}\right). \tag{4.5}$$

To be consistent with the structure of Equation (4.2), two types of errors can be modelled for including the multiplication factor F_S in the estimation of D_C across the channel width. The two errors are again expressed as a normal pdf with zero mean and a SD. According to Table 4.1, we define $e_{D_{C,ave}}$ that is the error in the calculation of $D_{C,ave}$ itself, which occurs when the reach is either straight or bended. The second error is e_{F_S}, which takes into account the error in the scour estimation where the river bends, i.e., it takes into account

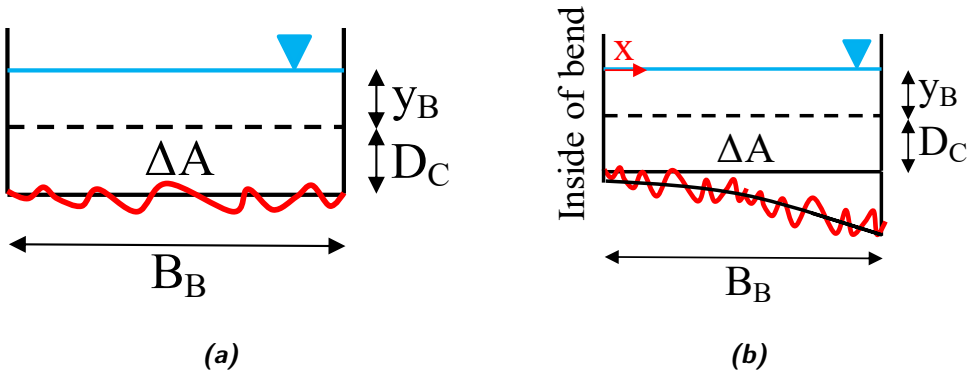

Figure 4.3: *Channel section with constriction scour depth profile in a* ***(a)*** *straight and* ***(b)*** *bended reach. ΔA is defined by BD97/12 as the increase in cross section area of flow due to constriction scour*

the additional component due to bend scour. This contribution to total scour is caused by the increase in velocity around the outside of the bend (Kirby *et al.*, 2015). Table 4.2 provides the two parameters defining the Normal pdf for the two errors in both limit cases.

Table 4.2: *Parameters of Normal pdfs defining the errors for constriction scour*

Location	$e_{D_{C,ave}}$	e_{F_S}
On bended reach	$\mathcal{N}(0, 0.25)$	$\mathcal{N}(0, [(x/B_B)^2 - 0.25])$
On straight reach	$\mathcal{N}(0, 0.25)$	0

Local scour

The formation of vortices at pier base is the principal mechanism causing the local scour (Lagasse *et al.*, 2007), and the pier width W_P is the primary controlling parameter, which is corrected by some factors depending on its shape, its inclination with respect to the river flow, and the local water level. The expression of the local scour depth according to Highway Agency (2012) is:

$$D_L = 1.5\, W_P\, f_{PS}\, f_{PA}\, f_y \left(1 + e_{D_L} +^{(j)} e_{D_L}\right), \tag{4.6}$$

where f_{PS} is the shape factor, f_{PA} is the pier alignment factor and f_y is the flood depth factor. Two model uncertainties are again added: the correlated one, e_{D_L} (i.e., the bias in the equation itself) and the uncorrelated one, ${}^{(j)}e_{D_L}$ (i.e., the error in the estimation in the jth pier). The total SD is set equal to 0.30 and divided equally between the two model uncertainties. The value of the prior SD is again taken from the work presented in Johnson *et al.* (2015).

Total scour

The depth of total scour D_T is simply the sum of the two components, constriction scour depth D_C and local scour depth D_L. This expression is assumed as deterministic, consequently no model uncertainties are added:

$$D_T = D_C + D_L. \tag{4.7}$$

4.3.1 Bayesian learning

With reference to the presented BN, it is assumed that three quantities can be monitored, that is, the river level upstream of the bridge y_U, the total scour depth D_T, and the constriction scour D_C^* in the middle of the channel. Environmental agencies can provide water level data from gauging stations while a wide range of SHM sensors can be employed to detect scour (Anderson *et al.*, 2007; Lin *et al.*, 2006; Michalis *et al.*, 2015; Prendergast and Gavin, 2014; Yu and Yu, 2009); therefore, a scour monitoring system can provide data about the two scour depths. When new observations become available, the BN model is used to propagate the new piece of information through the network and update probabilities (Jensen and Nielsen, 2007).

The solution of the BN can be broken down into three steps:

(i) defining the prior pdf of the root nodes, (grey nodes in Figure 4.4a): water flow Q,

grain size d, the correlated model uncertainties e_M, $e_{v_{B,c}}$ and e_{D_L} and the uncorrelated ones (not displayed in Figure 4.4a). Observations of y_U, D_C^* and D_T enter into the network (red nodes in Figure 4.4a);

(ii) splitting the BN into three sub-networks to have three different updating processes: y_U updates e_M; D_C^* and y_U update $e_{v_{B,c}}$ and d; D_T, y_U and D_C^* (through $D_{C,pier}$) update e_{DL} (Figure 4.4b);

(iii) updating the descendant nodes (light yellow nodes in Figure 4.4c).

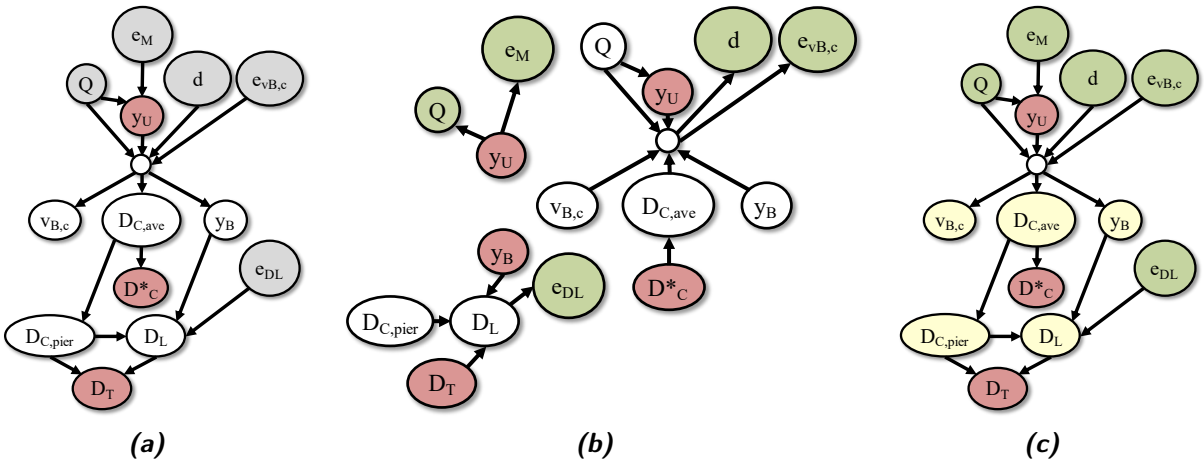

Figure 4.4: *Solution of the BN:* ***(a)*** *starting with prior pdfs;* ***(b)*** *updating of root nodes and;* ***(c)*** *descendant nodes.*

The BN can be extended to a second bridge with N piers because the scour estimation is based on the same models. For instance, Figure 4.5 shows a BN for scour estimation at two bridges, each of them with N piers. The estimation of the scour depth at the second bridge is based on the models corrected by the model uncertainty updated by direct observations of ${}^{(1)}D_C^*$ and ${}^{(1)}D_T$ at one pier of the first bridge. The three correlated model uncertainties are root nodes of each sub-network that represents a different bridge; these connections allow the BN to extend information gained from the scour monitoring system to each sub-network (i.e., unmonitored bridges) because the models used to estimate scour

depths are the same for any bridge. Consequently, the scour estimation at every pier is affected by the same correlated error.

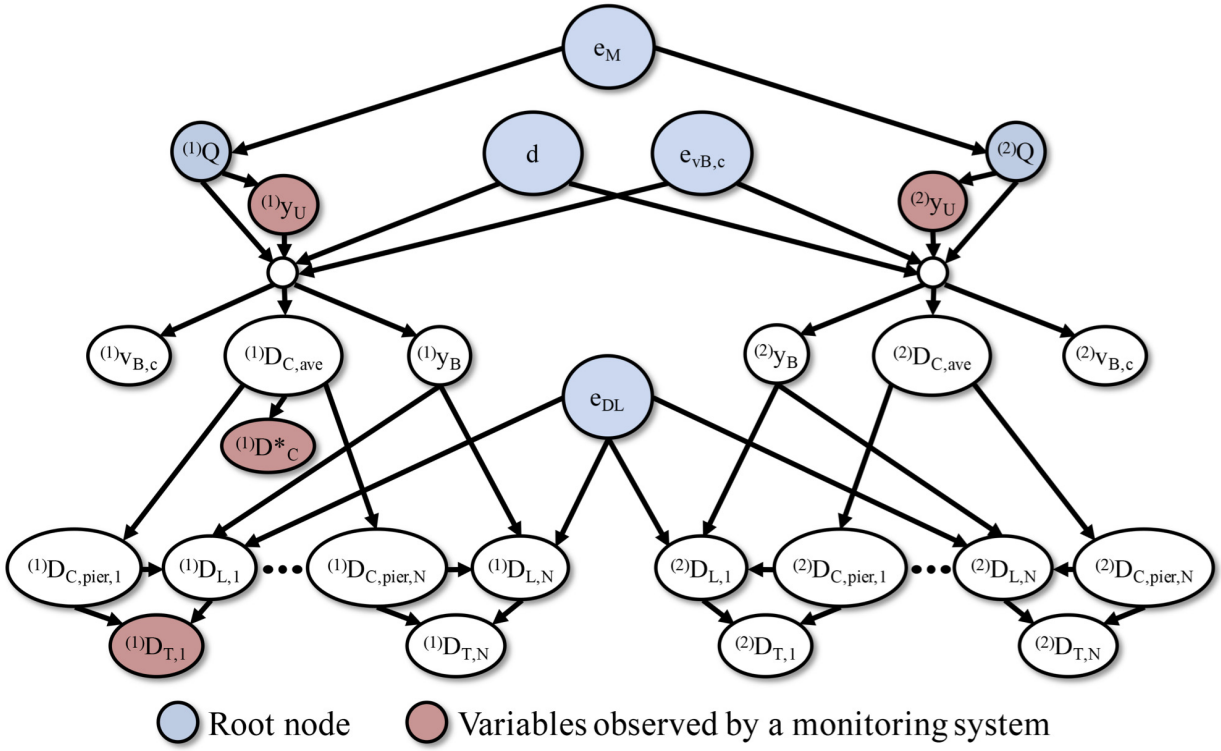

Figure 4.5: *BN for scour estimation at two bridges on the same river, both with N piers.*

It is worth mentioning that the above BN can be also used to perform predictive analysis, i.e., the first type of inference described in Section 4.2.1. As its name suggests, this analysis allows predicting the pdfs of the child nodes by starting from the prior pdfs of the parent nodes, without any observations entering the BN.

4.4 Numerical algorithm for model updating

Despite the numerous advantages associated with Bayesian Inference, its practical implementation involves some challenges, especially when continuous RVs are employed, as in the case of data collected by a monitoring system. A closed form solution of Equation (4.1)

is usually not available, and thus it is necessary to resort to numerical algorithms to calculate the posterior distribution's parameters (e.g., mean value vector and covariance matrix). Given this, Equation (4.1) can be rewritten as:

$$p(state|data) \propto p(data|state) \cdot p(data). \tag{4.8}$$

The class of algorithms belonging to the Markov chain Monte Carlo (MCMC) methods (Metropolis *et al.*, 1953) is a common choice when Bayesian inference must be carried out. These methods are a broad family of numerical algorithms that generate next sample values by performing a random sampling from the previous sample values. Their essential idea is using randomness to solve problems that might be deterministic in principle. Examples of these methods are Monte Carlo, Metropolis–Hasting and Transitional Markov chain Monte Carlo. These computer algorithms can be used to draw an (approximate) random sample from the posterior pdf, without having to completely evaluate it. The posterior pdf can be approximated to any accuracy level by taking a large number of samples.

The Metropolis–Hastings algorithm (Hastings, 1970) is the most used and simple approach to make inference for Bayesian parameter estimation. It allows to extract samples from the actual posterior pdf. However, the method has some disadvantages: it does not calculate the evidence, the required number of samples N might be huge in some cases, and it requires to always consider the burn-in period, i.e., a period after which the samples are independent from the starting choice of the parameter to estimate. In order to overcome the issues above, the transitional Markov chain Monte Carlo (TMCMC) method (Ching and Chen, 2007) has been proposed. In the TMCMC method, an iterative approach is used to generate samples from the unknown posterior distribution by changing the proposal pdf at each step until the target distribution is reached. Thus, n intermediate distributions p_j

are considered:

$$p_j \propto p\left(data|state\right)^{\beta_j} \cdot p(state), \tag{4.9}$$

where the index j denotes the step number. The likelihood function is scaled down by an exponent β_j, with $0 = \beta_0 < \ldots < \beta_j < \ldots < \beta_n = 1$. It is worth noting that this construction does not alter the Bayesian logic: the series of intermediate distributions starts from the prior pdf (i.e., $p_0 = p(state)$) and ends with the posterior (i.e., $p_n = p\left(state|data\right)$). The algorithm starts at the step j by generating samples from the prior pdfs using a Monte Carlo simulation. Then at the step $j + 1$, Markov chains with the Metropolis–Hasting algorithm are used to generate the p_{j+1} distribution, denoted by $\{state_{j+1,k} : \ k = 1, \ldots, N_{j+1}\}$, by choosing selected samples N_j taken from the p_j distribution, denoted by $\{state_{j,k} : \ k = 1, \ldots, N_j\}$, according to "plausibility weights", $w(state_{j,k})$, defined as:

$$w(state_{j,k}) = \frac{p\left(data|state_{j,k}\right)^{\beta_{j+1}} \cdot p(state_{j,k})}{p\left(data|state_{j,k}\right)^{\beta_j} \cdot p(state_{j,k})} = p\left(data|state_{j,k}\right)^{\beta_{j+1}-\beta_j} \tag{4.10}$$

where $k = 1, \ldots, N_j$. Before advancing to the next step, β_j is updated. The algorithm stops when β_j is equal to 1.

The TMCMC method is particularly convenient for dealing with complex joint pdfs (e.g., multimodal distributions) and does not require defining any prior proposal distribution or removing samples in the burn-in period. In Ching and Wang (2016), a comparison is made between the TMCMC and the Metropolis–Hastings algorithm, and the advantages of the former are highlighted.

4.5 Case Study

The functioning of the developed BN is demonstrated using a small bridge network, consisting of bridges managed by TS in south–west Scotland (Figure 4.6). The bridges cross the same river (River Nith) and only Bridge 1 is instrumented with a scour SHM system.

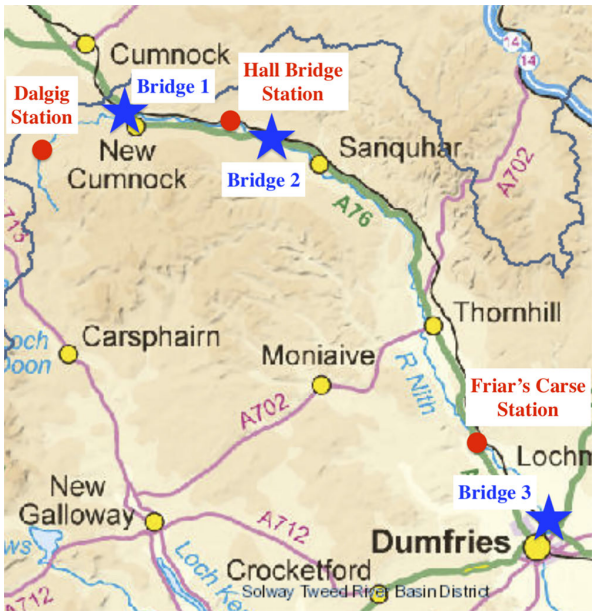

Figure 4.6: *Three bridges over the River Nith. Red circles represent environmental agency's gauging stations.*

The aim is to exploit the observations on Bridge 1 to update the pdf of the total scour depth at other bridge locations. Three bridges with significant scour events in the past are chosen from the TS scour database:

- *Bridge 1*: A76 200 Nith bridge in New Cumnock (Figure 4.7). It is a 3-span (9.1m, 10.7 m and 9.1 m) stone-masonry arch bridge, with two piers in the riverbed. Both the abutments and the piers are founded on spread footings on the natural riverbed.
- *Bridge 2*: A76 120 Guildhall bridge in Kirkconnel (Figure 4.8). It is a 3-span (8.8m, 11.3 m and 11.3 m) masonry arch bridge, with one pier in the riverbed. Both the abutments and the piers are founded on spread footings on natural ground, except one abutment's spread footing that is founded on rock.
- *Bridge 3*: A75 300 Dalscone bridge in Dumfries (Figure 4.9). It is a 7-span (spans of 35 m and two of 28 m) steel-concrete composite bridge, with one pier in the riverbed. Both the abutments and piers are founded on pile foundations on natural ground.

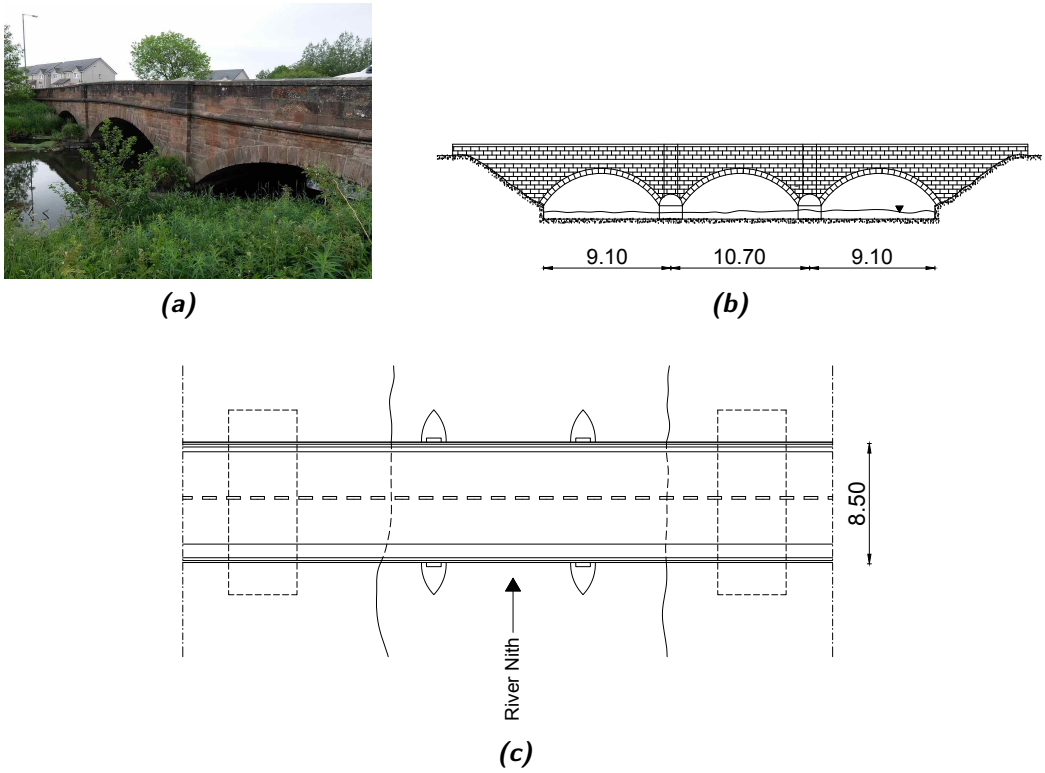

Figure 4.7: *(a) A76 200 Nith bridge, (b) bridge elevation and (c) and plan view*

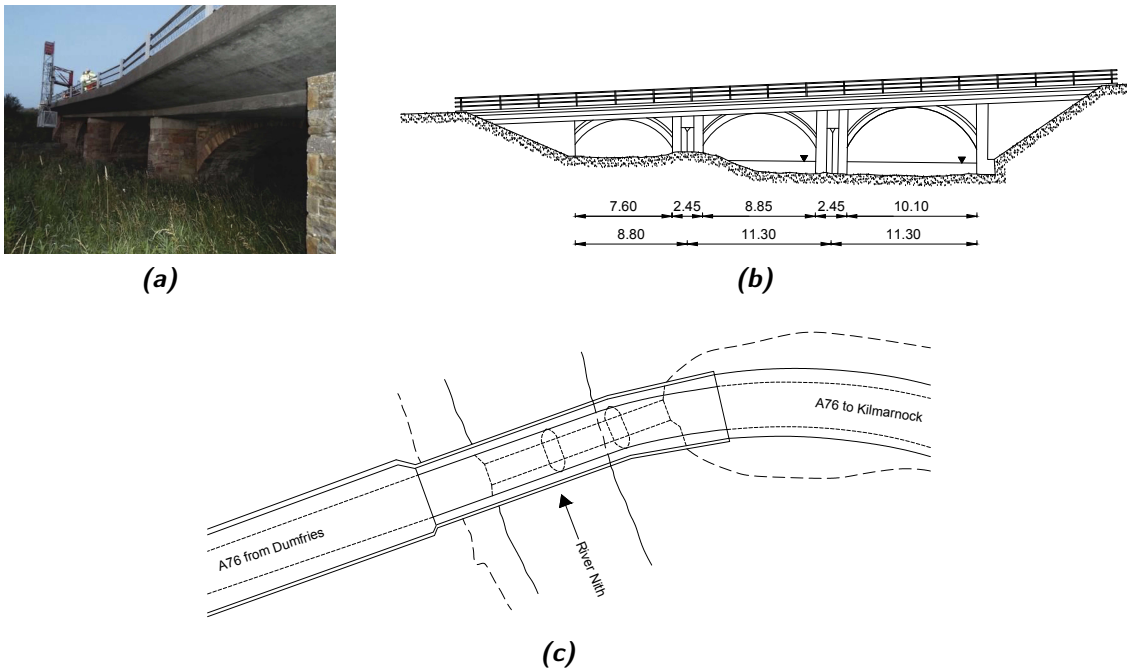

Figure 4.8: *(a) A76 120 Guildhall bridge, (b) bridge elevation and (c) and plan view*

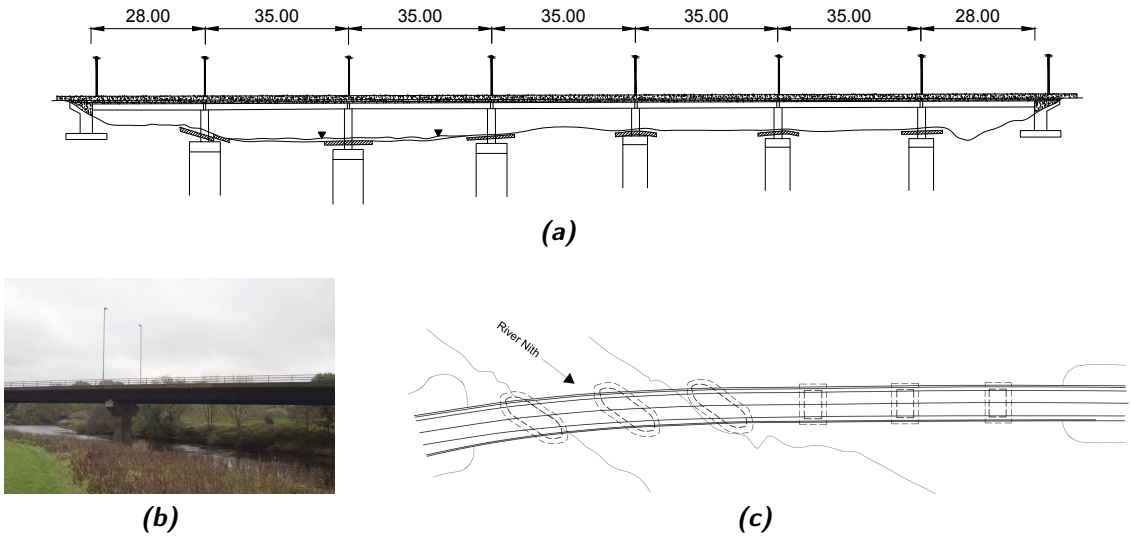

Figure 4.9: *(a) Bridge elevation, (b) A75 300 Dalscone bridge and (c) and plan view*

The final BN for the estimation of the total scour at every bridge pier is depicted in Figure 4.10. The subnetworks corresponding to the three bridges is identifiable; correlated errors and the bed material grain size are root nodes in common for all bridges. The river flow Q is not a common root node because the three bridges are far apart and numerous

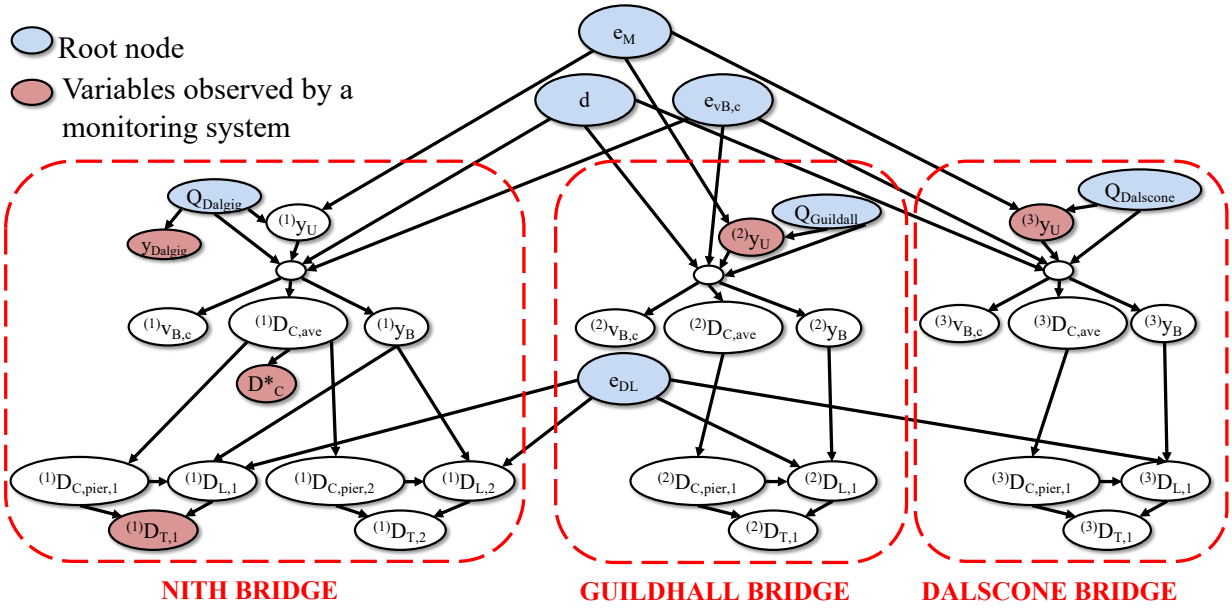

Figure 4.10: *BN developed for the case study*

tributaries of River Nith extend from Bridge 1 to Bridge 3. A model to correlate the river flow Q among the three subnetworks would introduce several uncertainties that are difficult to quantify. Furthermore, there is a gauge station measuring the flow before each bridge; therefore, upstream water flow data are available for each of the bridges.

4.6 Results

Normal pdfs are employed for every variable except for river flows, which are described by a log-normal pdf because the discharge cannot be negative. The parameters of the log-normal pdfs (i.e., mean and standard deviation of logarithmic values) are based on the gauging station data of the last ten years collected by the Scottish Environmental Protection Agency (SEPA). They are shown in Table 4.3 while Figure 4.11 depicts the pdfs

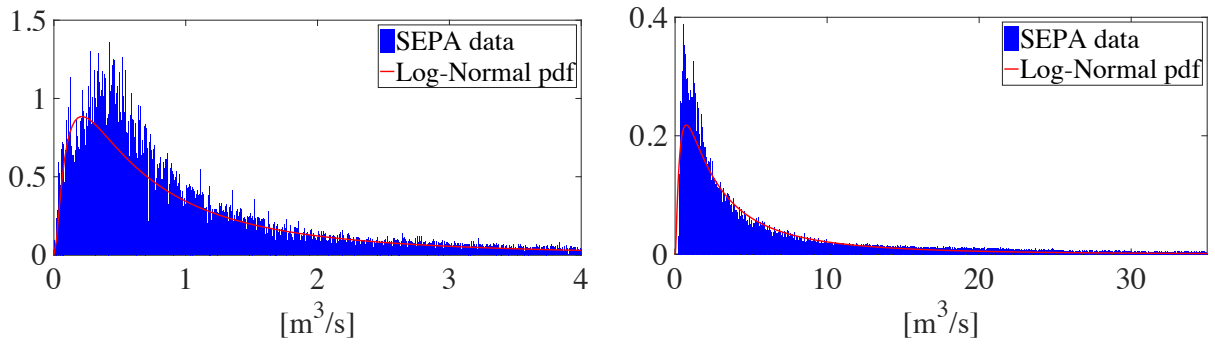

(a) *Dalgig gauging station*

(b) *Hall Bridge gauging station*

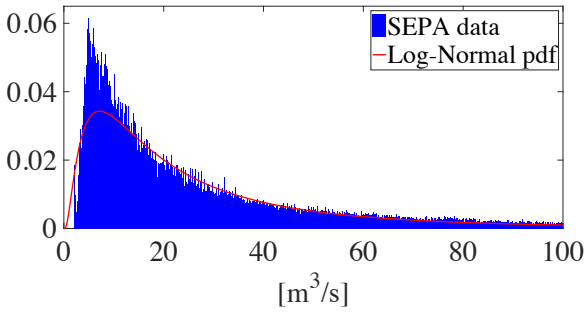

(c) *Friar's carse gauging station*

Figure 4.11: *Prior log-normal pdfs of the river flow*

fitting the data. The prior pdfs of the model errors are set as Normal distributions with zero mean and SDs defined previously.

Table 4.3: *Parameters defining water flow's prior pdfs based on SEPA's data*

SEPA gauging station	**Bridge**	$\boldsymbol{\mu}$ $[\boldsymbol{m^3/s}]$	$\boldsymbol{\sigma}$ $[\boldsymbol{m^3/s}]$
Dalgig	Nith	-0.281	1.1261
Hall Bridge	Guildhall	1.1126	1.2021
Friar's carse	Dalscone	2.9539	0.9925

The predictive analysis is carried out by running a Monte Carlo simulation. This type of analysis requires only the parent nodes' prior pdf and no observations enters into the BN to make a prediction of the distribution of the child nodes. A total of 10,000 samples of the root nodes pdfs is considered to estimate the prior pdf of the total scour depth $D_{T,pr}$ at each pier. The mean value, $\mu_{D_{T,pr}}$, and the SD, $\sigma_{D_{T,pr}}$, of the predictions are summarized in Table 4.4. It can be observed that the scour depth distributions at the various piers are characterized by a significant dispersion, with SD values of the order of 0.75 m.

Table 4.4: *Total scour depth prediction ("a priori") from the predictive analysis*

	Nith		**Guildhall**	**Dalscone**
	Pier 1	**Pier 2**	**Pier 1**	**Pier 1**
$\mu_{D_{T,pr}}$	1.979	1.992	2.297	1.855
$\sigma_{D_{T,pr}}$	0.739	0.762	0.798	0.752

The Bayesian learning is simulated by assuming that observations are available for the river levels y_U upstream of the three bridges, and for the contraction and total scour depth at pier 1 of A76 200 bridge. Table 4.5 shows the peak values recorded at the gauging stations, simulating a heavy flood scenario. The scour data are assumed equal to 0.20 m for constriction scour depth D_C^* and 0.45 m for total scour depth D_T.

The TMCMC algorithm (Ching and Chen, 2007) is then used to perform the Bayesian

Table 4.5: *Case scenario for river level observations*

SEPA gauging station	**Bridge**	**Water level [m] 12/30/13**
Dalgig	Nith	1.879
Hall Bridge	Guildhall	3.015
Friar's carse	Dalscone	1.512

learning analysis and update the root nodes. 1,000 samples are extracted at each stage of the TMCMC method, and this is repeated 100 times for each updating to eliminate the influence of randomness. To solve the whole network, five updates have to be performed. Each update is connected to one observed variable (i.e., water flow upstream of each bridge, constriction scour depth ${}^{(1)}D_C^*$ and local scour depth ${}^{(1)}D_T$ at first bridge). Considering that each TMCMC application requires on average seven stages, the number of extracted samples, which corresponds to how many times the calculation of the likelihood function is performed, is equal to $5 \times 100 \times 7 \times 10{,}000 = 3{,}500{,}000$ samples.

Figure 4.12 shows the comparison between the results of the total scour depth D_T obtained "a priori" with a Monte Carlo simulation (i.e., predictive analysis) and the estimations obtained after the Bayesian Learning with a TMCMC method. With regards to A76 200 Bridge, the total scour depth at pier 2 has a mean value equal to the one measured at pier 1 (Figure 4.12). This is indeed the most probable result, since the piers belong to the same bridge, have the same geometry, and the riverbed material and the water conditions are identical for them. However, it can be observed that while the value of the scour depth at pier 1 is known deterministically (assuming that the measurement is affected by no uncertainty), the one at pier 2 is uncertain, with a SD of 0.17 m. It is noteworthy that this value is significantly lower than the one corresponding to the prior pdf (0.76 m). This decrease of dispersion, of about 80%, is the result of the added information and the high correlation existing between the scour depths at the two piers of the bridge.

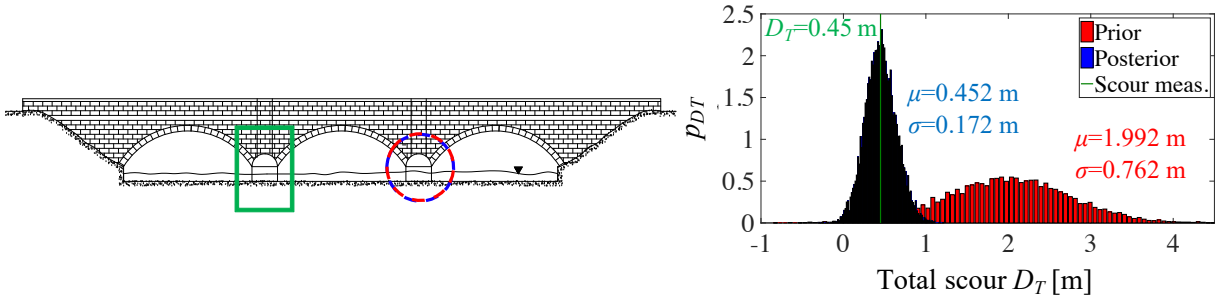

(a) *Pier 2 of Nith Bridge*

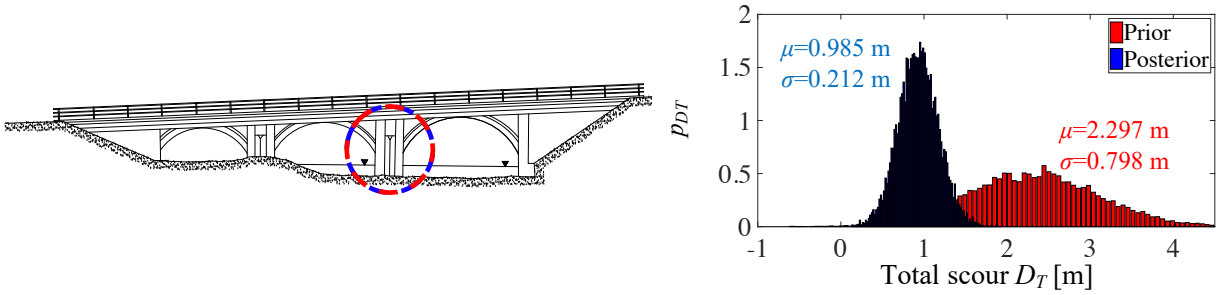

(b) *Pier 1 of Guildhall bridge*

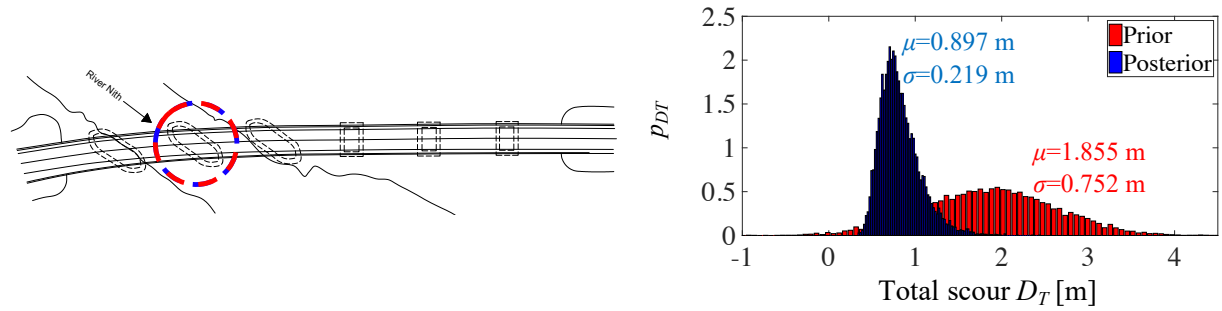

(c) *Pier 1 of Dalscone bridge*

Figure 4.12: *Comparison between prediction and estimation of total scour depths*

It can be observed in Figure 4.12b and c that the Bayesian learning allows the updating of the estimates of the total scour depth D_T at the piers of unmonitored bridges. In fact, the mean values of the total scour depth at these piers reduce significantly. Moreover, the standard deviations of the posterior distributions are close to 0.21m, which constitutes a significant reduction (more than 70%) of uncertainties compared to the prior estimates.

4.7 Conclusions

This Chapter shows the development of a probabilistic framework for scour hazard assessment that uses limited data from monitoring systems to update the probability distribution of the scour depth at the foundations of bridges in a network. The proposed framework is based on a Bayesian Network that describes the conditional dependencies between the scour depth at different piers within the same bridge or belonging to other bridges in the network. Once new observations on the river flow characteristics and/or scour data are available, Bayesian learning with a Transitional Markov Chain Monte Carlo algorithm is used to update the scour depth distribution at unmonitored locations.

A case study consisting of three bridges managed by Transport Scotland in south–west Scotland is considered to demonstrate the functioning of the BN. The bridges cross the same river, and only one bridge (Bridge 1) is instrumented with a scour monitoring system. The aim is to exploit direct observations of total scour depth D_T and the constriction scour D_C^* measured at Bridge 1 in order to predict the scour depth at other unmonitored piers. A flood event is simulated using river level data from gauging stations upstream of the bridges. It is shown that the available limited data from the scour monitoring system and the flow depths allow to increase significantly the precision of the scour estimates at unmonitored bridge piers. This reduction of uncertainties is in the order of 70%.

The implementation of real-time measurements of scour depth in the presented probabilistic framework will be addressed as further work. For the purpose of future work, a pilot scour device based on electromagnetic measurement has been developed at the University of Strathclyde. A pilot monitoring system, consisting of two probes, has been installed at A76 200 Nith Bridge and the measurement of the constriction and local scour will be used to update in real-time the estimates of the scour depth at other locations of the bridge network.

The only way to validate the estimates of the total scour depth at the piers of the unmonitored bridges would be to measure the scour after an event. In the next months, three more scour sensing probes will be installed at two other bridges. One candidate is the Whitehill Bridge (A76 100) in Sanquhar (i.e., it is a small village close to New Cumnock), which is over the River Nith and with one pier in the riverbed. Thus, the measurements from these probes will be also used to validate the scour estimates provided by the BN.

Furthermore, the impact of "monitored" nodes of the BN (i.e., water levels and scour depths) in the estimation of scour depth in unmonitored bridge will be studied as future work. An analysis will be carried out to investigate the sensitivity of the scour estimates (and in turn the scour risk classes) to bulk change in water flow rate or monitored scour depth. Finally, future research will also consider the extension of the BN with structural models, allowing to incorporate also information from sensors mounted on the bridges, such as accelerometers or inclinometers.

CHAPTER 5

SHM-based decision support system for bridge scour management

Abstract

Scour induced by river floods is the leading cause of bridge failure worldwide. Practical applications of scour monitoring systems are limited, but recent developments in sensor technology have resulted in more structures being instrumented and monitored. Alongside the development of structural health monitoring system for bridge scour, there is also a need of techniques to handle the data obtained from them and provide bridge owners and managers with useful information for optimal management of bridge scour risk. This Chapter illustrates the development and application of a decision support system (DSS) for bridge scour management, which is based on a probabilistic framework for the estimation of the scour risk, enhanced by real-time information from scour monitoring systems and in line with the current risk classification used by transport agencies. The proposed DSS can be used to produce measurement-informed thresholds triggering bridge closure to traffic under heavy floods. The application of the DSS is illustrated by considering as case study three bridges at risk of scour managed by Transport Scotland in south–west Scotland. It is shown that the proposed decision support system provides transport agencies with a real-time classification of the bridge scour risk. Moreover, the information from scour sensors allows

a reduction of the uncertainty in the scour estimates and results in higher values of the critical scour level at the bridge triggering closure to traffic compared to the one defined by transport agencies based on current risk rating procedures.

5.1 Introduction & background

Bridge scour is the excavation and removal of material from the bed of streams around bridge foundations as a result of the erosive action of flowing water. Scour process is classified according to the circumstances and structures that have caused it, and in general the following types of scour need to be considered at a bridge site: *(i)* degradation scour, *(ii)* constriction scour and *(iii)* local scour. The different type of scour are deeply described in Section 2.2.

In the UK, according to van Leeuwen and Lamb (2014), scour was identified as the most common cause of 138 bridge failures in 1846-2013. In contrast, in the United States, it has been recognised as the number one cause of bridge failure with an average annual rate of 22 bridges collapsing or being closed due to severe deformation (Briaud *et al.*, 2007). Moreover, a review of bridge collapses in the US in the 1990s carried out by Wardhana and Hadipriono (2003) has shown that the combined figure of 266 flood/scour-related cases constitutes the most dominant bridge failure cause (53% of the total cases of failures). Furthermore, the UK Climate Change Risk Assessment (CCRA) has identified scour bridge failures as one of the principal climate change risks for the transport sector (Thornes *et al.*, 2012).

Procedure BD 97/12 (Highway Agency, 2012) is used by Highways England and TS for evaluating the scour risk of railway and road bridges. The application of this procedure results in a scour risk classification of bridges based on an essentially deterministic approach, which estimates the scour risk with a prefixed flood scenario (e.g., the 1 in 200 years flood), and disregarding the various uncertainties that may characterize the problem (Johnson

et al., 2015; Pizarro and Tubaldi, 2019; Tubaldi *et al.*, 2017).

Transport agencies are also responsible for producing an action plan describing how they must respond to the threat of adverse weather. For instance, TS's decision of whether to close a bridge to traffic or not is based on the comparison between the water level at the upstream section of the bridge and the critical water level, represented by a marker installed on the bridge. Nevertheless, the critical water level cannot be directly associated to a precise level of scour at the bridge foundations, because there is a weak correlation between water level and scour depth due to many uncertainties that affect the problem (Pizarro and Tubaldi, 2019; Tubaldi *et al.*, 2017). Moreover, the probability of collapse of the bridge due to scour may differ significantly from the probability of exceedance of the critical water level (Pizarro *et al.*, 2020).

Hence, current scour risk management approaches could be improved *(i)* by adding a more explicit consideration of the various sources of uncertainty that affect the problem, thus enabling the shift from a deterministic to a probabilistic evaluation of the scour risk, and *(ii)* by integrating in the risk assessment the observations from scour sensors, allowing the reduction of the uncertainty in the scour risk estimates, and thus helping bridge operators in taking the optimal decisions concerning bridge scour risk management.

Structural health monitoring (SHM) sensors can significantly help to support risk mitigation strategies and decision-making processes under flood events, by allowing measuring more precisely the extent of scour at bridge foundations. However, alongside the development of SHM scour system, there is a need of techniques to handle the data obtained from them and provide bridge owners and managers with useful information for optimal management of bridge scour.

In this Chapter, a Decision Support System (DSS) is developed for road bridge scour management, which extends and complements current scour risk rating procedures and action plans of UK transport agencies. The propose DSS is based on a more fair and

accurate bridge assessment of the scour risk that reflects the uncertainties characterising the problem and allows the integration of real-time measurements of the scour depth in the decision-making process. The DSS also produces measurement-informed thresholds triggering bridge closure to traffic under heavy floods.Although earlier work on DSS, SHM and scour estimation methods have been singularly presented and SHM-based DSS were developed as well (Cappello *et al.*, 2016; Verzobio *et al.*, 2018), this is the first application of an SHM-based DSS for scour risk management of bridges.

The rest of the Chapter is structured as follows. Section 5.2 outlines only the principal concept of SHM-based decision-making processes (for a detailed state-of-the-art refers to Section 2.6). Section 5.3 briefly presents the scour risk management procedure currently followed by TS. Section 5.4 is broken down into two subsections: the first one illustrates how the developed DSS can complement the rating of bridge at scour risk while the second subsection presents the SHM-based scour thresholds, and outlines how they can inform decision in the bridge management. Section 5.5 describes the application of the DSS to a case study, and discusses the achieved outcomes. The Chapter ends with a conclusion and future works section.

5.2 SHM-based decision making

Visual inspections carried out at regular intervals are the predominant non-destructive evaluation technique used in bridge management to check the state of any bridge component (Moore *et al.*, 2001), but nonetheless, they are characterized by many drawbacks. Visual inspections are subjective, depending on the inspector's experience, their reliability might be affected by several factors (Megaw, 1979) and, above all, they are in general expensive and time-consuming.

A way to overcome these limitations is to install SHM systems, which are methods

aiming to provide a reliable diagnosis of the condition of structural components or the whole structure (Balageas *et al.*, 2006). The main benefits of SHM systems over visual inspections stem from their capacity to provide objective and quantitative information about the monitored structure, and to furnish continuous data about the structural state, even during extreme events such as an earthquake or floods (Farrar and Worden, 2007).

Although several studies have recognised the benefit of SHM campaigns (Pozzi and Der Kiureghian, 2011; Zonta, Glišić and Adriaenssens, 2014; Flynn and Todd, 2010*b*), asset owners and managers are still doubtful about the benefit of the deployment of SHM systems. They may prefer to undertake retrofitting work instead of investing in these systems, especially if they have a limited budget. The reasons are mainly two: first, the managers tend to act based on their experience because it is still unclear how an assets manager should practically make SHM-based decisions (Cappello, 2017); second, and it might explain why they are sceptical, SHM outputs are affected by several and severe uncertainties, which are often hard to quantify (Verzobio *et al.*, 2018).

A typical workflow to decision-making based on SHM is: *(i)* sensors are deployed on the structure; *(ii)* the SHM data are analysed; *(iii)* an algorithm recognises potential damage, and provides information on performance and structural health; *(iv)* the manager in charge makes the decision about to repair damage or not. SHM consists of the first three steps, while step four refers to decision-making (Cappello *et al.*, 2016). SHM is about monitoring the structure and acquiring information about its condition while decision-making is about choosing the optimal action based on this information. In fact, only part of the SHM data is normally used in the decision process. Thus, SHM-based decision support systems are frameworks aiming to provide suggestions for the structure management by taking the SHM data as an input and converting them into information for the manager (Wenzel, 2008).

Two examples of decision theories widely utilised in economy and finance, but recently becoming popular in civil engineering decision problems are the expected utility theory (von

Neumann and Morgenstern, 1953) and prospect theory (Kahneman and Tversky, 1977).

5.3 Current procedures for scour risk assessment and management

In the UK, Transport Scotland carries out the assessment of the scour risk at highway and railway structures in accordance to the Procedure BD 97/12 (Highway Agency, 2012). The procedure provides the scour estimation models before a flood event and a bridge scour risk classification through a scour vulnerability index.

The input parameter in the classification is the relative scour depth D_R, (i.e., the ratio between the total scour depth D_T and the foundation depth D_F). Furthermore, a priority factor PF enters the risk rating to account for several factors, such as the history of scour problems, the type of foundation and the importance of the bridge (i.e., vehicle traffic volume). TS classification consists of five classes, and bridges with the highest priority fall into class 1. Moreover, when a bridge is categorised into category 1 or 2, it is considered at high scour risk.

TS therefore defines a plan (Transport Scotland, 2018) describing the actions to be taken during or after the occurrence of a flood event and furnishing a systematic and structured approach to how to respond to the threat of adverse weather. The scheme identifies triggers that determine what actions needs to take place, with a "visual" decision scheme based on water level markers placed on the bridge upstream surface. When the water level exceeds these markers, specific actions must be taken. For instance, one action could be the closure of the bridge to traffic. After the closure, a structure inspection is undertaken, including underwater parts and the riverbed, when it is safely practicable to do so. The bridge may be re-opened to traffic once water levels have reduced sufficiently and only if there are no visible signs of deformation or structural distress. No direct or indirect measure of

the actual scour depth enters the decision process until water levels have receded so that inspectors can safely carry out checks.

TS's structures vulnerable to scour are provided with two different marker plates, the Flood Level Marker (FLM) plate that corresponds to the 1 in 200 year flood level according to the BD 97/12. The Red Plate is installed at the level of the bridge soffit in those structures where the 1 in 200 year flood level is higher than this. This marker is installed as a warning for deck uplifts (Transport Scotland, 2018).

In summary, the action plan specifies that any bridge at high-risk ought to be closed when the water level attains a critical threshold at which the structure is considered to be at risk of scour. The threshold's choice is conservative by nature in order to ensure road users safety by closing the bridge before the water rises to a level at which serious scour is expected to occur. However, this plan does not take into account the temporal evolution of the scour process. For example, in the case of live-bed scour condition, sediment may be partially redeposited in the scour pit when the flood event finishes (Hamill, 1999). Thus, a scour measure carried out at the end of a flood may not record the maximum scour that occurred during the event as the scour hole might have partly filled during the recession (Melville and Coleman, 2000).

Furthermore, scour depth formula are based on laboratory experiments and it is assumed that the designed flood acts over an infinite duration (Pizarro *et al.*, 2020). Conversely, real flood events are characterised by different hydrograph magnitude and duration. Therefore, high-flow events (i.e., corresponding to a high-water level) may not necessarily result in the development of a significant scour hole, especially if they have a short duration. Moreover, bridges are exposed to sequences of events, each potentially contributing to scouring. Thus, their safety could be jeopardized by the progressive accumulation of the excavations under multiple events with low return period (i.e., water levels below the FLM) occurring in sequence, as was the case of the Lamington viaduct (Rail Accident Investigation Branch,

2016).

For these reasons, the water level can be considered only a very rough indicator of the scour risk, also considering that no measurement of scour enters the action plan until the river flow and level are considerably reduced, thus allowing the diver teams to safety check the bridge foundations.

5.4 Proposed scour risk classification and DSS

The evaluation of the scour risk of bridges is a complex problem, involving many aleatoric and epistemic uncertainties. Probabilistic frameworks have been presented over the years to incorporate the effect of these uncertainties (Brandimarte *et al.*, 2006; Johnson *et al.*, 2015; Pizarro and Tubaldi, 2019; Tubaldi *et al.*, 2017). Comparisons between scour estimates according to formulas embedded in current assessment procedures and actual scour depths observed on site have shown that the first may be significantly biased on the conservative side (Johnson *et al.*, 2015). Thus, these overestimated scour depths might cause a misclassification of the bridge scour risk and even bring to unnecessary bridge closure as a precautionary action. Furthermore, a visual inspection is requited to re-open the bridge to traffic, and the structural integrity of the foundations can only be determined by a tactile inspection performed by a dive team. This inspection is extremely expensive and time-consuming because it cannot be carried out until the flow recedes and permits safe entry to the watercourse. Consequently, the bridge may have to be closed for many days, thus resulting in significant downtime.

This section illustrates a decision model for scour early warning risk management incorporating: *(i)* the various sources of uncertainty inherent to the hydrological and hydraulic parameters as well as the models employed for evaluating the scour depth at a bridge, and *(ii)* the information from scour sensors, leading to an uncertainty reduction. In

particular, the proposed decision model uses the probabilistic framework for bridge scour hazard assessment presented in Chapter 4, and the same classification scheme of current procedures of transport agencies to categorise the performance of bridges under a flood event. The updated scour risk estimates can then be used to inform the decisions to be taken concerning bridge closure or traffic management measures. The next two subsections describe the method for updating the bridge risk using the observations from SHM, and the decision support system based on SHM-informed scour estimates.

5.4.1 SHM-based classification of bridge risk

The bridge scour risk assessment under an extreme flood event is based on the framework developed in the previous Chapter. This framework employs a Bayesian network (BN) approach to update the a-priori estimates of the scour depth at any location of the bridge network with the information from the scour sensors installed at few locations. In particular, a-priori estimates of the probability density function (pdf) of the scour depth under an extreme flood event can be obtained with a Monte-Carlo approach, by generating samples of the parent nodes, starting from their pdf, and using the BN to propagate this uncertainty to the child nodes up to the scour total depth level. Information from the scour sensors are then used to update the pdf of the scour depth at the monitored location, and the BN is used to expand this information to other bridge locations in the bridge infrastructure network. In fact, while at the monitored locations quite accurate scour estimates can be achieved, depending on the sensor accuracy, at the unmonitored ones it is still possible to observe a reduction of uncertainty thanks to the correlation existing between the scour depths at different locations.

The BN's output is an updated pdf of the total scour depth, which is then used to classify the bridge performance under an extreme event. The same classification scheme used by TS is considered here (see Figure 2.9a), with the relative scour depth D_R discriminating among

the risk classes. However, while in BD 97/12 a deterministic approach is employed, leading to the identification of a unique risk class for bridges under an hypothetical flood scenario (e.g., the one with a return period of 200 years), the output of the proposed approach is the event-based bridge probability of being in a particular risk class.

Figure 5.1 illustrates an example of the risk classification, using only the relative scour

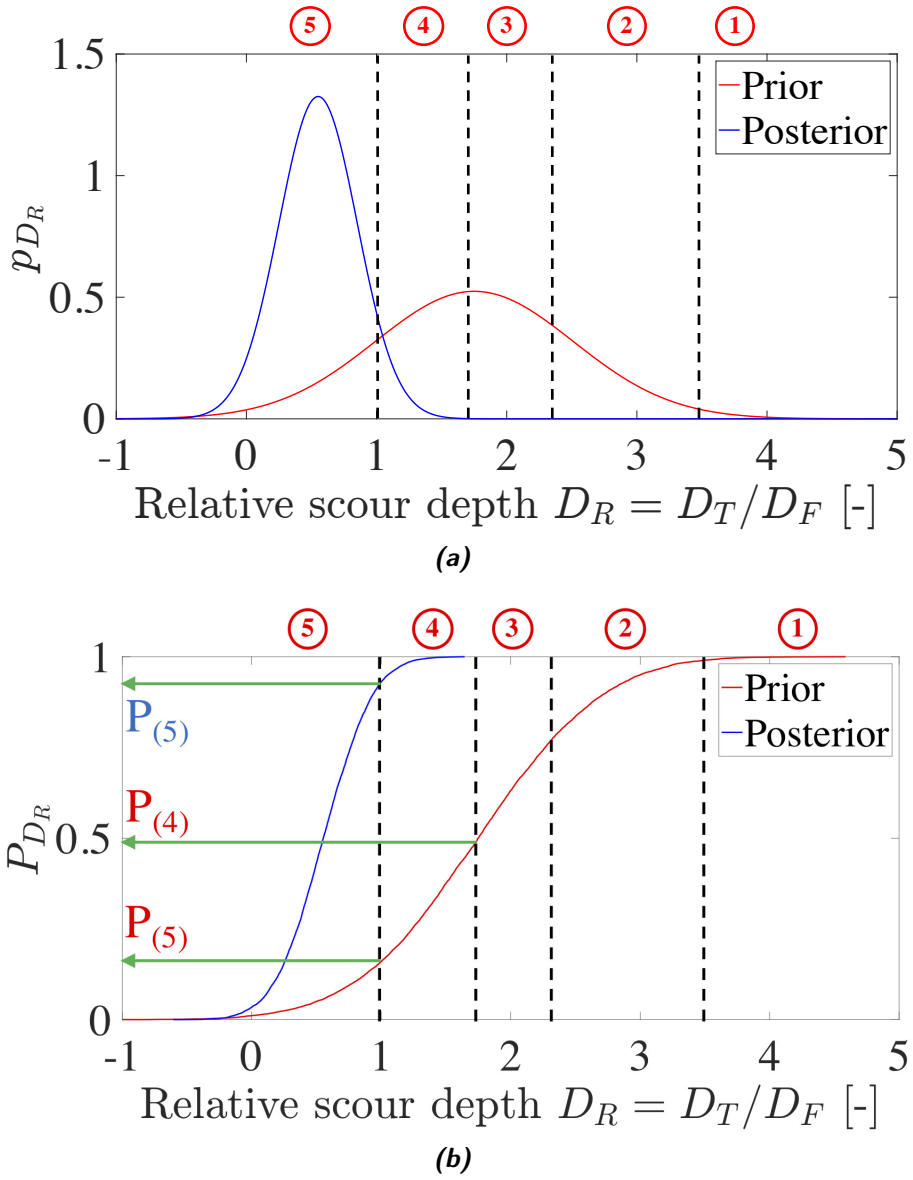

Figure 5.1: ***(a)*** *Probability density function, and* ***(b)*** *cumulative density function of prior and posterior relative scour depth provided by BN with corresponding risk classification* $(PF = 2)$

distribution obtained "a priori" (i.e., without observations entering the BN), and using the posterior distribution considering scour monitoring data. The probability $P_{(i)}$ of being in a particular class i is computed through the cumulative distribution function (cdf) of the relative scour depth (Figure 5.1b). Thus:

$$P_{(i)} = F_{D_R}\left(D_R^{(i)}\right) - F_{D_R}\left(D_R^{(i+1)}\right) \tag{5.1}$$

where $F_{D_R}\left(D_R^{(i)}\right)$ is the cdf calculated with the minimum value of D_R that is associated with the class i, and $F_{D_R}\left(D_R^{(6)}\right) = 0$.

The a-priori distribution of the scour depth is characterized by a significant dispersion, which is the effect of the uncertainties considered in the BN (i.e., those concerning the flow discharge and the hydrological and hydraulic models). This results in comparable values of the probability of the bridge being in class 2, 3, or 4, and very small probability of being in the two other classes (1 and 5). Information from monitoring systems is expected to reduce significantly the uncertainty in the scour estimation, thus allowing for a more precise

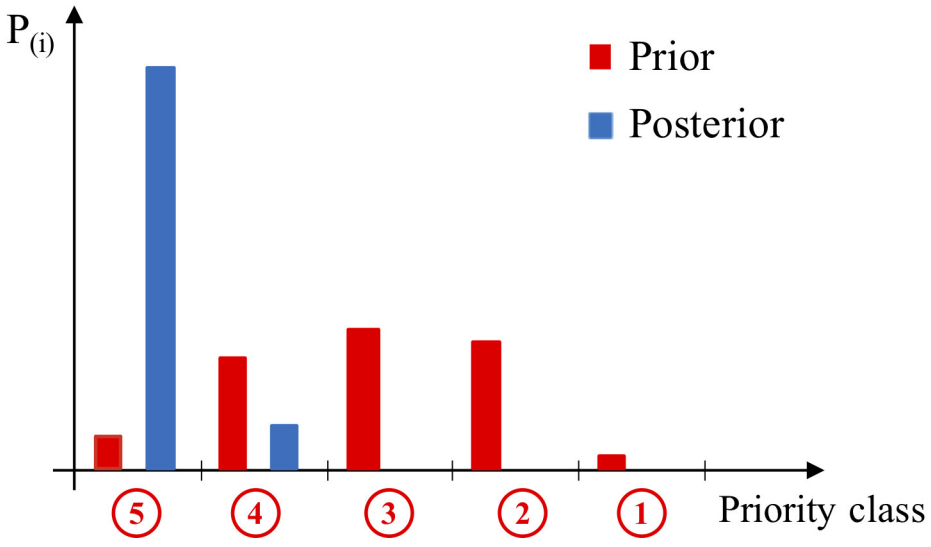

Figure 5.2: *TS prior and posterior risk class classification*

identification of the distribution of D_R and, in turn, of the scour risk (blue bars). Based on the updated pdf of D_R, the bridge most probably falls in class 5, with a small possibility of being in class 4 and a negligible probability of being in the other classes (Figure 5.2). In this example, the bridge will be therefore classified by the transport agency in the most probable class (i.e., class 5 thanks to scour observations from monitoring system).

5.4.2 SHM-based Decision Support System

This subsection describes an SHM-based DSS that integrates real-time measurements of the scour depth in the decision-making process to produce measurement-informed thresholds triggering bridge closure to traffic under heavy floods. Since the idea behind the development of the system is to introduce the information on the scour depth in the decision plan, the proposed DSS uses the relative scour depth D_R, employed by transport agencies to categorise bridges at high risk of scour, as the parameter triggering actions, instead of the water level. This choice is also motivated by the fact that there is not a perfect correlation between the scour depth at a location and the water level, and thus the two parameters cannot be used interchangeably.

When transport agencies fix a threshold (e.g., red marker) for triggering their actions, they implicitly choose a level of risk they are willing to accept, i.e., an acceptable probability of failure P_F for the structure. According to the simple decision tree depicted in Figure 5.3, a risk threshold can be generally defined such that the associated losses satisfy the following equation:

$$P_F \, C_F = C_{CB}, \tag{5.2}$$

where C_{CB} are the losses due to the bridge closure, and C_F are the losses (direct and indirect) due to the bridge failure. The threshold can be set such that the losses due to bridge closure and to bridge failure are equal.

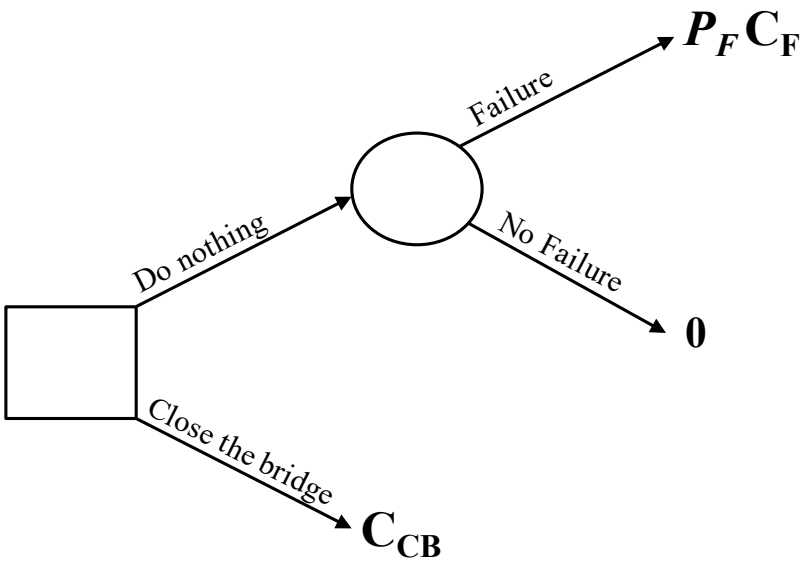

Figure 5.3: *Decision tree to define a threshold*

It is noteworthy that transport agencies usually do not carry out this risk/consequence analysis, but they fix the threshold based on their experience and engineering judgement. However, the knowledge of the value of the implicit probability of failure implicitly sought by transport agencies is essential for the development of the proposed DSS, which aims to use the information from real-time scour measurements to estimate a new scour threshold while targeting the same probability of failure.

In general terms, the probability of failure due to scour can be expressed as the probability that the scour demand is equal to or greater than the scour capacity of the bridge/foundation system. In the case of bridges with multiple piers, a series-system reliability model can be used, with the failure of the bridge occurring due to the scour depth at any pier exceeding the scour capacity. The relative values of the scour depth are considered hereinafter for expressing the scour demand and capacity, consistently with risk classifications. Both the demand and the capacity are random variables, due to the many uncertainties inherent to the problem.

The relative scour capacity model, relating D_R to the probability of failure P_F, can be

defined based on BD97/12. The model has been developed starting from typical values of failure probability (showed in the Table below) deriving from the reliability theory and, of course, engineering judgement. This model is assumed to follow a lognormal distribution as follows (Figure 5.4):

$$P_F\left(D_R\right) = P\left[C \leq D_R\right] = F_C(D_R) = \Phi\left(\frac{\ln D_R - \lambda}{\beta}\right), \tag{5.3}$$

where Φ is the standard normal cumulative distribution function, $\lambda = 3.58$ and $\beta = 0.75$ are the mean value and the standard deviation of the natural logarithm of D_R, respectively. The model (and, in turn, its defining parameters) has been fit to the acceptable values of the risk of failure for bridges belonging to different risk classes shown in the Table of Figure 5.4. Those values has been defined by assigning a probability of failure equal to $P_F = 10^{-3}$ to bridges in risk class 1 (i.e., the one at the highest risk). Instead, for bridges in risk class 4 or below, the probability of failure has been set equal to $P_F = 10^{-6}$. These figures usually simulate the failure probability of a bridge that exceeds its "Ultimate Limit State" and its "Serviceability Limit State", respectively, according the well-recognised reliability theory. It is noteworthy that similar models are used in other contexts such as Earthquake

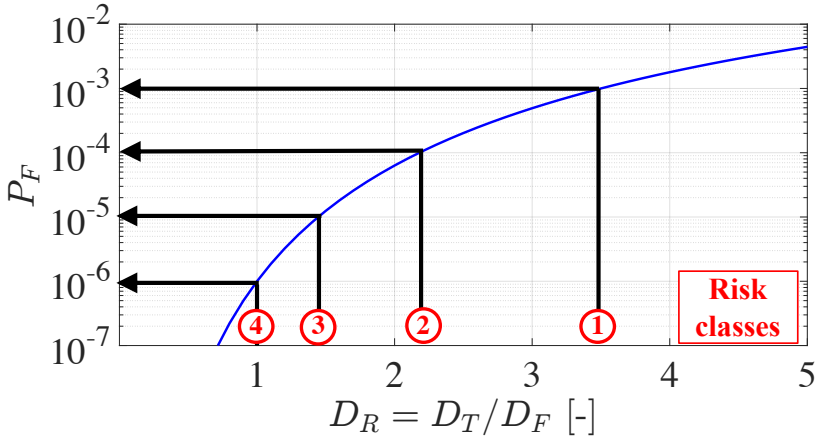

Risk class	P_F
1	10^{-3}
2	10^{-4}
3	10^{-5}
4 or below	10^{-6}

Figure 5.4: *Fragility function for scour capacity C*

Engineering (Gkimprixis *et al.*, 2019), where they are commonly referred to as fragility functions.

The relative scour demand model can be defined by exploiting the outcomes of the probabilistic framework developed in Chapter 4. In particular, for estimating the failure probability P_F implicitly associated to the current decision system of TS, a predictive analysis can be carried out, by generating through the BN a set of samples of the relative scour depth for the various bridge foundations under a flood discharge with a return period of 200 years. This approach is consistent with the choice of TS of setting a red marker in correspondence of the water level with a return period of 200 years. The obtained samples define the "a priori" distribution of the relative scour depth, $f_{D_{R0}}(D)$, and the corresponding a priori failure probability P_{F_0} can be expressed as:

$$P_{F0} = \int_0^\infty F_C(D)\ f_{D_{R0}}(D)\ dD\,. \tag{5.4}$$

This integral can be evaluated in closed form only if an assumption (e.g., normality or lognormality) is introduced for the demand. Alternatively, a pure Monte-Carlo based approach can be employed, by comparing each samples of the demand with a random sample generated from the fragility function expressing the capacity and counting the number of times that the demand exceeds the capacity.

It is worth stressing that the calculation of the failure probability is not essential per se, but it is important that, when a new source of information (e.g., scour monitoring data) is introduced to calculate the new scour threshold, the P_F is maintained constant in order to be consistent with TS's choice of threshold. The definition of the SHM-based scour depth thresholds triggering action for road bridges managed by TS is described in the following subsections.

5.4.2.1 Directly monitored locations

Scour sensors can achieve quite accurate estimates of the scour depth at the monitored locations under a flood event and for simplicity it is assumed that at these locations the scour demand is a deterministic variable, $D_{R,obs}$. In this case, the posteriori estimate of the probability of failure P_F is:

$$P_F\left(D_{R,obs}\right) = F_C\left(D_{R,obs}\right), \tag{5.5}$$

and the new SHM-based scour threshold can be obtained by solving the following inverse reliability problem:

$$P_{F0} = P_F\left(D_{R,obs}\right), \tag{5.6}$$

whose solution is $\overline{D}_R = F_C^{-1}\left(P_{F0}\right)$

This updated threshold incorporates the uncertainty of the scour capacity and the piece of information provided by the scour observation (i.e., that there is no uncertainty in the demand). It can be used under an extreme weather event to trigger bridge closure to traffic if the measured relative scour depth $D_{R,obs}$ exceeds $\overline{D}_R$. The updated scour threshold is valid only for monitored bridge locations, since for the unmonitored it is necessary to account also for the dispersion of the scour demand, as discussed in the following subsection.

5.4.2.2 Unmonitored locations

In the case of unmonitored locations, the relative scour demand is a random variable, and the corresponding failure probability due to scour at a generic location can be expressed as follows:

$$P_F\left(D_{R,obs}\right) = \int_0^\infty F_C\left(D\right)\ f_{D_R}\left(D|D_{R,obs}\right)\ dD \tag{5.7}$$

where $f_{D_R}\left(D|D_{R,obs}\right)$ is the posterior distribution of the scour depth at the unmonitored location, updated by entering into the BN with the direct observation of scour at the

monitored location.

It is noteworthy that this failure probability changes with the scour observation. To simplify the problem, the concept of pre-posterior distribution can be introduced (see e.g., Zonta, Cappello, Pozzi and Glišić, 2014). As explained in Chapter 4, Equation (4.1) (i.e., the Bayes' theorem) is the classical formulation used to update the state parameter after acquiring monitoring data. Instead, the pre-posterior distributions refers to a concept that is upstream of the data acquisition. The idea is indeed to infer a prior features of the posterior distribution by assuming that some data are going to be acquired, but these data have not been available yet. The pre-posterior analysis is often employed in the design phase of a monitoring system in order to estimate its accuracy in prior condition (i.e., before its deployment).

Introducing this concept, the scour demand can be assumed to follow a normal distribution with pre-posterior mean scour depth μ_{pp} and pre-posterior standard deviation σ_{pp}:

$$D_R \sim \mathcal{N}\left(\mu_{pp}, \sigma_{pp}\right). \tag{5.8}$$

Similar to the previous case (i.e., direct scour observation), the probability of failure must remain equal to the "a-priori" one, to be consistent with the approach followed by TS. Assuming that σ_{pp} remains unchanged, it is possible to find an updated value of the mean pre-posterior relative scour threshold μ_{pp} such that the corresponding failure probability equals P_{F0} expressed in (5.4):

$$\int_{D_R} F_C\left(D\right)\ f_{D_R}\left(\mu_{pp}, \sigma_{pp}\right)\ dD_R = P_{F0}. \tag{5.9}$$

The value of μ_{pp} that satisfies Equation (5.9) is the measurement-informed scour threshold $\overline{D}_R$ that should be considered to take decisions. In particular, the bridge closure at traffic under an extreme flood event can be triggered by comparing the SHM-based mean demand

to $\overline{D}_R$, and if it is higher, than the bridge should be closed.

5.5 Case study and results

The DSS is applied to the same case study presented in the previous Chapter. It is small bridge network, consisting of bridges managed by TS in south–west Scotland. The bridges cross the same river (River Nith) and only one pier of Bridge 1 is instrumented with a scour monitoring system. Three bridges with significant scour event in the past are chosen from TS scour database:

- *Bridge 1*: A76 200 Nith bridge in New Cumnock (Figure 5.5). It is a 3-span (9.1m, 10.7 m and 9.1 m) stone-masonry arch bridge, with two piers in the riverbed.
- *Bridge 2*: A76 120 Guildhall bridge in Kirkconnel (Figure 5.6). It is a 3-span (8.8m, 11.3 m and 11.3 m) masonry arch bridge, with one pier in the riverbed.
- *Bridge 3*: A75 300 Dalscone bridge in Dumfries (Figure 5.7). It is a 7-span (spans of 35 m and two of 28 m) steel-concrete composite bridge, with one pier in the riverbed.

The foundation depth D_F is unknown for all the three bridges; therefore, a depth of 1 m is assumed in the calculation of the relative scour depth D_R. The assumption is valid for

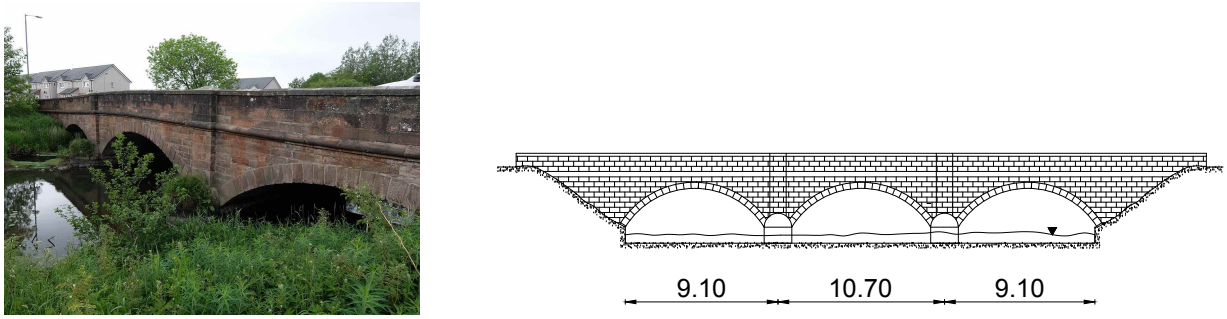

Figure 5.5: ***(a)*** *A76 200 Nith bridge and* ***(b)*** *bridge elevation*

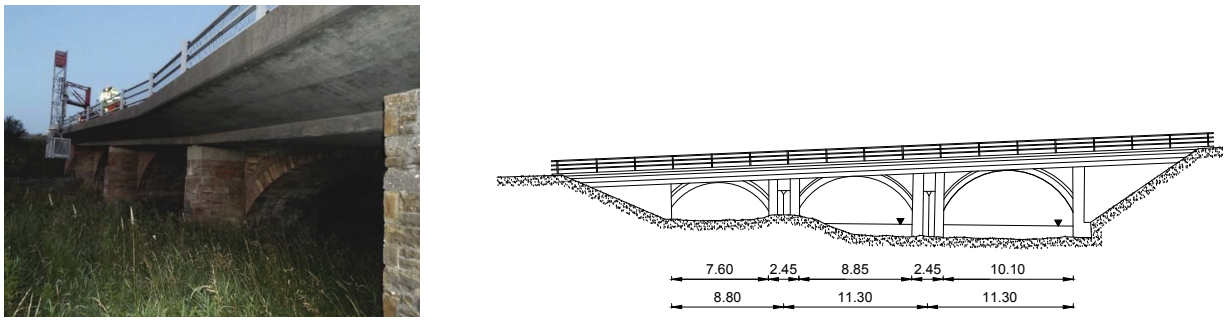

(a) *(b)*

Figure 5.6: ***(a)*** *A76 120 Guildhall bridge and* ***(b)*** *bridge elevation*

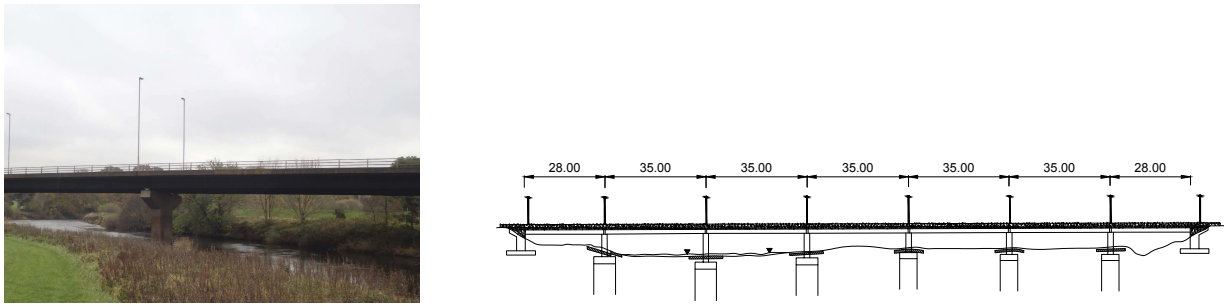

(a) *(b)*

Figure 5.7: ***(a)*** *A75 300 Dalscone bridge and* ***(b)*** *Bridge elevation*

the third bridge as well, because the BD 97/12 says that D_F is the underside of the pile cap in the case of a piled foundation.

Figure 5.8 shows the results of application of the procedure for the scour risk classification proposed in Section 5.4.1. In particular, the first column compares the prior and posterior probability mass functions of the scour depth at the unmonitored pier foundation of the A76 200 Nith bridge (i.e., the scour at pier 1 is directly monitored) and at the foundations of the other two unmonitored. These distributions are the results of the application of the BN, which is illustrated in Chapter 4.

The BN calculated the prior estimations starting from log-normal distributions of the water discharge based on the gauging station data of the last ten years collected by the Scottish Environmental Protection Agency. Peak water flow values recorded at the gauging stations, simulating a heavy flood scenario, and observation from scour sensors at the first

pier of Bridge 1 are then incorporated to update the scour estimates (i.e., posterior pdfs). The prior risk classification is uncertain, all the three bridges had similar probabilities to fall into class 2, 3, or 4. Following the procedure BD 97/12, with the classification based on the mean value of the scour depth estimated under a 200 years flood discharge, the bridges would fall into category 3, 2, and 3, respectively. Instead, according to the prior risk classification that incorporates the inherent uncertainties of the scour estimation, the most probable risk categories for the three bridges are 4, 2, and 4, respectively.

Figure 5.8 also shows how incorporating information from scour sensors into the BN

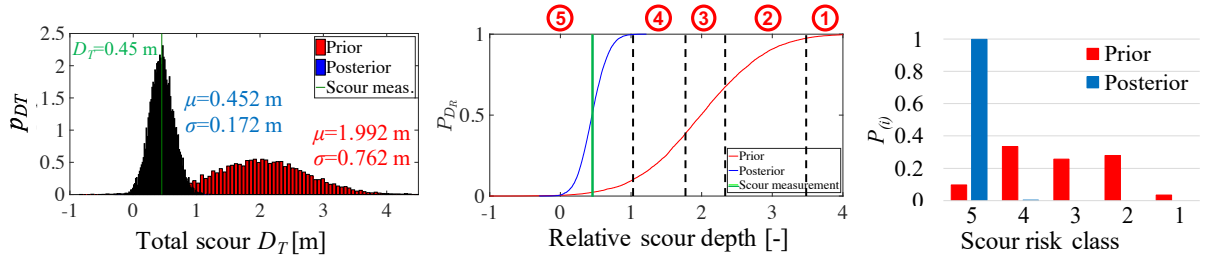

(a) *Pier 2 of Nith Bridge*

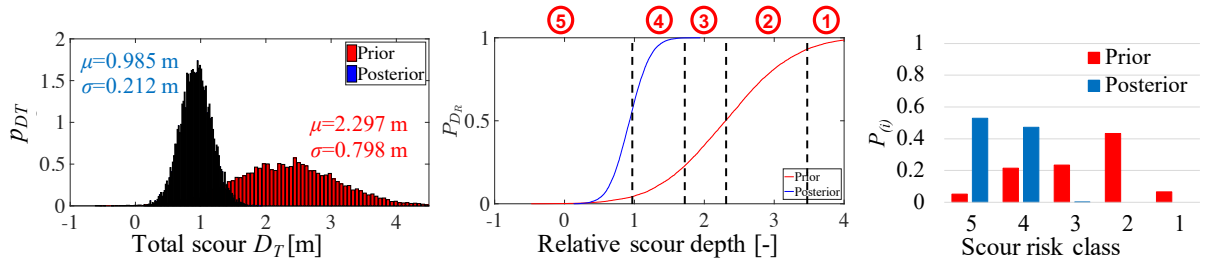

(b) *Pier 1 of Guildhall bridge*

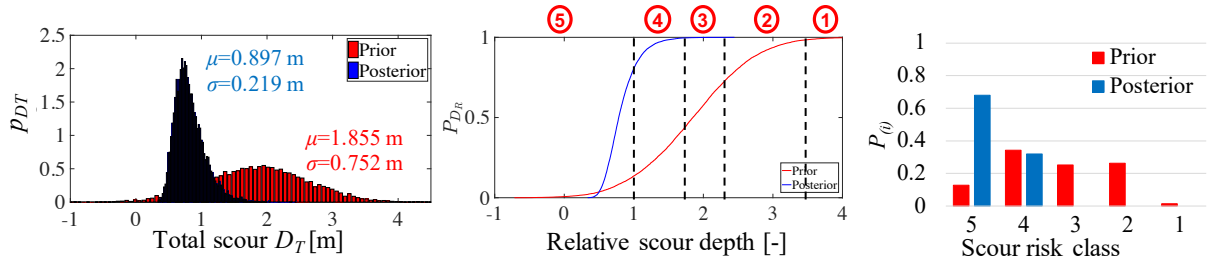

(c) *Pier 1 of Dalscone bridge*

Figure 5.8: *Risk classification of the three bridges making up our case study*

allows estimating the scour risk in the occurrence of a peak flood events. The SHM-based risk classification is indeed more explicit because of the uncertainty reduction thanks to scour monitoring data. By simulating a high-flow rate event (i.e., water level upstream the Bridge 1 assumed equal to 1.879 m) and envisaging a total scour depth at the first pier of Bridge 1 equal to 0.45m, the DSS categorises the second pier (i.e., not monitored) into category 5 (Figure 5.8a). The correlation existing between the scour depths at different locations allows to achieve a reduction of uncertainty even at unmonitored bridges. This reduction is reflected in the scour risk estimation: Bridge 3 has around the 70% of falling in the category at the lowest risk (Figure 5.8c), while Bridge 2 has around the same probability to be categorised in risk class 5 or 4 (Figure 5.8b). For this latter bridge there is not a clear classification because the mean value of D_T is 0.98 m, very close to the hypothesised foundation value D_F (1 m). Consequently, the numerical method used to solve the BN has evaluated the relative scour depth D_R greater than 1 in several extractions. This has led the method to classify the bridge within class 5 and 4 because this latter class is defined by values of relative scour falling within the interval $1 < D_R \leq 1.8$.

The outcomes of this analysis suggest that SHM-based risk classification could help the transport agencies in facilitating the bridge ranking and prioritising inspections in the aftermath of a flood event. The prior probabilistic scour risk classification furnishes a fairer and more accurate scour risk classification because it reflects the uncertainty characterising the scour problem. This information could be used for driving strategic maintenance, repair and rehabilitation (MR&R) actions and might help in reducing bridge misclassification.

The application of the SHM-based DSS and the measurement-informed scour thresholds is tested on the same bridge network. Firstly, the SHM-based scour threshold is calculated for the pier 1 of A76 200 Nith bridge because the total scour depth is monitored at this location. The prior threshold, corresponding to the mean relative scour depth under a flood discharge with return period of 200 years, is $E[D_{R0}] = 3.81$. The implicit probability of

failure corresponding to the scour demand is $P_{F0} = 2.08 \times 10^{-3}$. The updated threshold $\overline{D}_R$ at the monitored bridge location is therefore equal to:

$$\overline{D}_R = F_C^{-1}\left(P_{F0}\right) = \exp\left\{3.58 + 0.75 \cdot \Phi^{-1}\left(2.08 \times 10^{-3}\right)\right\}$$
$$\overline{D}_R = 4.15 > E\left[D_{R0}\right] = 3.81.$$

As expected, the inclusion of the scour measurements leads to a higher value of the scour threshold to classify the bridge at high risk. Therefore, A76 200 Nith bridge has to be closed to traffic if, during a flood event, its scour monitoring system measures a value of the relative scour depth equal or higher than 4.15, while following current procedures it would have to be closed for a measurement higher than 3.81. It is worth highlighting that the prior threshold is calculated with a set of equations develop for the estimation of the maximum scour depth, which, in the case study presented, may not be at the location of the probe. However, this does not invalidate the obtained results because it has confirmed the importance of the uncertainty reduction in scour estimation for triggering bridge closure.

The implicit values of the failure probability at the unmonitored locations of the Nith bridge and of the other bridges are illustrated in Figure 5.9, together with the pre-posterior estimates of the failure probability obtained following the procedure illustrated in subsection 5.4.2, for different values of the pre-posterior mean scour depth. Obviously, the prior failure probability values do not depend on the scour observation, and they are represented by a horizontal red line. On the other hand, the pre-posterior failure probability increases with an almost linear trend for increasing values of the mean scour relative demand. The critical scour threshold $\overline{D}_R$ for the various unmonitored locations can be found by intersecting the horizontal red line corresponding to P_{F0} with the line corresponding to the updated failure probability.

Starting from a prior threshold corresponding to the relative scour depth when the bridges are subjected to a flood event with a return period of 200 years, the pre-posterior

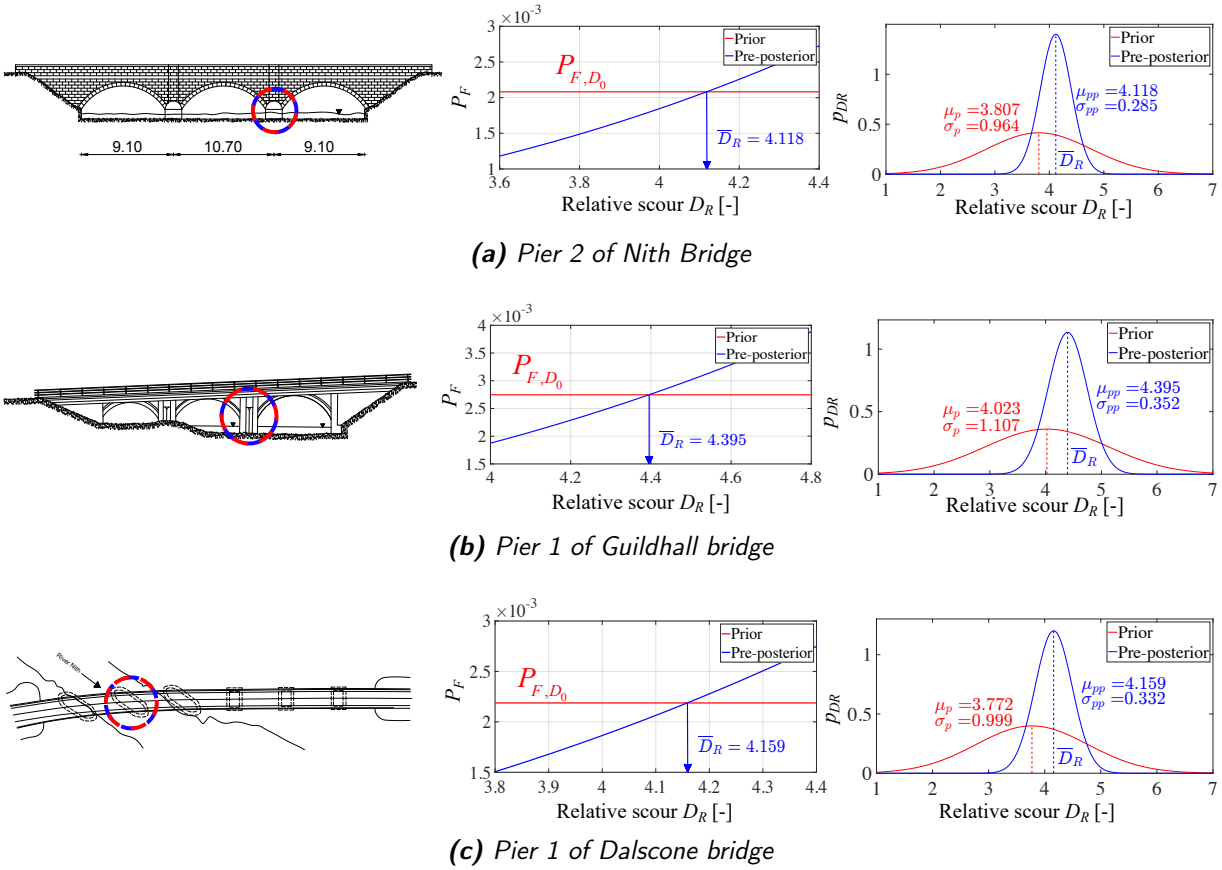

(a) *Pier 2 of Nith Bridge*

(b) *Pier 1 of Guildhall bridge*

(c) *Pier 1 of Dalscone bridge*

Figure 5.9: *Updating of the scour threshold from BN's outcomes of unmonitored components*

estimation of the scour depth accounting for the reduction of uncertainty due to scour monitoring allows an increase of the scour critical threshold for all the three unmonitored bridges. This increase is of the order of 10%.

Figure 5.9 also compares the prior distribution of the scour depth (fitted by a normal distribution) with the pre-posterior one, centred in correspondence of the updated scour threshold. This comparison is useful for illustrating how the reduction of uncertainty, thanks to the observation from the scour monitoring system, allows increasing the critical scour threshold triggering bridge closure.

5.6 Conclusions

Although structural health monitoring (SHM) systems are increasingly installed on civil engineering infrastructures, it is still unclear how the collected observations can be exploited by bridge owners and managers in making decisions for managing their asset.

This Chapter presents an SHM-based scour risk classification for bridge scour risk rating and a Decision Support System (DSS) for bridge management under extreme flood events.

The risk classification accounts for the relevant sources of uncertainty characterizing the problem, leading to a fairer probabilistic classification of the scour risk and allowing to quantify the benefits of SHM in terms of uncertainty reduction. The DSS extends and complements current action plans of UK transport agencies. It integrates the real-time measurements of the scour depth in the decision-making process, by producing measurement-informed scour thresholds triggering bridge closure to traffic under heavy floods. Both the risk classification and the DSS are based on a Bayesian network (BN) approach for modelling the scour risk assessment and the updating based on the available observations.

A small network consisting of three bridges at risk of scour managed by Transport Scotland in south–west Scotland is considered to illustrate the application of the proposed risk rating system and the DSS. Based on the study results, the following conclusions can be drawn:

(i) Starting from an uncertain prior risk classification (i.e., all the three bridges have similar probabilities to fall into class 2, 3, or 4), the integration of scour monitoring data leads to an overall reduction of uncertainty that is reflected in the proposed scour risk classification. Under the considered flood scenario, Bridge 1 clearly falls into class 5, Bridge 3 has the 70% of probability of being classified in the lowest risk class, whereas Bridge 2 can be classified in either Class 5 or 4 (i.e., it has a negligible probability of being in the more risky classes);

(ii) The DSS is found to benefit from the incorporation of scour SHM data for the management of bridge assets under extreme flood events. For instance, Bridge 1 can stay open to traffic until its scour monitoring system measures a value of the relative scour depth equal or higher than 4.15 at the monitored location. The prior threshold, according to current procedures, would have been equal to 3.81 (i.e., relative scour depth due to a flood event with a return period of 200 yrs.). The system also allows increasing the critical scour threshold triggering bridge closure at the unmonitored locations, e.g., passing from 4.023 to 4.395, thanks to a reduction of uncertainty of 70% (e.g. from 1.107 to 0.352). The scour threshold increases of about 10% compared to the prior thresholds.

The proposed scour risk classification provides information that can be of paramount importance for strategic maintenance, repair and rehabilitation actions and can help in reducing the scour risk misclassification, thus prioritising inspections according to the scour risk classification in the aftermath of a flood event. Moreover, the measurement-informed scour thresholds might help bridge asset operators in reducing the times that bridges might be closed unnecessarily as a precautionary action, by comparing these thresholds to scour measured from SHM systems and scour estimates (i.e., the expected value) provided by the BN. Therefore, both features of the DSS will provide quantitative and robust information about scour estimates, risk classes and bridge closure management. This will be beneficial for transport agencies because, as public bodies, it might help them in reducing their expenses for unnecessary scour inspections or bridge closures (e.g., downtime costs), thus allowing them to optimally manage their budgets.

Future studies will aim at applying expected utility theory to the developed SHM-based DSS in order to identify financially optimal decisions to be taken under extreme events. Furthermore, the concept of measurement-informed scour threshold will be extended to develop adaptive flood level thresholds triggering bridge closure changing with the real-time

information provided by the sensors.

CHAPTER 6

Concluding remarks and outlook

The aim of this thesis was to propose a framework for improving current scour risk assessment and management procedures of transport agencies, by incorporating the various sources of uncertainty inherent to the problem, and by using information from scour monitoring sensors.

In order to achieve the proposed aim, the research presented the following contributions to the field of bridge scour risk management:

(i) *Chapter 3* described the concept, installation and functioning of a pilot scour monitoring system based on the use of smart electromagnetic probes and installed on the A76 200 bridge over the River Nith in New Cumnock, UK. The principle of operation of the probe was introduced, together with the procedure implemented for calibrating and testing the sensors.

(ii) *Chapter 4* illustrated the development of the probabilistic framework for scour hazard assessment based on a Bayesian network (BN) approach, to *(a)* explicitly account for the various sources of uncertainty inherent to the hydrological and hydraulic parameters as well as the models employed for evaluating the scour depth at a bridge, and *(b)* exploit information from scour sensors to reduce the uncertainty in the scour risk estimates. The aim was to exploit the direct observation of scour at a monitored

bridge to predict the scour depth at other unmonitored piers.

(iii) *Chapter 5* presented a SHM-based scour risk classification for bridge scour risk rating under extreme flood events. The risk classification accounts for the relevant sources of uncertainty characterizing the problem, using the outcomes of the probabilistic framework and SHM scour data.

(iv) *Chapter 5* also showed a SHM-based event-based decision support system (DSS) that produces measurement-informed scour thresholds triggering bridge closure to traffic under heavy floods by incorporating real-time scour measurements in the decision-making process.

A case study consisting of three bridges managed by Transport Scotland in South-West Scotland was considered to demonstrate the functioning of the developed BN and DSS. The bridges cross the same river, and only one bridge is assumed to be instrumented with a scour monitoring system.

6.1 Summary of key findings

Chapter 3

- After a peak flood event, the probe P_2 (i.e., installed in the middle of the channel) measured 30 cm of scour, and the recorded data were consistent with the survey of the riverbed in vicinity of the probe carried out using a telescopic pole during a bridge inspection. This has proved the potential of the technology in providing continuous scour monitoring, even during extreme flood events, thus avoiding the deployment of divers for underwater examination.

- Even though the recorded scour might be the result of the turbulence of water around the steel pipe, this pipe-induced scour did not invalidate the obtained results, and in

fact, it has confirmed the probe capacity to detect scour.

- To the author's knowledge, this was the first time that smart probes were applied to a real world setting for the continuous monitoring of scour.

Chapter 4

- The probabilistic framework showed that the limited data from the scour monitoring system allow a significant increase in the accuracy of the scour estimates at unmonitored bridge piers. This increase was in the order of 70%. It is noteworthy that this is the first application of BNs for bridge scour risk assessment.

- To the author's knowledge, this study constitutes the first application of Bayesian networks to bridge scour risk assessment.

Chapter 5

- Starting from an uncertain prior risk classification (i.e., all the three bridges have similar probabilities to fall into class 2, 3, or 4), the integration of scour monitoring data leads to an overall reduction of uncertainty that is reflected in the proposed scour risk classification. Under the considered flood scenario, Bridge 1 clearly falls into class 5, Bridge 3 has the 70% of probability of being classified in the lowest risk class, whereas Bridge 2 can be classified in either Class 5 or 4 (i.e., it has a negligible probability of being in the more risky classes).

- The DSS is found to benefit from the incorporation of scour SHM data for the management of bridge assets under extreme flood events. For instance, Bridge 1 can stay open to traffic until its scour monitoring system measures a value of the relative scour depth equal or higher than 4.15 at the monitored location. The prior threshold, according to current procedures, would have been equal to 3.81 (i.e., relative scour

depth due to a flood event with a return period of 200 yrs.). The system also allows increasing the critical scour threshold triggering bridge closure at the unmonitored locations, e.g., passing from 4.023 to 4.395 thanks to a reduction of uncertainty of 70% (e.g. from 1.107 to 0.352). This constitutes an increase of about 10% compared to the prior thresholds.

- Although earlier work on SHM-based DSSs have been developed, to the author's knowledge, this is the first application of a SHM-based DSS for scour risk management of bridges.

The proposed decision model and the results of the analyses are relevant to the scour management of bridges, in particular for activities, such as bridge risk ranking and decision-making. In fact, the developed DSS could help the transport agencies in reducing the "false positive" in the bridge scour assessment, that is, directing reactive inspections according to a more accurate scour risk classification. Moreover, this may help bridge asset operators in reducing the times that bridges might be closed unnecessarily as a precautionary action.

6.2 Future research

Future studies and additional investigations that would extend the analyses presented in this thesis are illustrated as follows:

- As continuation of the work presented in *Chapter 3*, a better characterisation of the sensor response could be proposed by including the study of the effect of temperature, investigating how long-term drift could impact the accuracy of the sensor and including the collection of soil samples in order to perform more representative lab tests. Furthermore, the effect of debris (e.g., hay), ice formation and vegetable growth (e.g., biofouling of algae or plants) on the sensor response will be studied.

- The scour recorded by probe P_2 (i.e., the one installed in the middle of the channel) might be the result of the turbulence of water around the steel pipe. This raised a concern about the design of the protective system for the probe; an improved design must be pursued to have a system that protects the probe alone, and not induce the scour to be monitored. Shortening the steel protective tube and replacing its bottom part with a cage (e.g., wider than the tube diameter and welded at its bottom part) could be a starting idea to avoid (or at least highly reduce) water turbulence around the pipe. Furthermore, the response of the sensors in the presence of a very localised/non-uniform scour holes must be studied in laboratory.

- The data collected by the scour monitoring system described in *Chapter 3* have shown that empirical formulas overestimate the scour depth, proving that several uncertainties affect scour models. The overestimation can be also observed comparing the prior pdf of the scour depth provided by BD97/12 and the estimations provided by the BN in *Chapter 4*. Therefore, scour monitoring systems and the developed probabilistic framework could be used to help in quantifying the scour model errors, validating and improving current formulas (or developing new and more accurate ones) for estimating the scour depth under transient flood conditions.

- The only way to validate the estimates of the total scour depth at the piers of the unmonitored bridges would be to measure the scour after an event. In the next months, three more scour sensing probes will be installed at two other bridges. One candidate is the Whitehill Bridge (A76 100) in Sanquhar (i.e., it is a small village close to New Cumnock), which is over the River Nith and with one pier in the riverbed. Thus, the measurements from these probes will be also used to validate the scour estimates provided by the BN in *Chapter 4*.

- The impact of "monitored" nodes of the BN (i.e., water levels and scour depths) in the

estimation of scour depth in unmonitored bridge will be also studied as future work. An analysis will be carried out to investigate the sensitivity of the scour estimates (and risk classes) to bulk change in water flow rate or monitored scour depth.

- Furthermore, future research should address the implementation of real-time scour measurements collected by the monitoring system into the BN shown in *Chapter 4*. This may involve extending the BN into a dynamic one, which is an enhanced version including time-variant parameters, thus allowing a real-time updating of the estimates of the scour depth at unmonitored bridge locations.

- Future research will also consider the extension of the BN with structural models, allowing to incorporate also information from sensors mounted on the bridges, such as accelerometers or inclinometers.

- As continuation of the work presented in *Chapter 3*, a rational methodology could be proposed to quantify the performance of scour SHM systems. This methodology may be based on indicators such as the "pre-posterior variance" (Zonta, Cappello, Pozzi and Glišić, 2014) or the "relative entropy reduction" (Capellari *et al.*, 2018). By considering the case study of New Cumnock bridge, a comparison may be carried out between the effectiveness of different scour monitoring approaches, one based on the smart scour probes presented in *Chapter 3*, and the others based on new devices to be installed (e.g., sonar devices, inclinometers or total stations). The monitoring effectiveness could be linked to the uncertainty reduction in the estimate of the bridge condition due to scour monitoring, which can be quantified once information from the sensors enter the BN developed in *Chapter 4*. The impact of the monitoring techniques on scour early warning and risk management could also be quantified by evaluating how the deployment of different SHM devices affect the estimation of scour threshold triggering bridge closure.

- More studies are required to characterise the vulnerability of bridges to the effects of scour and produce fragility curves to be employed in scour risk assessment.

- The integration of data from different sensors in the scour risk assessment of bridges could be addressed by extending the BN developed in *Chapter 4*. The framework for sensor data fusion could incorporate river flow measurements or information from different scour monitoring techniques, including the indirect ones, monitoring the response of the bridge to scour (e.g., pier rotation). The data-fusion framework could exploit information from multiple sources to update the scour knowledge or even detect aberrations from the normal state of a structure, indicating an imminent structural health problem.

- The proposed probabilistic framework could be further developed by implementing a rainfall-runoff model able to predict the peak discharge Q given by extreme rainfall events. With this information entering as evidence in the parent node Q, the BN would be able to predict the corresponding scour depth, thus simulating the impact of the potential extreme weather events on transport agencies' networks and planning in advance appropriate emergency procedures and countermeasures.

- Future studies will aim at applying expected utility theory to the developed SHM-based DSS shown in *Chapter 5* in order to identify financially optimal decisions to be taken under extreme events.

- Finally, future studies will aim at implementing the concept of scour threshold, shown in *Chapter 5* to develop an adaptive flood level threshold that triggers the bridge closure. This is because transport agencies check the water level not only for scour warning, but also for ensuring that the bridge will not be inundated or possibly struck with floating debris.

Bibliography

Addin, O., Sapuan, S. M., Mahdi, E. and Othman, M. (2007), 'A Naïve-Bayes classifier for damage detection in engineering materials', *Materials & Design* **28**(8), 2379–2386.

Alipour, A., Shafei, B. and Shinozuka, M. (2013), 'Reliability-Based Calibration of Load and Resistance Factors for Design of RC Bridges under Multiple Extreme Events: Scour and Earthquake', *Journal of Bridge Engineering* **18**(5), 362–371.

Anderson, N. L., Ismael, A. M. and Thitimakorn, T. (2007), 'Ground-penetrating radar: a tool for monitoring bridge scour', *Environmental & Engineering Geoscience* **13**(1), 1–10.

ASCE (2017), '2017 Report Card for America's Infrastructure – Bridges', American Society of Civil Engineers (ASCE), Reston, VA, USA (accessed on 23/11/19).
URL: *https:// bit.ly/ 3bdJzZn*

Bakht, B. and Jaeger, L. G. (1990), 'Bridge Testing—A Surprise Every Time', *Journal of Structural Engineering* **116**(5), 1370–1383.

Balageas, D., Fritzen, C.-P. and Güemes, A. (2006), *Structural Health Monitoring*, first edn, ISTE Ltd., London, UK.

Bamler, R. and Hartl, P. (1998), 'Synthetic aperture radar interferometry', *Inverse Problems* **14**, R1–R54.

Barbato, M., Petrini, F., Unnikrishnan, V. U. and Ciampoli, M. (2013), 'Performance-Based Hurricane Engineering (PBHE) framework', *Structural Safety* **45**, 24–35.

Barbetta, S., Camici, S. and Moramarco, T. (2015), 'A reappraisal of bridge piers scour vulnerability: a case study in the Upper Tiber River basin (central Italy)', *Journal of Flood Risk Management* **10**(3), 283–300.

Baumhardt, R. L., Lascano, R. J. and Evett, S. R. (2000), 'Soil Material, Temperature, and Salinity Effects on Calibration of Multisensor Capacitance Probes', *Soil Science Society of America Journal* **64**(6), 1940–1946.

Bayraktarli, Y. Y., Ulfkjaer, J. P., Yazgan, U. and Faber, M. H. (2005), On the application of Bayesian probabilistic networks for earthquake risk management, *in* 'Proceedings of Structural Health Monitoring and Intelligent Infrastructures (SHMII-1)', Rome, Italy, June 19-23.

Ben Gal, I. (2007), Bayesian Networks, *in* F. Ruggeri, F. Faltin and R. Kenett, eds, 'Encyclopedia of Statistics in Quality & Reliability', John Wiley & Sons, Chichester, UK.

Benn, J. (2013), 'Railway bridge failure during flooding in the UK and Ireland', *Proceedings of the Institution of Civil Engineers - Forensic Engineering* **166**(4), 163–170.

Bensi, M. T., Der Kiureghian, A. and Straub, D. (2011), 'A Bayesian Network Methodology for Infrastructure Seismic Risk Assessment and Decision Support', PEER Report 2011/02, Pacific Earthquake Engineering Research Center, College of Engineering, University of California, Berkeley, CA, USA.

Betti, R., Sloane, M. J. D., Khazem, D. and Gatti, C. (2016), 'Monitoring the structural health of main cables of suspension bridges', *Journal of Civil Structural Health Monitoring* **6**(3), 355–363.

Bolognani, D., Verzobio, A., Cappello, C., Glišić, B. and Zonta, D. (2017), An application of Prospect Theory to a SHM-based decision problem, *in* 'Proceedings of SPIE 10170, Health Monitoring of Structural and Biological Systems', p. 101702G.

Bolognani, D., Verzobio, A., Tonelli, D., Cappello, C., Glišić, B., Zonta, D. and Quigley, J. (2018), 'IWSHM 2017: Quantifying the benefit of structural health monitoring: what if the manager is not the owner?', *Structural Health Monitoring* **17**(6), 1393–1409.

Bolstad, W. M. (2004), *Introduction to Bayesian Statistics*, first edn, John Wiley & Sons, Hoboken, NJ, USA.

Brandimarte, L., Montanari, A., Briaud, J.-L. and D'Odorico, P. (2006), 'Stochastic Flow Analysis for Predicting River Scour of Cohesive Soils', *Journal of Hydraulic Engineering* **132**(5), 493–500.

Brandimarte, L., Paron, P. and Baldassarre, G. D. (2012), 'Bridge Pier Scour: A Review of Processes, Measurements And Estimates', *Environmental Engineering and Management Journal* **11**(5), 975–989.

Breusers, H. N. C., Nicollet, G. and Shen, H. W. (1977), 'Local Scour Around Cylindrical Piers', *Journal of Hydraulic Research* **15**(3), 211–252.

Briaud, J. L., Brandimarte, L., Wang, J. and D'Odorico, P. (2007), 'Probability of scour depth exceedance owing to hydrologic uncertainty', *Georisk: Assessment and Management of Risk for Engineered Systems and Geohazards* **1**(2), 77–88.

Briaud, J. L., Hurlebaus, S., Chang, K.-A., Yao, C., Sharma, H., Yu, O.-Y., Darby, C., Hunt, B. E. and Price, G. R. (2011), 'Realtime Monitoring of Bridge Scour Using Remote Monitoring Technology', FHWA/TX-11/0-6060-1, Texas Transportation Institute, The Texas A&M University System, College Station, TX, USA.

Briaud, J. L., Ting, F. C. K., Chen, H. C., Gudavalli, R., Perugu, S. and Wei, G. (1999), 'SRICOS: Prediction of scour rate in cohesive soils at bridge piers', *Journal of Geotechnical and Geoenvironmental Engineering* **125**(4), 237–246.

Brooks, N. (2003), 'Vulnerability, risk and adaptation: A conceptual framework', Working Paper No. 38, Tyndall Centre for Climate Change Research and Centre for Social and Economic Research on the Global Environment (CSERGE), Norwich, UK.

Brownjohn, J. M. W. (2007), 'Structural health monitoring of civil infrastructure', *Philosophical Transactions of the Royal Society A: Mathematical, Physical and Engineering Sciences* **365**, 589–622.

Brownjohn, J. M. W., Kripakaran, P., Harvey, B., Kromanis, R., Jones, P. and Huseynov, F. (2016), 'Structural Health Monitoring of short to medium span bridges in the United Kingdom', *Structural Monitoring and Maintenance* **3**(3), 259–276.

Byrne, P. (2009), 'The Northside bridge collapse', The Guardian.
URL: *https://bit.ly/2UoU4nf*

Calvi, G. M., Pinho, R., Magenes, G., Bommer, J. J., Restrepo-Vélez, L. F. and Crowley, H. (2006), 'Development of seismic vulnerability assessment methodologies over the past 30 years', *ISET Journal of Earthquake Technology* **43**(3), 75–104.

Capellari, G., Chatzi, E. and Mariani, S. (2018), 'Structural Health Monitoring Sensor Network Optimization through Bayesian Experimental Design', *ASCE-ASME Journal of Risk and Uncertainty in Engineering Systems, Part A: Civil Engineering* **4**(2), 04018016–14.

Cappello, C. (2017), Theory of Decision Based on Structural Health Monitoring, PhD thesis, Doctoral School in Civil, Environmental and Mechanical Engineering, University of Trento, Italy.

Cappello, C., Zonta, D. and Glišić, B. (2016), 'Expected utility theory for monitoring-based decision making', *Proceedings of IEEE* **104**(8), 1647–1661.

Cappello, C., Zonta, D., Pozzi, M., Glišić, B. and Zandonini, R. (2015), 'Impact of prior perception on bridge health diagnosis', *Journal of Civil Structural Health Monitoring* **5**(4), 509–525.

Çelebi, M. and Sanli, A. (2002), 'GPS in Pioneering Dynamic Monitoring of Long-Period Structures', *Earthquake Spectra* **18**(1), 47–61.

Chabert, J. and Engeldinger, P. (1956), *Etude des affouillements autour des piles des ponts*, Laboratoire National d'Hydraulique, Chatou, France.

Chanzy, A., Gaudu, J.-C. and Marloie, O. (2012), 'Correcting the Temperature Influence on Soil Capacitance Sensors Using Diurnal Temperature and Water Content Cycles', *Sensors* **12**(7), 9773–9790.

Ching, J. and Chen, Y.-C. (2007), 'Transitional Markov Chain Monte Carlo Method for Bayesian Model Updating, Model Class Selection, and Model Averaging', *Journal of Engineering Mechanics* **133**(7), 816–832.

Ching, J. and Wang, J.-S. (2016), 'Application of the transitional Markov chain Monte Carlo algorithm to probabilistic site characterization', *Engineering Geology* **203**, 151–167.

Clubley, S., Manes, C. and Richards, D. (2015), 'High-resolution sonars set to revolutionise bridge scour inspections', *Proceedings of the Institution of Civil Engineers - Civil Engineering* **168**(1), 35–42.

Cook, W., Barr, P. J. and Halling, M. W. (2015), 'Bridge Failure Rate', *Journal of Performance of Constructed Facilities* **29**(3), 04014080–8.

Cooksey, A. (1990), 'Report on the Collapse of Glanrhyd Bridge on 19th October 1987 in the Western Region of British Railways', Her Majesty's Stationery Office, London, UK.

Cumbria Intelligence Observatory (2010), 'Cumbria Floods November 2009: An Impact Assessment', Cumbria Intelligence Observatory, Cumbria, UK (accessed on 11th July 2018).
URL: *https://bit.ly/35Anses*

Dalton, P. A. (2008), 'Physical Infrastructure: Challenges and Investment Options for the Nation's Infrastructure', United States Government Accountability Office, Washington, DC, USA.

Daraghi, B. (1990), 'Controlling mechanism of local scour', *Journal of Hydraulic Engineering* **116**(10), 1197–1214.

Davey & Maynard Agricultural Consulting (2001), 'Irrigation Scheduling with Capacitance Probes', Department of Primary Industries, Water & Environment, Hobart, Tasmania.

DEFRA (2012), 'UK Climate Change Risk Assessment: Government Report', The Stationary Office, London, UK.

DeGroot, M. H. (1984), 'Changes in utility as information', *Theory and Decision* **17**(3), 287–303.

Del Soldato, M., Tomas, R., Pont, J., Herrera, G., Garcia Lopez-Davalillos, J. C. and Mora, O. (2016), A multi-sensor approach for monitoring a road bridge in the Valencia harbor (SE Spain) by SAR Interferometry (InSAR), Technical report.

Deng, L. and Cai, C. S. (2010), 'Bridge Scour: Prediction, Modeling, Monitoring, and Countermeasures - Review', *Practice Periodical on Structural Design and Construction* **15**(2), 125–134.

Deng, L., Wang, W. and Yu, Y. (2016), 'State-of-the-Art Review on the Causes and Mechanisms of Bridge Collapse', *Journal of Performance of Constructed Facilities* **30**(2), 04015005–14.

Department for Traffic (2015), '£40 million to help rebuild flood-hit roads for people in Cumbria and Lancashire', (accessed on 10th July 2018).
URL: *https://bit.ly/2WrDV0A*

Dikanski, H. (2018), Planning and Asset Management for Climate Change Adaptation, PhD thesis, Faculty of Engineering and Physical Sciences, University of Surrey, UK.

Dikanski, H., Hagen-Zanker, A., Imam, B. and Avery, K. (2016), 'Climate change impacts on railway structures: bridge scour', *Proceedings of the Institution of Civil Engineers - Engineering Sustainability* **170**(5), 237–248.

Doebling, S. W., Farrar, C. R. and Prime, M. B. (1998), 'A summary review of vibration-based damage identification methods', *Shock and vibration digest* **30**(2), 91–105.

Downing, T. E., Butterfield, R., Cohen, S., Huq, S. and Moss, R. (2001), 'Vulnerability indices: climate change impacts and adaptation', UNEP Policy Series, Nairobi, Kenya.

Dundee Tunnel Research (2012), 'Bridge pier scour [Online image]', Dundee Tunnel Research.
URL: *http://goo.gl/ZpY2U7*

Ebrahimi, M., Djordjević, S., Panici, D., Tabor, G. and Kripakaran, P. (2020), 'A method for evaluating local scour depth at bridge piers due to debris accumulation', *Proceedings of the Institution of Civil Engineers - Bridge Engineering* **173**(2), 86–99.

Ebrahimi, M., Kripakaran, P., Prodanović, D. M., Kahraman, R., Riella, M., Tabor, G., Arthur, S. and Djordjević, S. (2018), 'Experimental Study on Scour at a Sharp-Nose Bridge Pier with Debris Blockage', *Journal of Hydraulic Engineering* **144**(12), 04018071–12.

Ekuje, F. T. (2018), Bridge Scour – Climate Change Effect and Modelling Uncertainties, PhD thesis, Faculty of Engineering and Physical Sciences, University of Surrey, UK.

Elsaid, A. and Seracino, R. (2014), 'Rapid assessment of foundation scour using the dynamic features of bridge superstructure', *Construction and Building Materials* **50**, 42–49.

Enright, M. P. and Frangopol, D. M. (1999), 'Condition Prediction of Deteriorating Concrete Bridges Using Bayesian Updating', *Journal of Structural Engineering* **125**(10), 1118–1125.

Faber, M. H., Kroon, I. B. and Kragh, E. (2002), 'Risk assessment of decommissioning options using Bayesian networks', *Journal of Offshore Mechanics and Artic Engineering, ASME* **124**, 231–238.

Fan, W. and Qiao, P. (2010), 'Vibration-based Damage Identification Methods: A Review and Comparative Study', *Structural Health Monitoring* **10**(1), 83–111.

Farrar, C. R. and Worden, K. (2007), 'An introduction to structural health monitoring', *Philosophical Transactions of the Royal Society A: Mathematical, Physical and Engineering Sciences* **365**(1851), 303–315.

Federico, F., Silvagni, G. and Volpi, F. (2003), 'Scour vulnerability of river bridge piers', *Journal of Geotechnical and Geoenvironmental Engineering* **129**(10), 890–899.

FEMA (2005), 'Hazus MR4 technical manual: Flood model', Federal Emergency Management Agency, U.S. Department of Homeland Security, Washington DC, USA.

Fisher, M., Chowdhury, M. N., Khan, A. A. and Atamturktur, S. (2013), 'An evaluation of scour measurement devices', *Flow Measurement and Instrumentation* **33**, 55–67.

Flint, M. M., Fringer, O., Billington, S. L., Freyberg, D. and Diffenbaugh, N. S. (2017), 'Historical Analysis of Hydraulic Bridge Collapses in the Continental United States', *Journal of infrastructure systems* **23**(3), 04017005–16.

Flynn, E. B. and Todd, M. D. (2010*a*), 'A Bayesian approach to optimal sensor placement for structural health monitoring with application to active sensing', *Mechanical Systems and Signal Processing* **24**(4), 891–903.

Flynn, E. B. and Todd, M. D. (2010*b*), 'Optimal Placement of Piezoelectric Actuators and Sensors for Detecting Damage in Plate Structures', *Journal of Intelligent Material Systems and Structures* **21**(3), 265–274.

Flynn, E. B., Todd, M. D., Croxford, A. J., Drinkwater, B. W. and Wilcox, P. D. (2011), 'Enhanced detection through low-order stochastic modeling for guided-wave structural health monitoring', *Structural Health Monitoring* **11**(2), 149–160.

Forde, M. C., McCann, D. M., Clark, M. R. and Broughton, K. J. (1999), 'Radar measurement of bridge scour', *NDT&E International* **32**(8), 481–492.

Fornaro, G., Reale, D. and Verde, S. (2012), Monitoring Thermal Dilations with Millimetre sensitivity via Multi-Dimensional SAR Imaging, *in* 'Proceedings of the Tyrrhenian Work. Adv. Radar Remote Sens. From Earth Obs. to Homel. Secur TyWRRS', Naples, Italy, 12-14 Sept.

Foti, S. and Sabia, D. (2011), 'Influence of Foundation Scour on the Dynamic Response of an Existing Bridge', *Journal of Bridge Engineering* **16**(2), 295–304.

Friis-Hansen, A. (2000), Bayesian networks as a decision support tool in marine applications, PhD thesis, Department of Naval Architecture and Offshore Engineering, Technical University of Denmark, Kgs Lyngby, DK.

Fujino, Y. and Siringoringo, D. M. (2008), Structural health monitoring of bridges in Japan: an overview of the current trend, *in* 'Proceedings of Fourth International Conference on FRP Composites in Civil Engineering CICE', Zurich, Switzerland, 22-24 July.

Gehl, P. and D'Ayala, D. (2016), 'Development of Bayesian Networks for the multi-hazard fragility assessment of bridge systems', *Structural Safety* **60**, 37–46.

Geiß, C. and Taubenböck, H. (2012), 'Remote sensing contributing to assess earthquake risk: from a literature review towards a roadmap', *Natural Hazards* **68**(1), 7–48.

Giordano, P. F., Prendergast, L. J. and Limongelli, M. P. (2020), 'A framework for assessing the value of information for health monitoring of scoured bridges', *Journal of Civil Structural Health Monitoring* **10**(3), 485–496.

Gkimprixis, A., Tubaldi, E. and Douglas, J. (2019), 'Comparison of methods to develop risk-targeted seismic design maps', *Proceedings of the Institution of Civil Engineers-Forensic Engineering* **17**(7), 3727–3752.

Hamill, L. (1999), *Bridge Hydraulics*, E & FN Spon, London, UK.

Hastings, W. K. (1970), 'Monte Carlo sampling methods using Markov chains and their applications', *Biometrika* **57**(1), 97–109.

Hayes, D. C. and Drummond, F. E. (1995), 'Use of fathometers and electrical-conductivity probes to monitor riverbed scour at bridge piers', Water-Resource Investigation Report 94-4164, U.S. Geological Survey, Richmond, Virginia, USA.

Heywood, R., Roberts, W., Taylor, R. and Andersen, R. (2000), 'Fitness-for-Purpose Evaluation of Bridges Using Health Monitoring Technology', *Transportation Research Record: Journal of the Transportation Research Board* **1696**(1), 193–201.

Highway Agency (2012), 'The Assessment of Scour at and Other Hydraulic Actions at Highway Structures - Procedure BD97/12', Vol. 3 of Design manual for roads and bridges, The Stationery Office Ltd, London, UK.

Hofmann-Wellenhof, B., Lichtenegger, H. and Collins, J. (1992), *Global Positioning System (GPS). Theory and practice*, third edn, Springer, Wien, Austria.

HR Wallingford (1993), 'Hydraulic Aspects of Bridges - Assessment of the Risk of Scour', Report EX 2502, HR Wallingford Ltd., Wallingford, UK.

Hung, C.-C. and Yau, W.-G. (2014), 'Behavior of scoured bridge piers subjected to flood-induced loads', *Engineering Structures* **80**, 241–250.

Hunt, B. E. (2009), 'Monitoring scour critical bridges', National Cooperative Highway Research Program (NCHRP) Synthesis no. 396, Transportation Research Board, Washington, DC, USA.

Huw Evans Agency (1987), 'The Glanrhyd bridge collapse', Wales Online.
URL: *https://bit.ly/379YMKG*

Imam, B. and Chryssanthopoulos, M. K. (2010), A review of metallic bridge failure statistics, *in* 'Proceedings 5th International Conference on Bridge Maintenance, Safety and Management (IABMAS'10)', Philadelphia, USA, 11-15 July.

Imhof, D. (2004), Risk Assessment of Existing Bridge Structures , PhD thesis, Ph. D. thesis, University of Cambridge, UK.

Jensen, F. V. and Nielsen, T. D. (2007), *Bayesian networks and decision graphs*, second edn, Information Science and Statistics, Springer, Berlin, Germany.

Johnson, P. A., Clopper, P. E., Zevenbergen, L. W. and Lagasse, P. F. (2015), 'Quantifying Uncertainty and Reliability in Bridge Scour Estimations', *Journal of Hydraulic Engineering* **141**(7), 04015013.

Kahneman, D. and Tversky, A. (1977), 'Prospect Theory: An Analysis of Decision Making Under Risk', *Econometrica* **47**(2), 263–292.

Kariyawasam, K., Fidler, P., Talbot, J. P. and Middleton, C. R. (2019), Field Deployment of an Ambient Vibration-Based Scour Monitoring System at Baildon Bridge, UK, *in*

'Proceedings of International Conference on Smart Infrastructure and Construction 2019 (ICSIC)', ICE Publishing, Cambridge, UK, 8-10 July, pp. 711–719.

Kay, A. L., Crooks, S. M., Davies, H. N. and Reynard, N. S. (2011), 'An assessment of the vulnerability of Scotland's river catchments and coasts to the impacts of climate change: Work Package 1 Report', Centre for Ecology & Hydrology, Crowmarsh Gifford, UK.

Kessler, S. S., Spearing, S. M., Atalla, M. J., Cesnik, C. E. S. and Soutis, C. (2002), 'Damage detection in composite materials using frequency response methods', *Composites: Part B* **33**, 87–95.

Kirby, A. M., Roca, M., Kitchen, A., Escarameia, M. and Chesterton, O. J. (2015), 'Manual on scour at bridges and other hydraulic structures', Report C742, CIRIA, London, UK.

Klinga, J. V. and Alipour, A. (2015), 'Assessment of structural integrity of bridges under extreme scour conditions', *Engineering Structures* **82**, 55–71.

Koh, B. H. and Dyke, S. J. (2007), 'Structural health monitoring for flexible bridge structures using correlation and sensitivity of modal data', *Computers & Structures* **85**(3-4), 117–130.

Korb, K. B. and Nicholson, A. E. (2010), *Bayesian artificial intelligence*, Chapman and Hall/CRC, Boca Raton, FLA, USA.

Lagasse, P. F., Clopper, P. E., Zevenbergen, L. W. and Girard, L. G. (2007), 'Countermeasures to Protect Bridge Piers from Scour', National Cooperative Highway Research Program (NCHRP) Report no. 593, Transportation Research Board, Washington, DC, USA.

Lagasse, P. F., Clopper, P. E., Zevenbergen, L. W., Spitz, W. J. and Girard, L. G. (2010), 'Impacts of Debris on Bridge Pier Scour', National Cooperative Highway Research Program (NCHRP) Report no. 653, Transportation Research Board, Washington, DC, USA.

Lauchlan, C. S. and Melville, B. W. (2001), 'Riprap protection at bridge piers', *Journal of Hydraulic Engineering* **127**(5), 412–418.

Lin, Y. B., Lai, J. S., Chang, K. C. and Li, L. S. (2006), 'Flood scour monitoring system using fiber Bragg grating sensors', *Smart Materials and Structures* **15**(6), 1950–1959.

Liu, Z., Nadim, F., Garcia-Aristizabal, A., Mignan, A., Fleming, K. and Luna, B. Q. (2015), 'A three-level framework for multi-risk assessment', *Georisk: Assessment and Management of Risk for Engineered Systems and Geohazards* **9**(2), 59–74.

Lowe, J. A., Bernie, D., Bett, P., Bricheno, L., Brown, S., Calvert, D., Clark, R., Eagle, K., Edwards, T., Fosser, G. *et al.* (2019), '*UKCP18 Science Overview Report*', Met Office, Exeter, UK (accessed on 17th September 2019).
URL: *https://bit.ly/2Wkzhmk*

Luque, J. and Straub, D. (2015), Probabilistic modeling of system deterioration with inspection and monitoring data using Bayesian networks, *in* 'Proceeding of 12th International Conference on Applications of Statistics and Probability in Civil Engineering (ICASP12)', Vancouver, Canada, 12-15 July.

Lynch, J. P. (2007), 'An overview of wireless structural health monitoring for civil structures', *Philosophical Transactions of the Royal Society A: Mathematical, Physical and Engineering Sciences* **365**(1851), 345–372.

Malings, C. and Pozzi, M. (2015), Sensor network optimization using Bayesian networks, decision graphs, and value of information, *in* 'Proceedings of Structural Health Monitoring and Intelligent Infrastructures (SHMII-1)', Vancouver, Canada, 12-15 July.

Maroni, A. (2015), After-earthquake damage detection: numerical and experimental uncertainty analyses of different monitoring strategies, Master's thesis, Department of Civil, Environmental and Mechanical Engineering, University of Trento, Italy.

Marsh, T., Kirby, C., Muchan, K., Barker, L., Henderson, E. and Hannaford, J. (2016), 'The winter floods of 2015/2016 in the UK - a review', Centre for Ecology and Hydrology, Wallingford, UK.

Marzocchi, W., Garcia-Aristizabal, A., Gasparini, P., Mastellone, M. L. and Di Ruocco, A. (2012), 'Basic principles of multi-risk assessment: a case study in Italy', *Natural Hazards* **62**(2), 551–573.

Megaw, E. D. (1979), 'Factors affecting visual inspection accuracy', *Applied Ergonomics* **10**(1), 27–32.

Melville, B. W. (1984), 'Live-bed scour at bridge piers', *Journal of Hydraulic Engineering* **110**(9), 1234–1247.

Melville, B. W. (1997), 'Pier and Abutment Scour: Integrated Approach', *Journal of Hydraulic Engineering* **123**(2), 125–136.

Melville, B. W. (2008), The physics of local scour at bridge piers, *in* 'Proceedings of Structural Health Monitoring and Intelligent Infrastructures (SHMII-1)', Tokyo, Japan.

Melville, B. W. and Chiew, Y.-M. (1999), 'Time Scale for Local Scour at Bridge Piers', *Journal of Hydraulic Engineering* **125**(1), 59–65.

Melville, B. W. and Coleman, S. E. (2000), *Bridge Scour*, Water Resources Publication, Highland Ranch, Colorado, USA.

Melville, B. W. and Dongol, D. M. (1992), 'Bridge Pier Scour with Debris Accumulation', *Journal of Hydraulic Engineering* **118**(9), 1306–1310.

Metropolis, N., Rosenbluth, A. W., Rosenbluth, M. N., Teller, A. H. and Teller, E. (1953), 'Equation of State Calculations by Fast Computing Machines', *The Journal of Chemical Physics* **21**(6), 1087–1092.

Michalis, P., Tarantino, A., Tachtatzis, C. and Judd, M. D. (2015), 'Wireless monitoring of scour and re- deposited sediment evolution at bridge foundations based on soil electromagnetic properties', *Smart Materials and Structures* **24**(12), 1–15.

Moore, M., Phares, B., Graybeal, B., Rolander, D. and Washer, G. (2001), 'Reliability of visual inspection for highway bridges', volume I (No. FHWA-RD-01-105), Research, Development, and Technology Turner-Fairbank Highway Research Center, McLean, VA, USA.

Mussi, S. (2004), 'Putting value of information theory into practice: a methodology for building sequential decision support systems', *Expert Systems* **21**(2), 92–103.

Naidu, A. S., Soh, C. K. and Pagalthivarthi, K. V. (2006), 'Bayesian network for E/M impedance-based damage identification', *Journal of Computing In Civil Engineering* **20**(4), 227–236.

Network Rail (2017), 'Scotland Adverse and Extreme Weather Plan', Network Rail, Glasgow, UK.

Nguyen, M., Wang, X., Su, Z. and Ye, L. (2004), Damage identification for composite structures with a Bayesian network, *in* 'Proceedings of the Intelligent Sensors, Sensor

Networks and Information Processing Conference', Melbourne, Australia, 14-17 Dec, pp. 307–311.

Olofsson, I., Elfgren, L., Bell, B., Paulsson, B., Niederleithinger, E., Sandager Jensen, J., Feltrin, G., Täljsten, B., Cremona, C., Kiviluoma, R. and Bien, J. (2005), 'Assessment of European railway bridges for future traffic demands and longer lives – EC project "Sustainable Bridges"', *Structure and Infrastructure Engineering: Maintenance, Management, Life-Cycle Design and Performance* **1**(2), 93–100.

Or, D. and Wraith, J. M. (1999), 'Temperature effects on soil bulk dielectric permittivity measured by time domain reflectometry: A physical model', *Water Resources Research* **35**(2), 371–383.

Pagliara, S. and Carnacina, I. (2011), 'Influence of Wood Debris Accumulation on Bridge Pier Scour', *Journal of Hydraulic Engineering* **137**(2), 254–261.

Parola, A. C., Apelt, C. J. and Jempson, M. A. (2000), 'Debris Forces on Highway Bridges', National Cooperative Highway Research Program (NCHRP) Report no. 445, Transportation Research Board, Washington, DC, USA.

PCSG (2019), 'Gaist boosts winter resilience with bridge system', Professional Construction Strategies Group Ltd, Croydon, UK (accessed on 1st May 2019).
URL: *https://bit.ly/2A7oi7b*

Pearson, D., Stein, S. and Jones, J. S. (2002), 'HYRISK Methodology and User Guide', Report FHWA-RD-02-XXX, U.S. Department of Transportation, Federal Highway Administration, Virginia, USA.

Pizarro, A., Manfreda, S. and Tubaldi, E. (2020), 'The Science behind Scour at Bridge Foundations: A Review', *Water* **12**(2), 374–26.

Pizarro, A. and Tubaldi, E. (2019), 'Quantification of Modelling Uncertainties in Bridge Scour Risk Assessment under Multiple Flood Events', *Geosciences* **9**, 445–15.

Porter, K. A. (2003), An overview of PEER's performance-based earthquake engineering methodology, *in* 'Proceedings of 9th International Conference on Applications of Statistics and Probability in Civil Engineering (ICASP9)', San Francisco, USA, 6-9 July.

Pozzi, M. and Der Kiureghian, A. (2011), Assessing the value of information for long-term structural health monitoring, *in* 'Proceedings of SPIE7984, Health Monitoring of Structural and Biological Systems', SPIE, p. 79842W.

Pozzi, M. and Der Kiureghian, A. (2013), Gaussian Bayesian network for reliability analysis of a system of bridges , *in* 'Proceedings of 11th International Conference on Structural Safety and Reliability (ICOSSAR'13)', New York, USA, 16-20 June.

Prendergast, L. J. and Gavin, K. (2014), 'A review of bridge scour monitoring techniques', *Journal of Rock Mechanics and Geotechnical Engineering* **6**(2), 138–149.

Rail Accident Investigation Branch (2016), 'Structural failure caused by scour at Lamington viaduct, South Lanarkshire 31 December 2015 ', Report 22/2016, Rail Accident Investigation Branch, Department for Transport, Derby, UK.

Rail Safety & Standards Board (2005), 'Safe management of railway structures - flooding and scour risk', Rail Safety & Standards Board, Skipton, UK.

Richardson, E. V. and Davis, S. R. (2001), 'Evaluating Scour at Bridges', Hydraulic Engineering Circular No.18, Publication No. FHWA NHI 01-001, U.S. Department of Transportation, Federal Highway Administration, Washington DC, USA.

Robinson, D. A., Jones, S. B., Blonquist, J. M. and Friedman, S. P. (2005), 'A Physically Derived Water Content/Permittivity Calibration Model for Coarse-Textured, Layered Soils', *Soil Science Society of America Journal* **69**(5), 1372–1378.

Roca, M. and Whitehouse, R. (2012), Scour risk assessment at river crossings, *in* 'Proceeding of Sixth Conference on Scour and Erosion (ICSE6)', Paris, France, 27-31 August.

Roth, C. H., Malicki, M. A. and PLAGGE, R. (1992), 'Empirical evaluation of the relationship between soil dielectric constant and volumetric water content as the basis for calibrating soil moisture measurements by TDR', *Journal of Soil Science* **43**(1), 1–13.

Roth, K., Schulin, R., Flühler, H. and Attinger, W. (1990), 'Calibration of time domain reflectometry for water content measurement using a composite dielectric approach', *Water Resources Research* **26**(10), 2267–2273.

Schwank, M., Green, T. R., Mätzler, C., Benedickter, H., Schulin, R. and Flühler, H. (2006), 'Characterization of EnviroSMART capacitance sensors for measuring soil water content', Swiss Federal Institute of Technology (ETH), Zürich, Switzerland.

Scozzese, F., Ragni, L., Tubaldi, E. and Gara, F. (2019), 'Modal properties variation and collapse assessment of masonry arch bridges under scour action', *Engineering Structures* **199**, 109665.

Selvakumaran, S., Plank, S., Geiß, C., Rossi, C. and Middleton, C. (2018), 'Remote monitoring to predict bridge scour failure using Interferometric Synthetic Aperture Radar (InSAR) stacking techniques', *Int J Appl Earth Obs Geoinformation* **73**, 463–470.

Sentek technologies (2011), 'Calibration manual for Sentek soil moisture sensors', Sentek Pty. Ltd, Kent Town, South Australia (accessed on 1st November 2017).
URL: *https://bit.ly/35FBJqn*

Sentek technologies (2015), 'Sentek PLUS All-in-One & Sentek PLUS Compact DTU', Sentek Pty. Ltd, Kent Town, South Australia (accessed on 1st November 2017).
URL: *https://bit.ly/2WaQ4bs*

Sentek technologies (2017), 'Factory literature for the EnviroSCAN', Sentek Pty. Ltd, Kent Town, South Australia (accessed on 25th May 2017).
URL: *https://bit.ly/2W5xyB0*

Sheppard, D. M. and Renna, R. (2005), 'Florida bridge scour manual', Florida DOT, Tallahassee, Fla., USA.

Sohn, H. and Law, K. H. (1997), 'A Bayesian probabilistic approach for structure damage detection', *Earthquake Engineering and Structural Dynamics* **26**, 1259–1281.

Sousa, J. J., Hlaváčová, I., Bakoň, M., Lazecký, M., Patrício, G., Guimarães, P., Ruiz, A. M., Bastos, L., Sousa, A. and Bento, R. (2014), 'Potential of Multi-temporal InSAR Techniques for Bridges and Dams Monitoring', *Procedia Technology* **16**, 834–841.

Straub, D. (2005), Natural hazards risk assessment using Bayesian networks, *in* 'Proceedings of Structural Health Monitoring and Intelligent Infrastructures (SHMII-1)', Rome, Italy, 19-23 June.

Straub, D. (2009), 'Stochastic modeling of deterioration processes through dynamic Bayesian networks', *Journal of Engineering Mechanics* **135**(10), 1089–1099.

Straub, D. and Der Kiureghian, A. (2010*a*), 'Bayesian network enhanced with structural reliability methods: Application', *Journal of Engineering Mechanics* **136**(10), 1259–1270.

Straub, D. and Der Kiureghian, A. (2010*b*), 'Bayesian network enhanced with structural reliability methods: Methodology', *Journal of Engineering Mechanics* **136**(10), 1248–1258.

Sustainable Bridges (2008), 'Publishable Final Activity Report', FP6-SUSTDEV, European Railway Bridge Demography: Assessment for Future Traffic Demands and Longer Lives (2003-2007).
URL: *https://cordis.europa.eu/project/id/1653*

Szoenyi, M., May, P. and Lamb, R. (2015), 'Flooding in Cumbria after Storm Desmond', Zurich Insurance Group, Zurich, Switzerland, JBA Trust, North Yorkshire, UK (accessed on 20th July 2019).
URL: *https://bit.ly/2YzesoJ*

Tanasić, N., Ilić, V. and Hajdin, R. (2013), 'Vulnerability Assessment of Bridges Exposed to Scour', *Transportation Research Record: Journal of the Transportation Research Board* **2360**, 36–44.

Tarantino, A. (2019), personal communication.

Tarantino, A., Ridley, A. M. and Toll, D. G. (2008), 'Field Measurement of Suction, Water Content, and Water Permeability', *Geotechnical and Geological Engineering* **26**(6), 751–782.

Texas A&M Transportation Institute (2014), 'Bridge failure due to scour [Online image]', Texas A&M Transportation Institute.
URL: *https://goo.gl/QEL74P*

The Boston Globe (2009), 'Aging Bridge [Online image]', The Boston Globe.
URL: *https://bit.ly/2WEh0PQ*

The Guardian (2019*a*), 'Morandi bridge collapse in Genova [Online image]', The Guardian.
URL: *https://bit.ly/2WGONYv*

The Guardian (2019*b*), 'What caused the Genoa bridge collapse – and the end of an Italian national myth?', (accessed on 10th July 2018).
URL: *https://bit.ly/35MuLQI*

Thöns, S. and Faber, M. H. (2013), Assessing the value of structural health monitoring, *in* 'Proceedings of 11th International Conference on Structural Safety and Reliability (ICOSSAR'13)', New York, USA, 16-20 June.

Thornes, J., Rennie, M., Marsden, H. and Chapman, L. (2012), 'Climate Change Risk Assessment for the Transport Sector', Department for Environment, Food and Rural Affairs, London, UK.

Tien, I. and Der Kiureghian, A. (2017), 'Reliability Assessment of Critical Infrastructure Using Bayesian Networks', *Journal of infrastructure systems* **23**(4), 04017025.

Tinkler, K. J. (1982), 'Avoiding Error When Using the Manning Equation', *The Journal of Geology* **90**(3), 326–328.

Topp, G. C., Davis, J. L. and Annan, A. P. (1980), 'Electromagnetic determination of soil water content: Measurements in coaxial transmission lines', *Water Resources Research* **16**(3), 574–582.

Transport Scotland (2018), 'Scour Management Strategy and Flood Emergency Plan', Transport Scotland, Glasgow, UK.

Tritech (2018), 'Bridge Inspection - Hammerhead mechanical sonar', Tritech International Limited, Westhill, UK (accessed on 1st May 2019).
URL: *https://bit.ly/2L2BAUx*

Tubaldi, E., Macorini, L. and Izzuddin, B. A. (2018), 'Three-dimensional mesoscale modelling of multi-span masonry arch bridges subjected to scour', *Composites: Part B* **165**, 486–500.

Tubaldi, E., Macorini, L., Izzuddin, B. A., Manes, C. and Laio, F. (2017), 'A framework for probabilistic assessment of clear-water scour around bridge piers', *Structural Safety* **69**, 11–22.

Umbrell, E. R., Young, G. K., Stein, S. M. and Jones, J. S. (1998), 'Clear-water contraction scour under bridges in pressure flow', *Journal of Hydraulic Engineering* **124**(2), 236–240.

United States Geological Survey (2016), 'Local Scour [Online image]'.
URL: *https://on.doi.gov/2UkFUn7*

van Leeuwen, Z. and Lamb, R. (2014), 'Flood and scour related failure incidents at railway assets between 1846 and 2013', Project W13 - 4224, JBA Trust Limited 2014, Skipton, UK.

Vanik, M. W., Beck, J. L. and Au, S. K. (2000), 'Bayesian Probabilistic Approach to Structural Health Monitoring', *Journal of Engineering Mechanics* **126**(7), 738–745.

Verzobio, A., Tonelli, D., Bolognani, D., Cappello, C., Bursi, O. S. and Zonta, D. (2018), Monitoring-based Decision Support System for optimal management of Colle Isarco Viaduct, *in* 'Proceedings of SPIE 10600, Health Monitoring of Structural and Biological Systems XII', p. 106002C.

Vogel, K., Riggelsen, C., Korup, O. and Scherbaum, F. (2014), 'Bayesian network learning for natural hazard analyses', *Natural Hazards and Earth System Science* **14**(9), 2605–2626.

von Neumann, J. and Morgenstern, O. (1953), *Theory of Games and Economic Behavior*, third edn, Princeton University Press, Princeton, USA.

Wang, C. Y., Wang, H. L., Wu, C. Y. and Chen, C. H. (2003), Development of bridge health monitoring systems in Taiwan, *in* Z. Wu and M. Abe, eds, 'Proceedings of Structural Health Monitoring and Intelligent Infrastructures (SHMII-1)', pp. 1067–1072.

Wang, C., Yu, X. and Liang, F. (2017), 'A review of bridge scour: mechanism, estimation, monitoring and countermeasures', *Natural Hazards* **87**(3), 1881–1906.

Wardhana, K. and Hadipriono, F. C. (2003), 'Analysis of recent bridge failures in the United States', *Journal of performance of constructed facilities* **17**(3), 144–150.

Wenzel, H. (2008), *Health Monitoring of Bridges*, John Wiley & Sons, Chichester, UK.

Whalley, W. R., Dean, T. J. and Izzard, P. (1992), 'Evaluation of the Capacitance Technique as a Method for Dynamically Measuring Soil Water Content', *Journal of Agricultural Engineering Research* **52**, 147–155.

Woodward, R. J. (2002), 'BRIME - Bridge Management in Europe Final Report D14', (accessed on 23/11/19).
URL: *https://bit.ly/3b75odm*

Yu, X. and Yu, X. (2009), 'Time Domain Reflectometry Automatic Bridge Scour Measurement System: Principles and Potentials', *Structural Health Monitoring* **8**(6), 463–476.

Yue, Y., Zonta, D., Pozzi, M., Bortot, F. and Zandonini, R. (2012), Application of the Bayesian Network to Seismic Vulnerability Assessment in Bridge Management System,

in 'Proceedings of XIV ANIDIS L'Ingegneria sismica in Italia, Sep 18-22', Bari, Italy, 18-22 Sep.

Zarafshan, A., Iranmanesh, A. and Ansari, F. (2012), 'Vibration-Based Method and Sensor for Monitoring of Bridge Scour', *Journal of Bridge Engineering* **17**(6), 829–838.

Zonta, D., Cappello, C., Pozzi, M. and Glišić, B. (2014), On Evaluating Monitoring Design Effectiveness, *in* 'EWSHM-7th European Workshop on Structural Health Monitoring', Nantes, France, 8-11 July.

Zonta, D., Glišić, B. and Adriaenssens, S. (2014), 'Value of information: impact of monitoring on decision-making', *Structural Control and Health Monitoring* **21**(7), 1043–1056.